

**2018 Fall**

# ***Advanced Solidification***

**11.23.2018**

**Eun Soo Park**

**Office: 33-313**

**Telephone: 880-7221**

**Email: [espark@snu.ac.kr](mailto:espark@snu.ac.kr)**

**Office hours: by appointment**

**Solidification of Pure Metal**

**: Thermal gradient dominant**



**Solidification of single phase alloy: Solute redistribution dominant**

**a) Constitutional Supercooling (C.S.)**

Planar	→ Cellular growth	→ cellular dendritic growth	→ Free dendritic growth
Thin zone formation by C.S. at the sol. Interface	Dome type tip / (surrounding) hexagonal array	T↓ → Increase of C.S. zone Pyramid shape of cell tip / Square array of branches / Growth direction change toward Dendrite growth direction	formed by releasing the latent heat from the growing crystal toward the supercooled liquid Dendrite growth direction/ Branched rod-type dendrite

→ “Nucleation of new crystal in liquid” which is at a higher temp. than the interface at which growth is taking place.

**b) Segregation**

**: normal segregation, grain boundary segregation, cellular segregation, dendritic segregation, inverse segregation, coring and intercrystalline segregation, gravity segregation**

**: undesirable ~ deleterious effects on mechanical properties**

→ subsequent **homogenization heat treatment**, but diffusion in the solid far too slow

→ **good control of the solidification process**

## 5.10. Types of Segregation

\* Last discussion on “**solute redistribution in single phase alloys**”

→ “**Various types of segregation**”

\* Segregation: result of rejection of solute at the interface during solidification

**The difference depends on the “rejection direction / distance / solute motion”.**

### \* Segregation

**(a) Macrosegregation** : Large area

**composition changes over distances comparable to the size of the specimen.**

**Four important factors** that can lead to **macrosegregation**

- a) **Shrinkage** due to solidification and thermal contraction.
- b) **Density differences** in the interdendritic liquid.
- c) **Density differences** between the solid and liquid.
- d) **Convection currents** driven by temperature-induced density differences in the liquid.

**(b) Microsegregation** : in secondary dendritic arms

**occur on the scale of the secondary dendrite arm spacing.**

**Fig.** Simulation of macrosegregation formation in a large steel casting, showing liquid velocity vectors during solidification (left) and final carbon macrosegregation pattern (right).

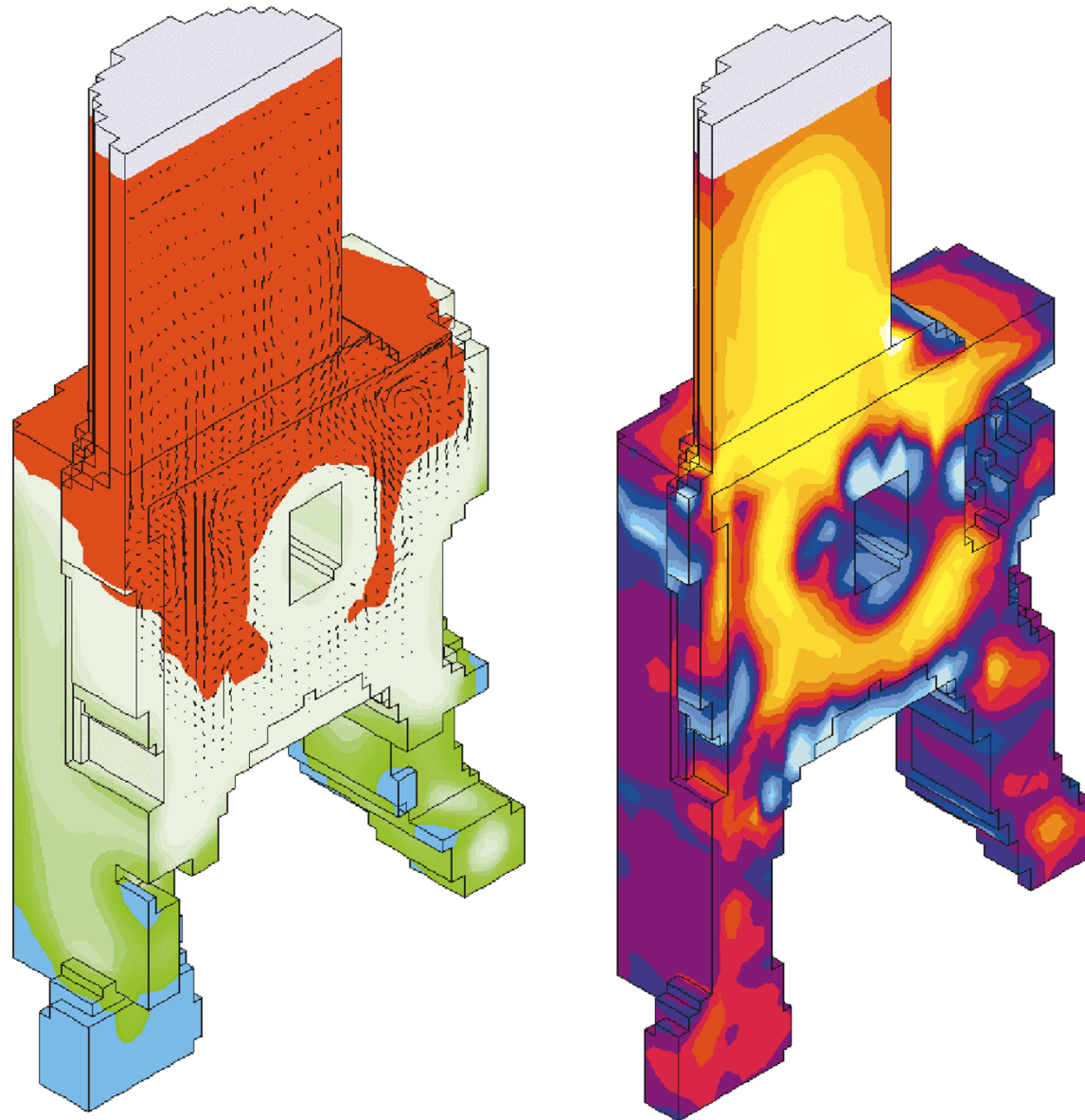


**Fig.**

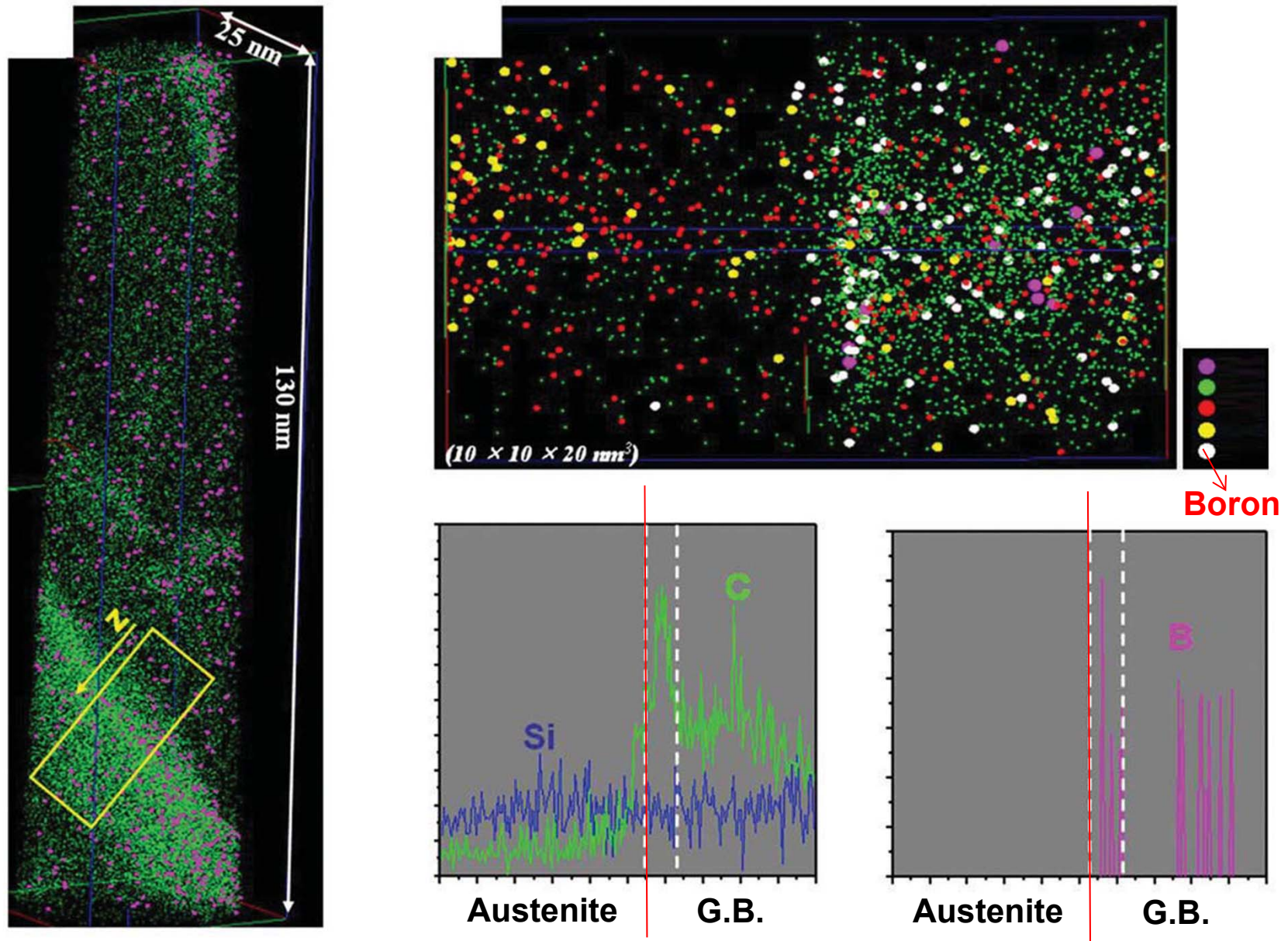
**Freckles** in a single-crystal nickel-based superalloy prototype blade (left) and close-up of a single freckle (right) (courtesy of A. F. Giamei, United Technologies Research Center).



**Fig.**

Sulfur print showing centerline segregation in a continuously cast steel slab (courtesy of IPSCO Inc.).





The result obtained by APT analysis. (a) 3D Atom map of **Boron steel containing 100 ppm Boron** and (b) composition profile showing **solute segregation within retained austenite and grain boundary** 7

# 1) Normal segregation

**: motion of solute parallel to the direction of solidification**

**The form of curve depends on ① equilibrium distribution coefficient  $k_0$ , ② the rate of R of solidification (or the time-distance relationship if R is not constant), and ③ the amount of mixing by fluid motion.**

→ **Actual segregation:** depends very much on “**sample geometry**”

**influences both ① solidification rate ② amount of convection**

→ **difficult to state general rule for predicting the result**

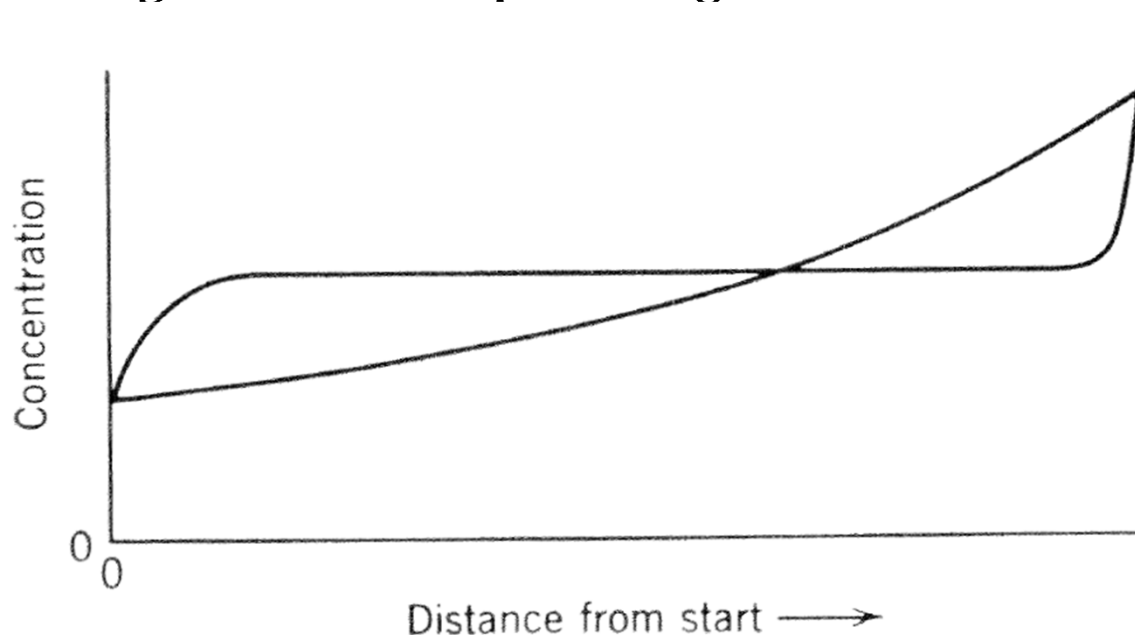


**Fig. 5.42. Extreme cases of normal segregation**

# 1) Normal segregation

**: motion of solute parallel to the direction of solidification**

The form of curve depends on ① equilibrium distribution coefficient  $k_0$ , ② the rate of R of solidification (or the time-distance relationship if R is not constant), and ③ the amount of mixing by fluid motion.

→ Actual segregation: depends very much on “sample geometry”

influences both ① solidification rate ② amount of convection

→ difficult to state general rule for predicting the result

- **Variation of Segregation pattern**

**Solidification rate**

Below 2 cm/hr  $\longleftrightarrow$  Above 20 cm/hr

Mixing dominant      Diffusion control

→ Oversimplification, because **the form of the interface**, which depends on the extent of constitutional supercooling, has an important influence on the mixing process.

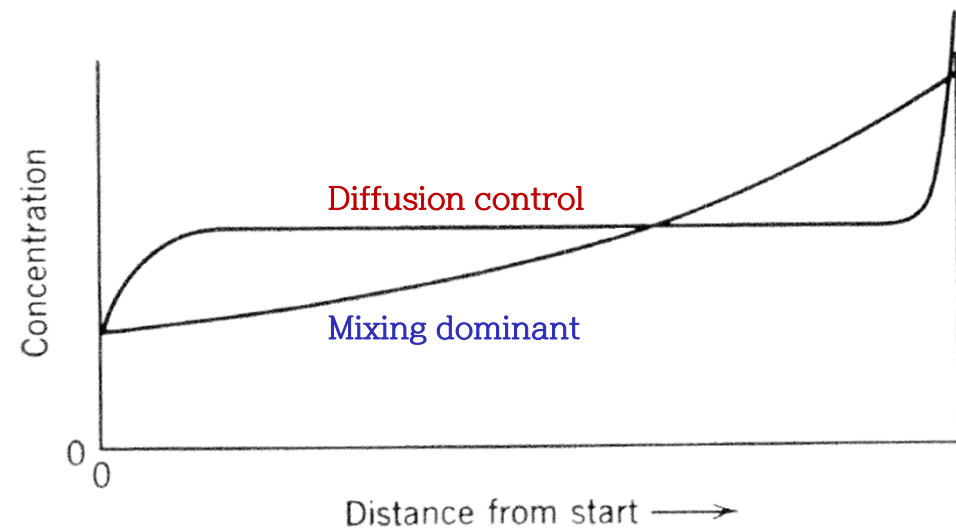


Fig. 5.42. Extreme cases of normal segregation

## 2) Grain boundary segregation during the process of solidification

: This is not to be confused with equilibrium segregation at GB.

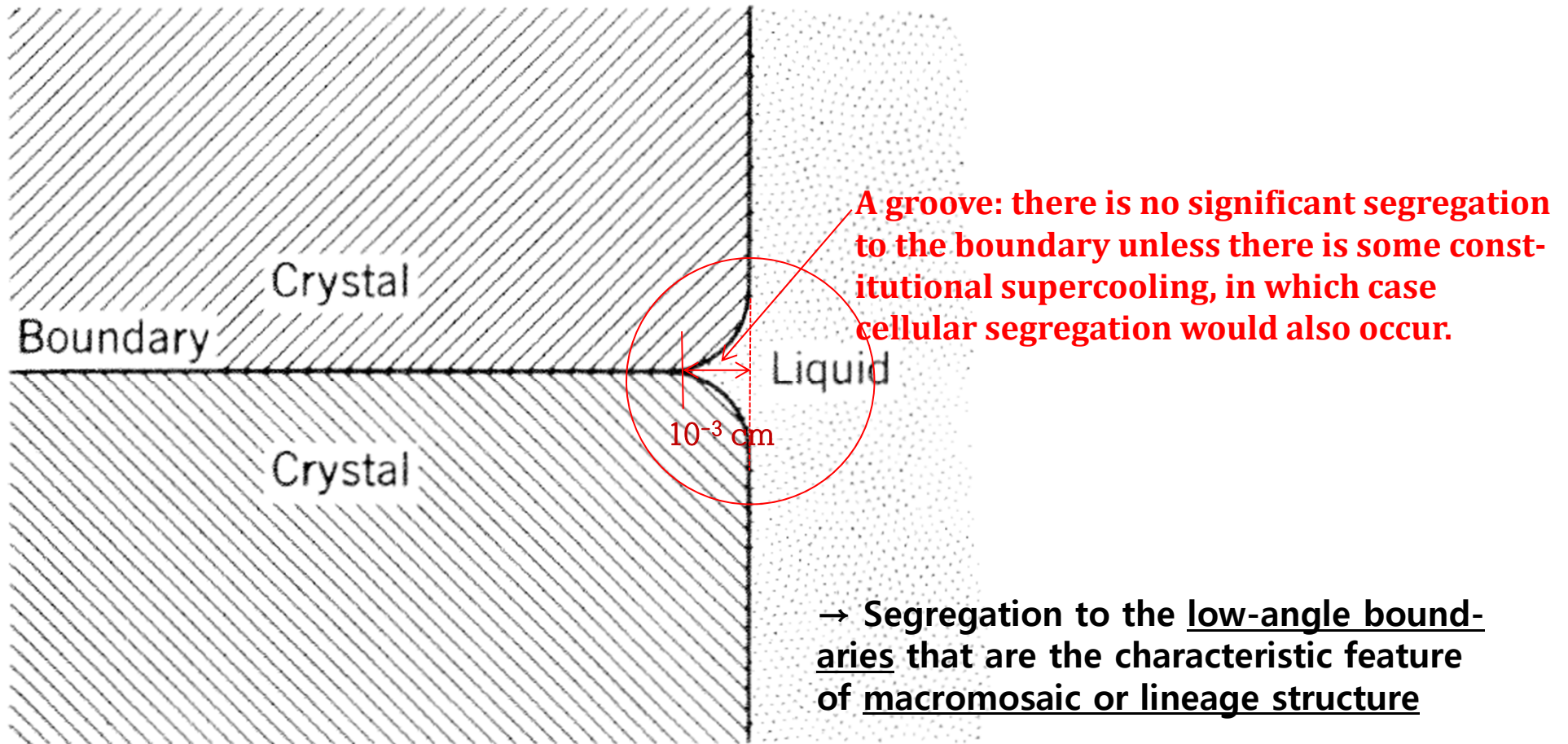


Fig. 5.43. Conditions for grain boundary segregation

# Whose mobility would be high between special and random boundaries?

By considering grain boundary structure,

(Mobility depending on GB structures)

High energy G.B. → relatively open G.B. structure → High mobility

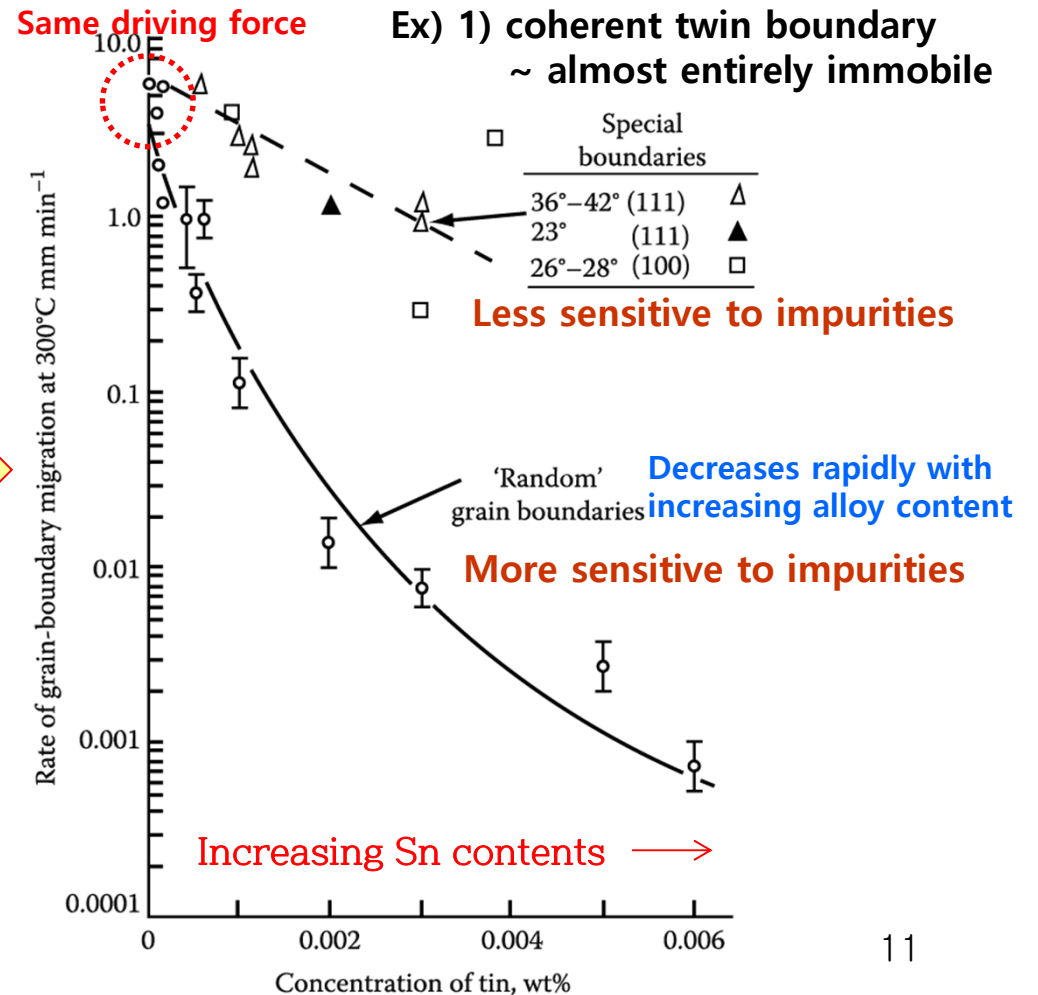
Low energy G.B. → closed (or denser) G.B. structure → Low mobility

But, **Ideal** ↔ **Real**

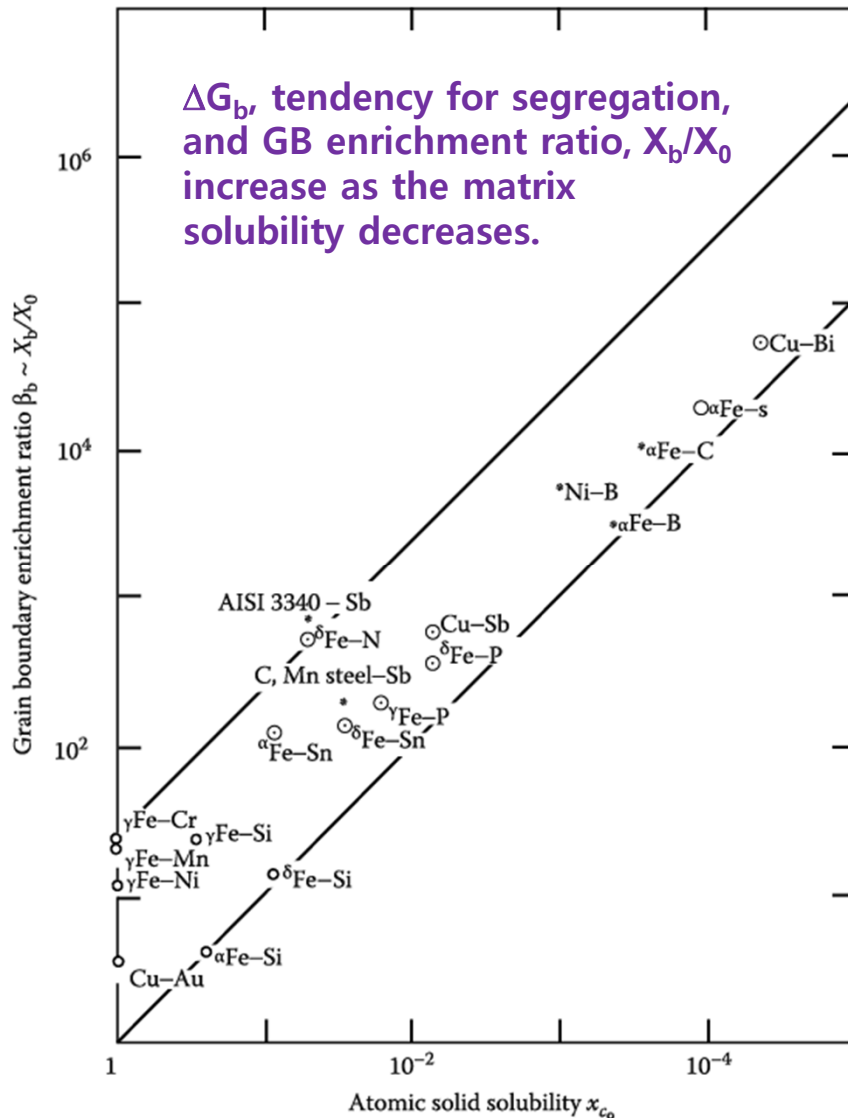
2) The other special boundaries are usually more mobile than random high-angle boundary. Why?

If the metal were “perfectly” pure the random boundaries would have the higher mobility.

⇒ Due to differences in the interactions of alloy elements or impurities with different boundaries



Migration rate of special and random boundaries at 300 °C in zone-refined lead alloyed with tin under equal driving forces



<Increasing GB enrichment with decreasing solid solubility in a range of system>

$X_0$  : matrix solute concentration/  $X_b$  : boundary solute concentration

$\Delta G_b$  : free energy reduced when one mole of solute is moved to GB from matrix.

→ The high mobility of special boundaries can possibly be attributed to a low solute drag on account of the relatively more close-packed structure of the special boundaries.

\* Solute drag effect

In general,  $G_b$  (grain boundary E) and mobility of pure metal decreases on alloying.

~Impurities tend to stay at the GB.

Generally,  $\Delta G_b$ , tendency of segregation, increases as the matrix solubility decreases.

$$X_b = X_0 \exp \frac{\Delta G_b}{RT}$$

$X_b/X_0$ : GB enrichment ratio

- Decreases as temp. increases, i.e., the solute "evaporates" into the matrix

Low T or  $\Delta G_b$  ↑  $X_b$  ↑ Mobility of G.B. ↓

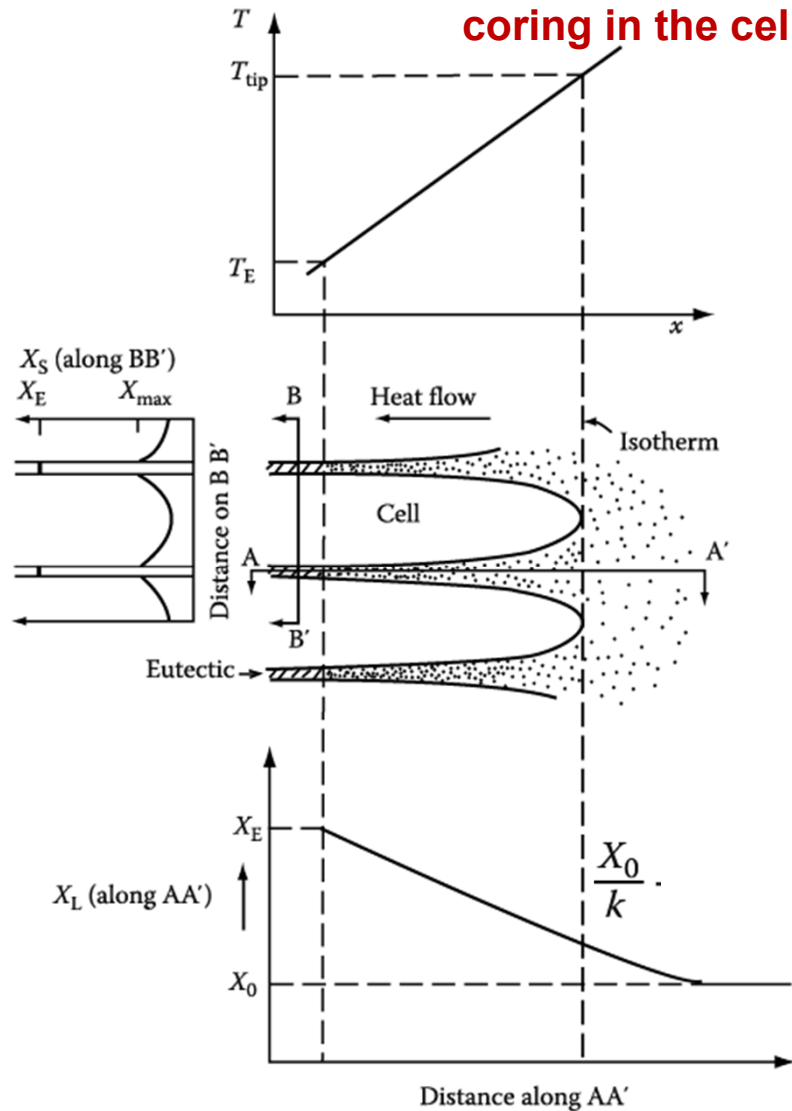
→ Alloying elements affects mobility of G.B.

### 3) Cellular segregation

: after cellular solidification, **at the “terminal transient” region**

\* **Temp. and solute distributions associated with cellular solidification.**

1) Note that solute enrichment in the liquid between the cells, and **coring in the cells with eutectic in the cell walls.**



2) **Tips of the cells grow into the hottest liquid and therefore contain the least solute.**

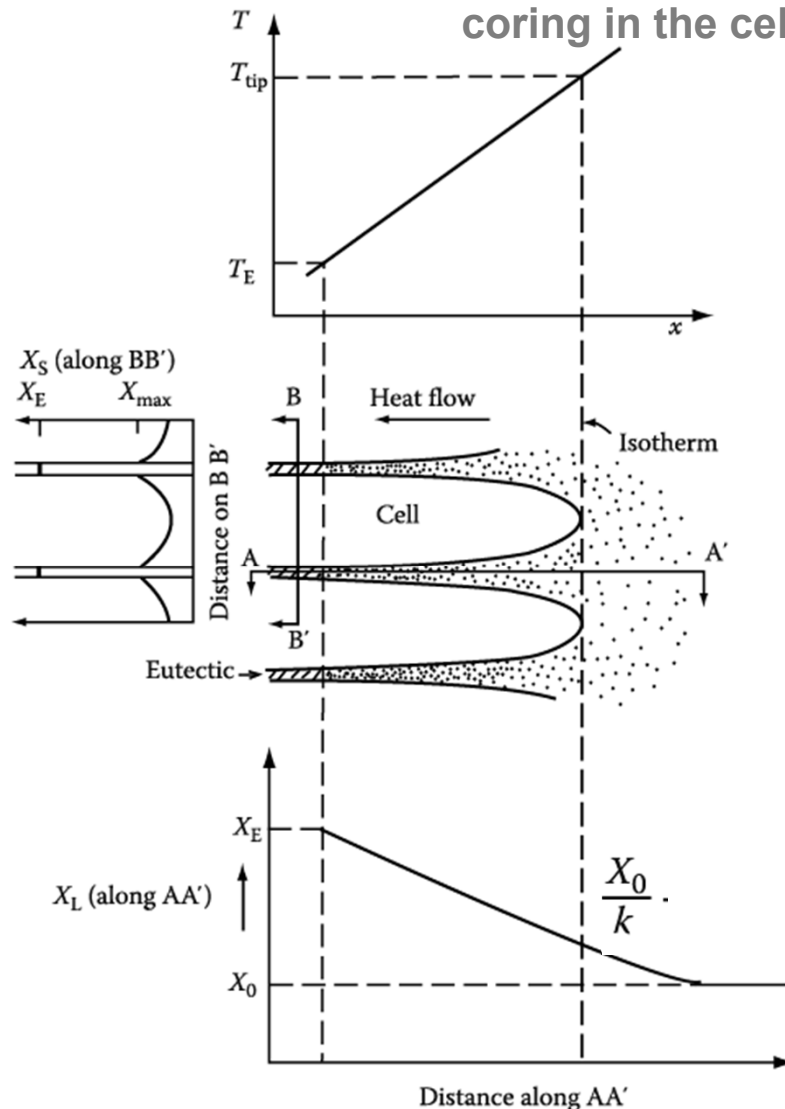
3) **Even if  $X_0 \ll X_{max}$  Solute pile up  $\rightarrow$  eutectic solidification  $\rightarrow$  formation of 2<sup>nd</sup> phases at the cell wall**

### 3) Cellular segregation

: after cellular solidification, **at the “terminal transient” region**

\* Temp. and solute distributions associated with cellular solidification.

1) Note that solute enrichment in the liquid between the cells, and coring in the cells with eutectic in the cell walls.



2) Tips of the cells grow into the hottest liquid and therefore contain the least solute.

3) Even if  $X_0 \ll X_{max}$   
Solute file up  $\rightarrow$  eutectic solidification  
 $\rightarrow$  formation of 2<sup>nd</sup> phases at the cell wall

- Segregation decreases as a result of diffusion

- ① during cooling down after solidification

- ② any subsequent annealing process

$\rightarrow$  but, “dislocation” associated with the solute at the cell walls may tend to stabilize it and limit the homogenizing effect of annealing.

## 4) Dendritic segregation

: Almost all work on micro-segregation in alloys has been on cellular-dendritic structure



Fig. 5.44. Distribution of Cu in an Al-4.5% Cu alloy

**Cu segregation**

: light contrast in microradiograph

most concentrated close to the plates



Fig. 5.45. Segregation in Al-Cu alloy

used Biloni's epitaxial film technique

to show the segregation in Al-Cu alloys

## 4) Dendritic segregation

: Almost all work on micro-segregation in alloys has been on cellular-dendritic structure

**Quantitative work on the actual distribution of solute** has been carried out using electron microprobe technique, with which they were able to establish solute **“iso-concentration lines”**, it is apparent that the plate-like structure is in this case built up of a main stem and coalesced branches. → The **extremely complicated geometry** of the cellular structure makes it very difficult to form realistic theoretical predictions with which to compare the experimental results. → **“Phase field modeling”**

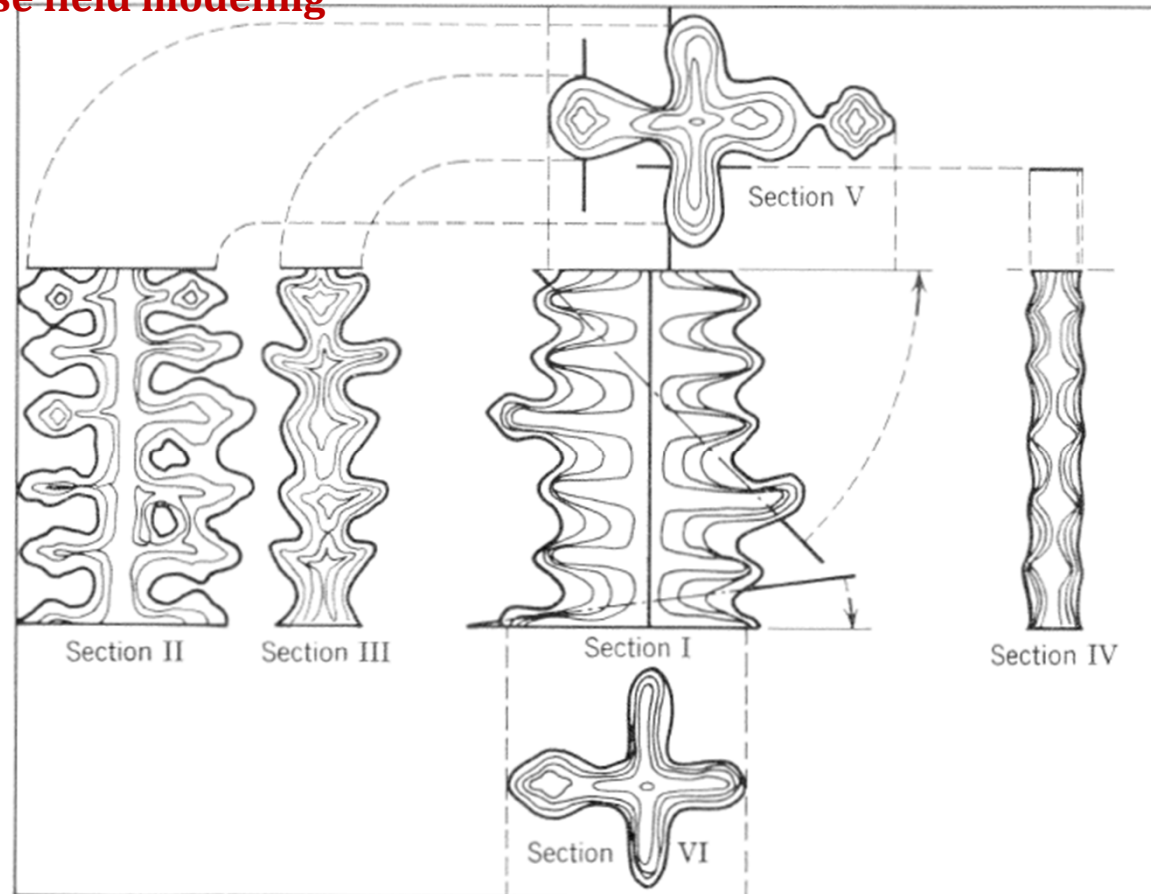


Fig. 5.46. Quantitative results on distribution of solute in columnar dendritic crystal

## 4) Dendritic segregation

: Almost all work on micro-segregation in alloys has been on cellular-dendritic structure

But, Flemings and Brody have shown that good agreement with the electron-probe results can be obtained from calculations based on a very simple model

(solidification is regarded as taking place inward from two plane “walls” whose spacing is equal to that of the cell walls.

The calculated distribution using

$$C_s = k_E C_0 (1 - g)^{k_0 - 1}$$

is shown in Fig. 5.47 for some Al-Cu alloys.

- The speed of solidification does not appear explicitly in this solution, because the cell wall spacing depends upon speed.
- Thus, the distribution of solute is independent of speed if it is plotted in the dimensionless form of Fig.5.47.

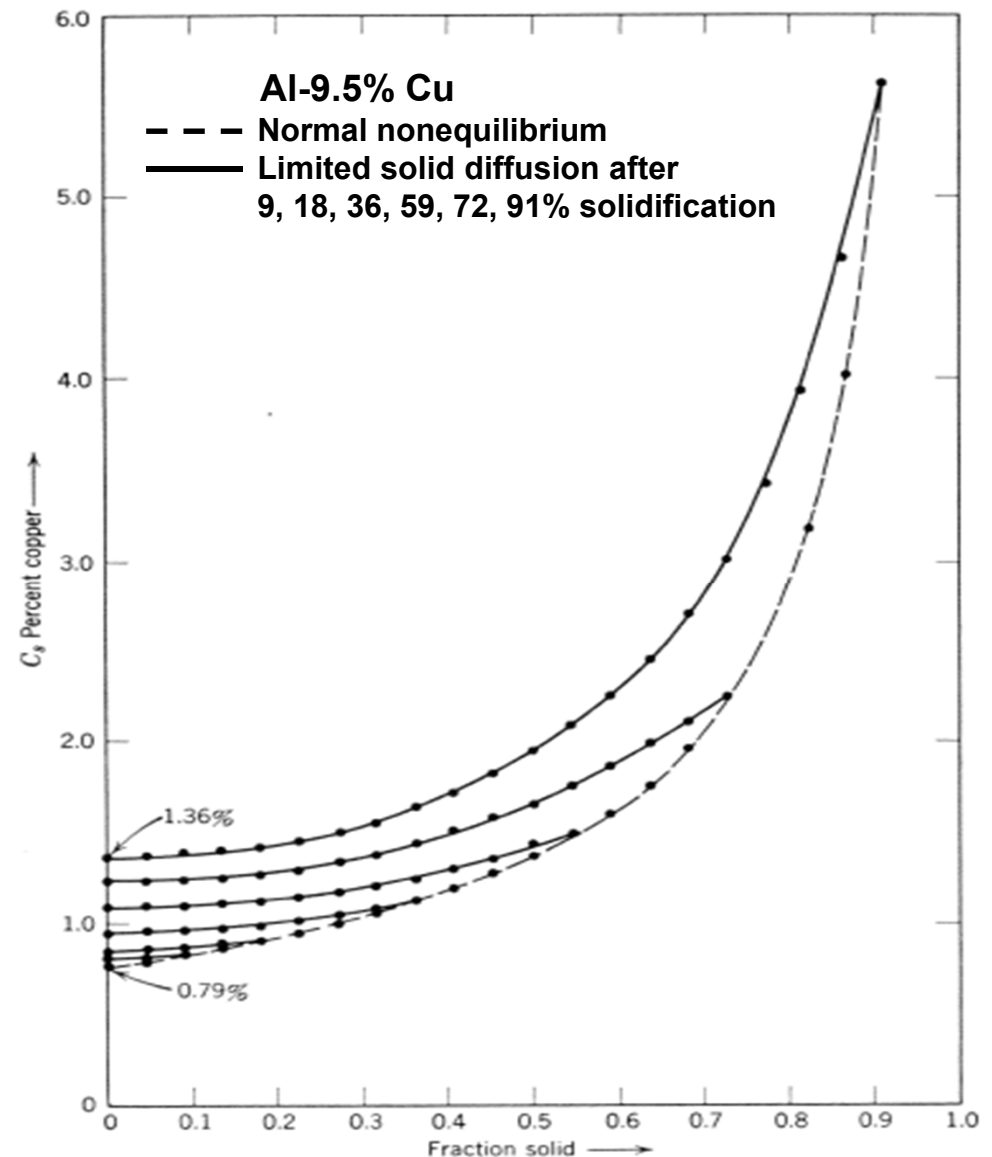


Fig. 5.47. Calculated distribution of solute between walls of cellular dendritic structure

## 4) Dendritic segregation

: Almost all work on micro-segregation in alloys has been on cellular-dendritic structure

- \* **Maximum concentration (eutectic composition & independent of the rate of solidification)**  
→ compared experimental results with theoretical values based on various assumptions of the amount of diffusion that occurs in the solid during solidification

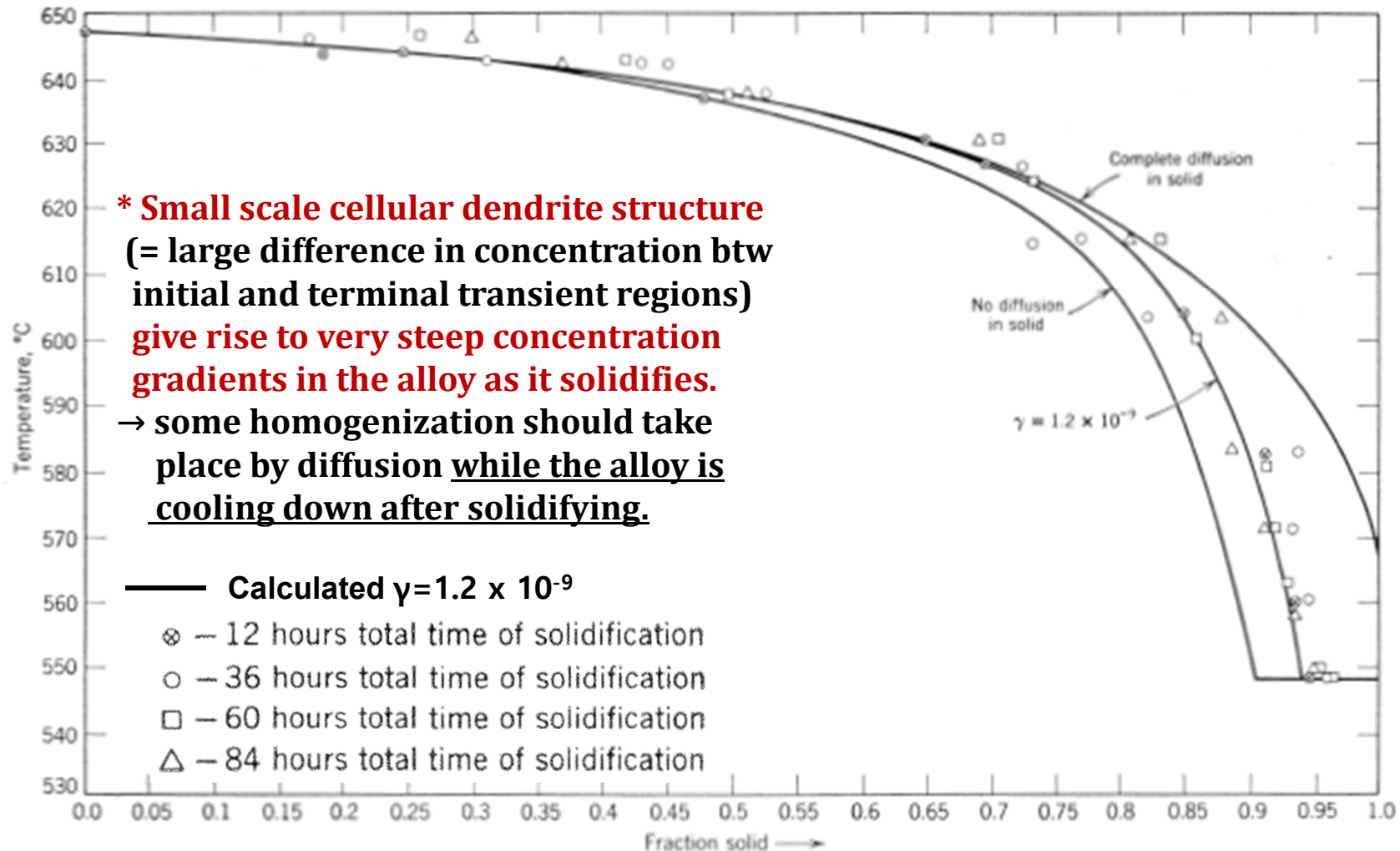


Fig. 5.48. Comparison between calculated and experimental distributions of solute.

## 4) Dendritic segregation

: Almost all work on micro-segregation in alloys has been on cellular-dendritic structure

\* Flemings and Poirier have shown that the amount of homogenization during cooling can be predicted with reasonable accuracy if the initial distribution is calculated in the manner discussed above. → Fig. 5.49.

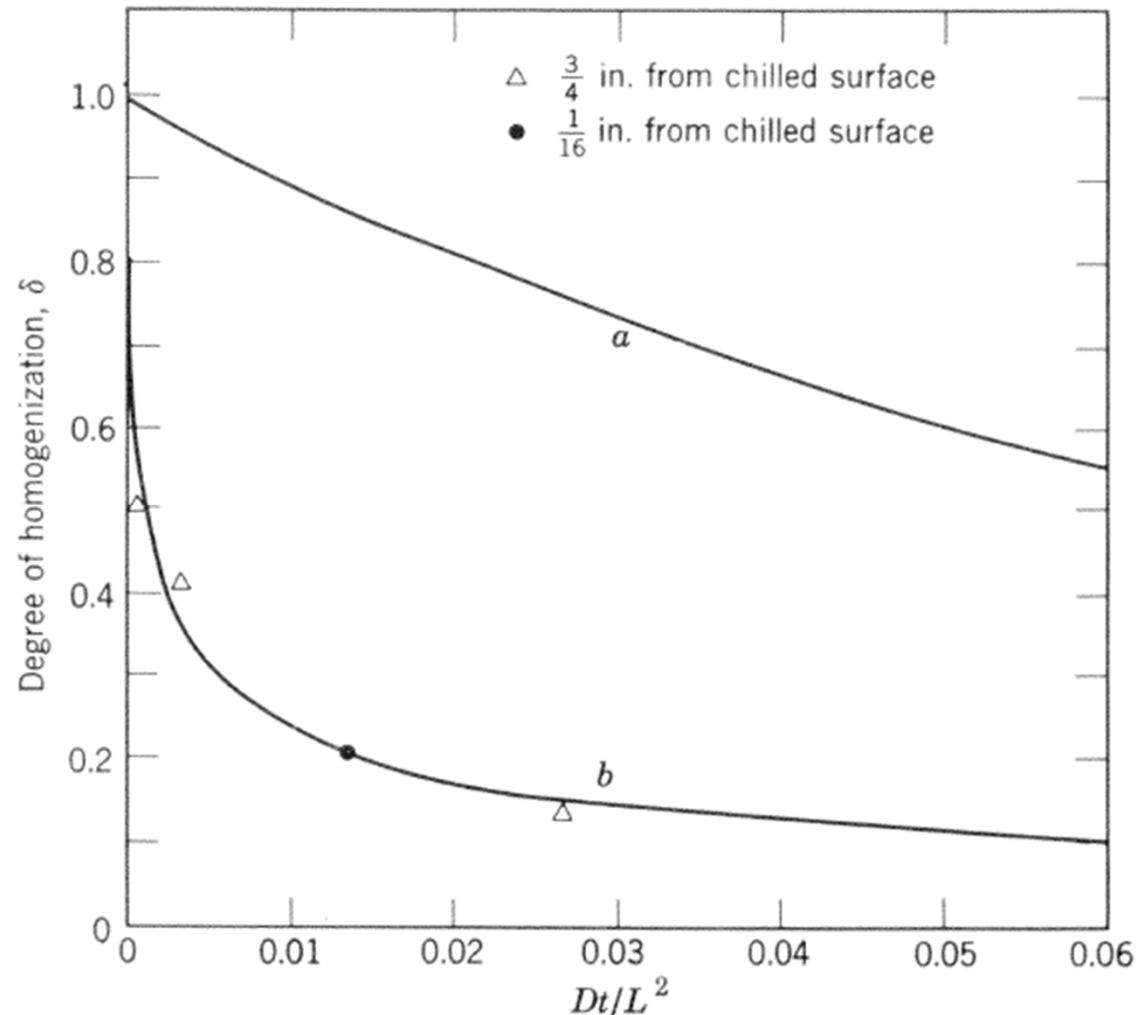


Fig. 5.49. Experimental and calculated results for homogenization during cooling.

## 5) Inverse segregation

: occurs when a solute that is rejected during solidification is present at a higher concentration in regions that solidified earlier than in those that solidified later. (=solute moves in the direction opposite to that of normal segregation)

→ **Formation mechanism originally proposed by Scheil.**

**\* Shrinkage** that in most alloys accompanies solidification may cause motion of the most “solute enriched” liquid in a direction opposite to that of the general solidification front.

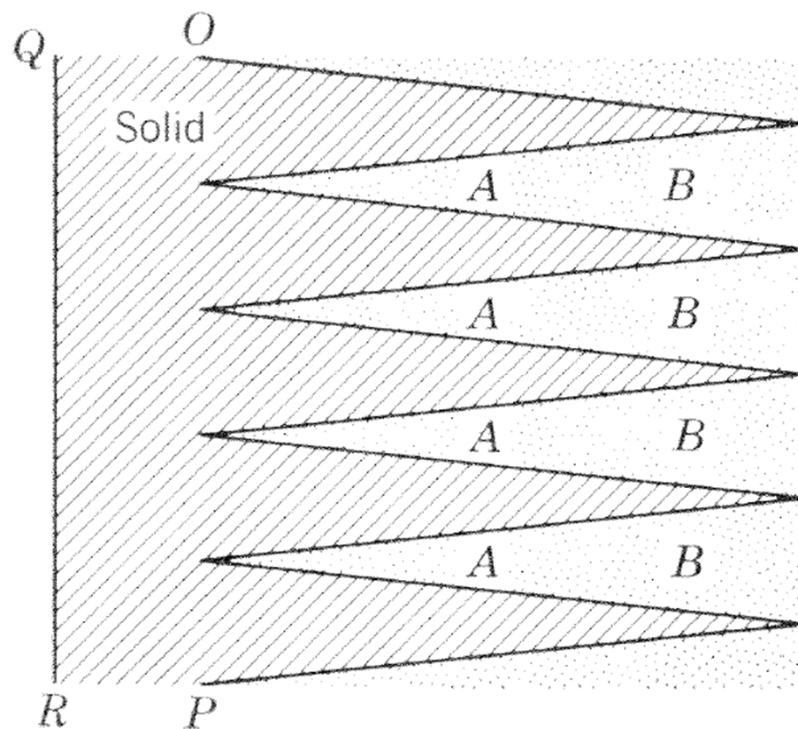


Fig. 5.50. mechanism of inverse segregation

\* Left of OP line: completely solidified.

→ As the region AA solidify, shrinkage takes place, causing the solute enriched liquid at BB to move toward the left.

Liquid

\* The effect is larger than might be expected due to the highly enriched composition of the liquid in the terminal transient condition, i.e. when there is only a small amount remaining in a given region.

\* General validity of this theory : inverse segregation does not occur in alloys that expand on solidification.

## 5) Inverse segregation

\* Quantitative approach of inverse segregation (by Kirkaldy & Youdelis)

**(Assumption1) No shrinkage void → liquid: compensate completely for the shrinkage**

**(Assumption2) Liquid in the interdendritic region is always of uniform composition.**

**& it is always in equilibrium with the solid that has just been deposited on dendrite.**

**However, the dendrites are not of uniform composition, since they formed from a liquid of continuously changing composition.**

\* This theory describes an alloy system in which enrichment of the liquid is limited by a eutectic composition; the case considered by Kirkaldy and Youdelis was that of the Al-Cu system, of which the relevant part of the diagram is shown in Fig. 5.51.

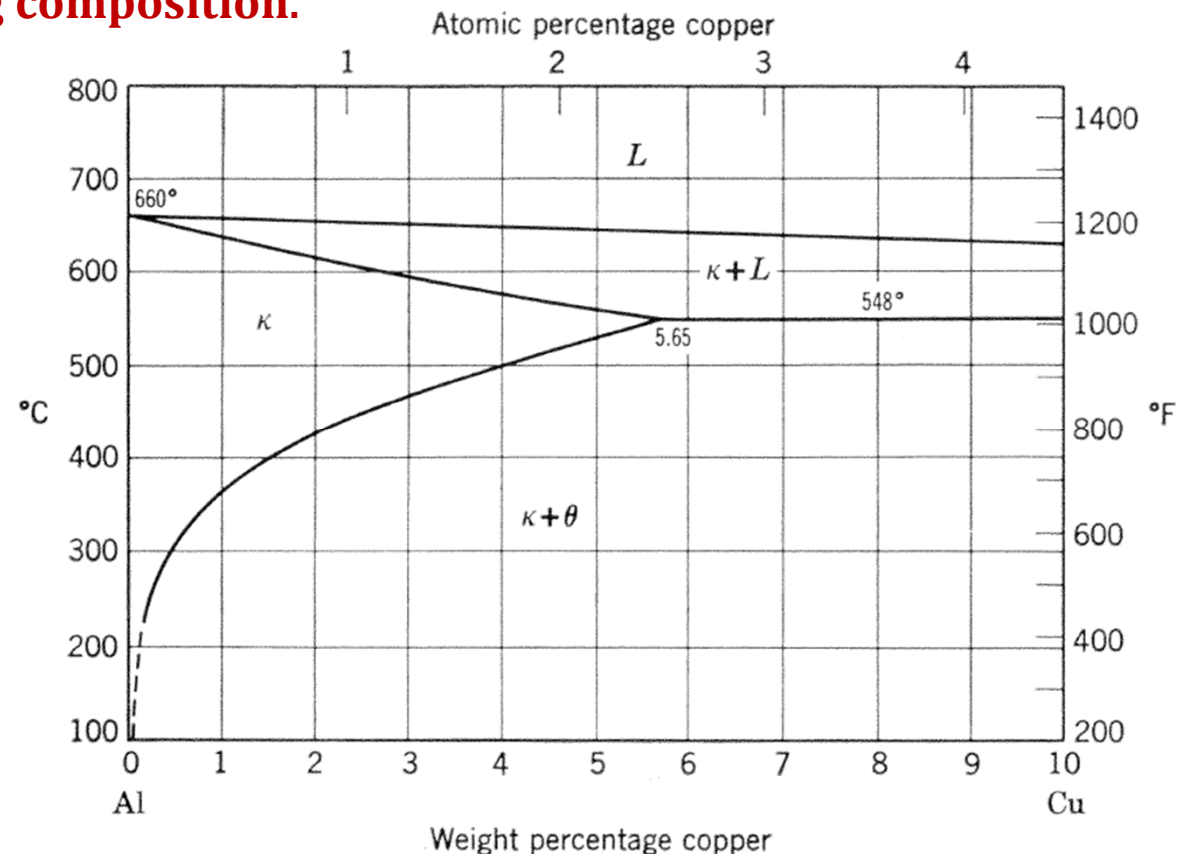


Fig. 5.51. Part of the phase diagram for the Cu-Al system.

**\* Good agreement btw theory and experiment in inverse segregation of Al-Cu alloy.**

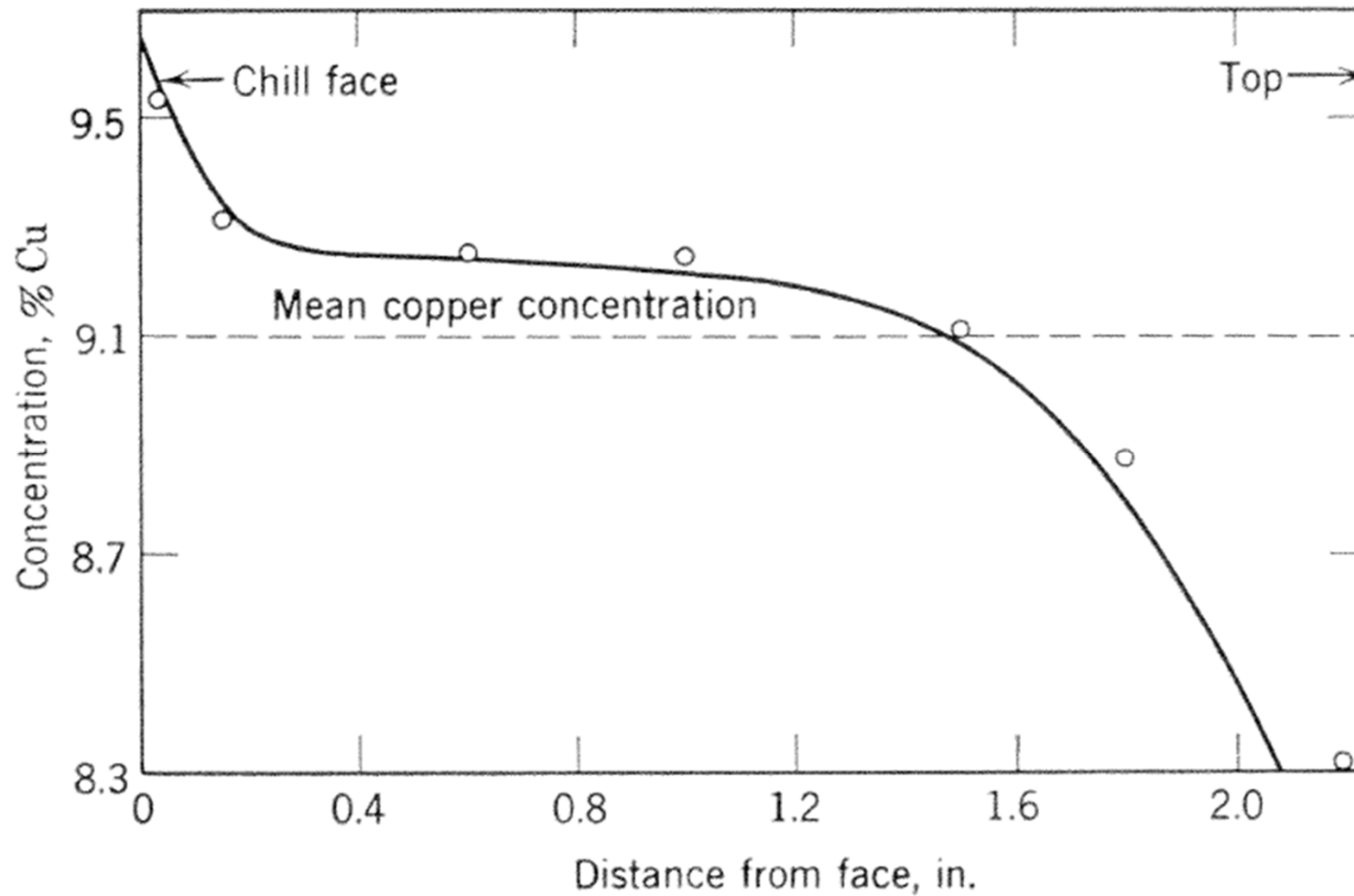


Fig. 5.52. Comparison between experimental and calculated inverse segregation in Al-Cu.

\* Case of Al-Zn system studied by Youdelis & Colton (Fig. 5.53)

: somewhat more complicated, because

- a) Assumption of constant  $k_0$  can no longer be regarded as correct,
- b) stepwise integration is used.

However, Fig. 5.54 shows good agreement btw experimental and calculated inverse segregation.

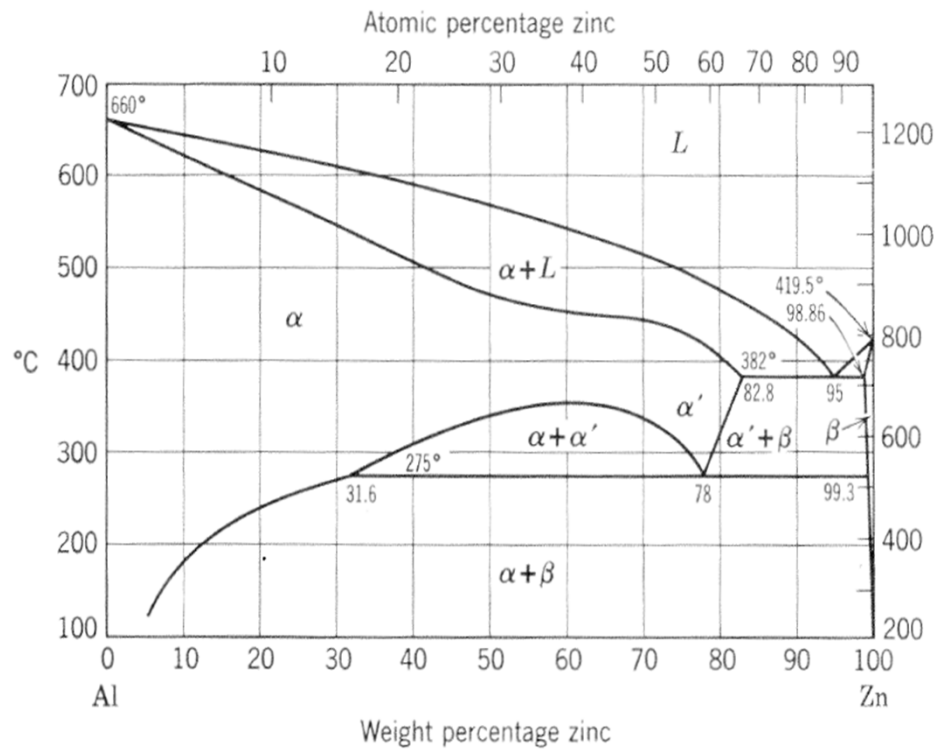


Fig. 5.53. Part of phase diagram for the Al-Zn system

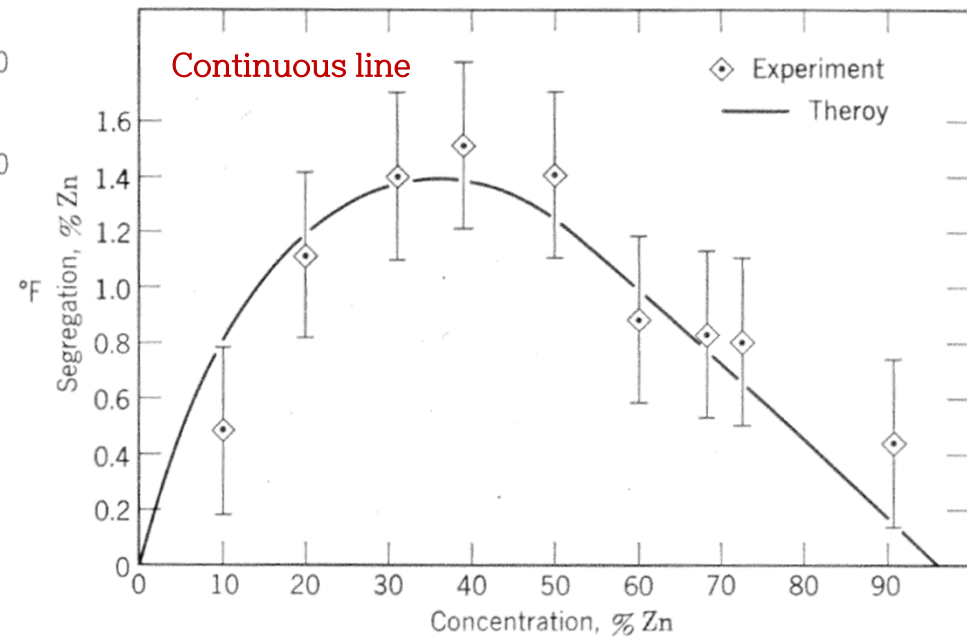
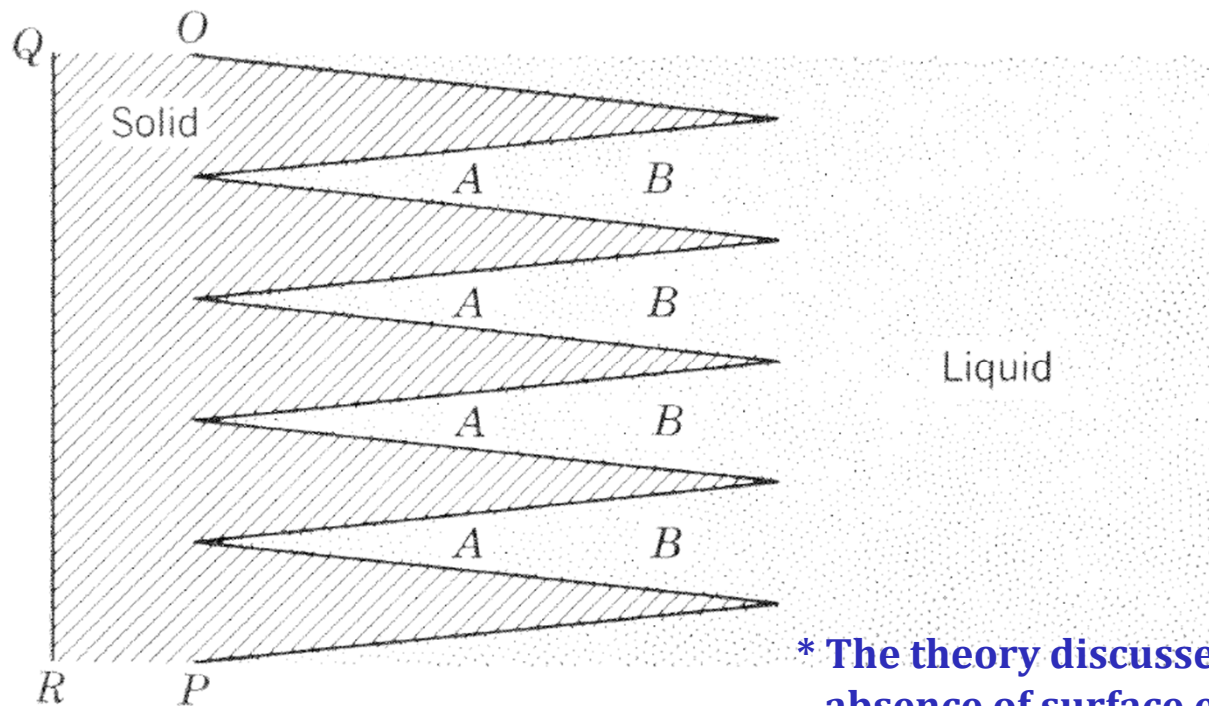


Fig. 5.54. Predicted and measured inverse segregation in Al-Zn

## 5) Inverse segregation

\* A much more drastic form of inverse segregation occurs when liquid is sucked out through the boundary **QR (the first region to solidify)** by a difference of the pressure arising from the separation of the metal from the mold.

→ The liquid which has exuded solidifies on surface of the metal btw it and the mold, in the form of small “drops”, known as “sweat”, which are usually much harder than the neighboring metal due to their high alloy content.



\* The theory discussed above assumes the absence of surface exudation.

Fig. 5.50. mechanism of inverse segregation

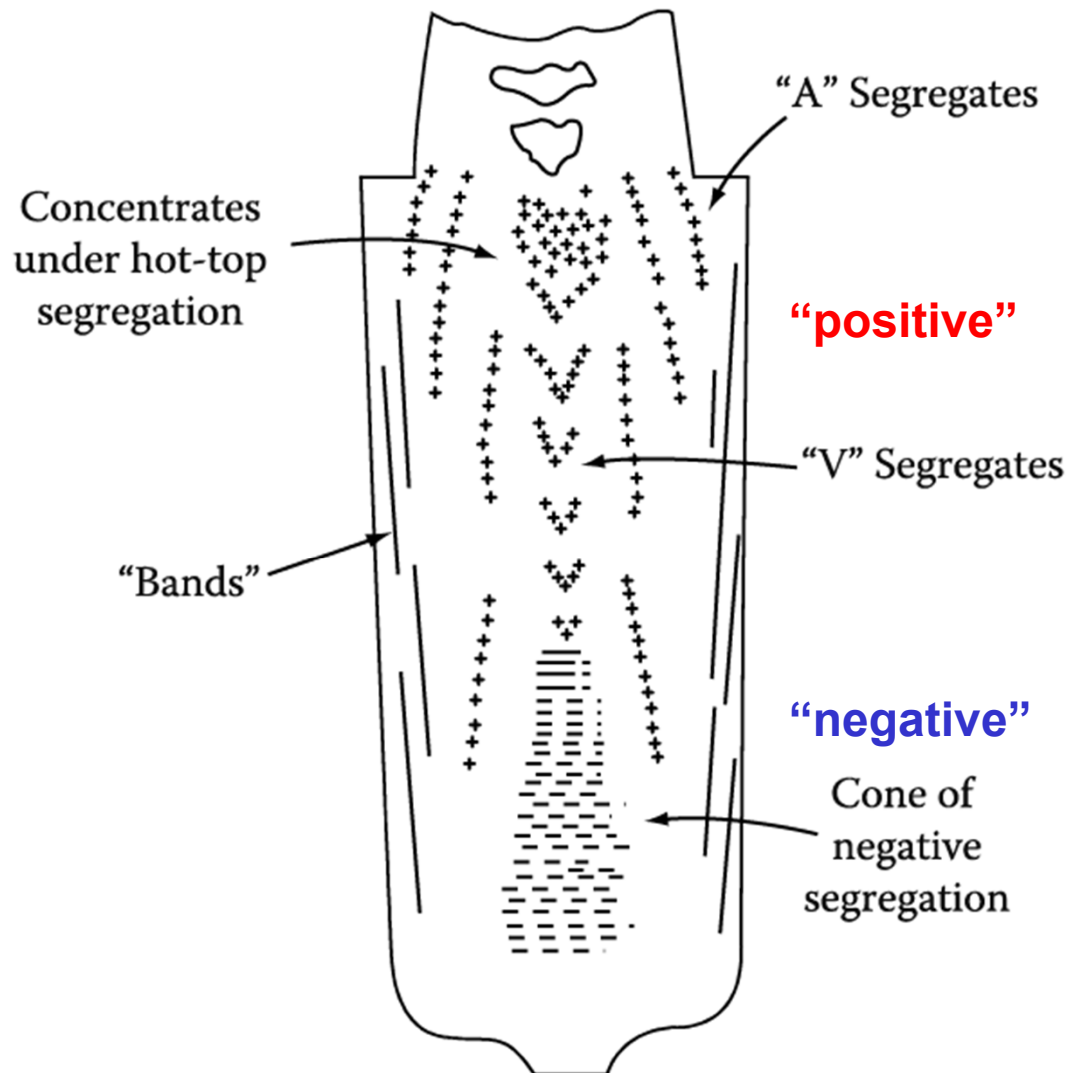
## 6) Coring and intercrystalline segregation

- \* The discussion of normal segregation was developed from a macroscopic point of view. → However, each crystal is likely to exhibit normal segregation on a microscopic scale; the earliest part of it to form has a lower concentration of solute (unless  $k_0 > 1$ ) than the later parts; "**Coring**", locally highest solute content
- found in the terminal regions where two or more crystals grow toward each other and finally form a grain boundary.

## 5. 10 Gravity segregation

- \* When the mass of liquid is sufficiently large, convection causes motion of the solute away from the limit of the boundary layer.
  - If **solute changes the density of the liquid**, it may set up a convection current that carries it toward the top or the bottom of the space in which the liquid can move.
- \* This is a type of **transverse segregation** that is much more significant in large, real system than in the idealized ones discussed in this chapter.

- \* **Segregation:** undesirable ~ deleterious effects on mechanical properties
  - subsequent **homogenization heat treatment**, but diffusion in the solid far too slow
  - **good control of the solidification process**



**Inverse segregation:** As the columnar dendrites thicken solute-rich liquid (assuming  $k < 1$ ) must flow back between the dendrites to **compensate for (a) shrinkage** and this raises the solute content of the outer parts of the ingot relative to the center.

EX) Al-Cu and Cu-Sn alloys with a wide freezing range (relatively low  $k$ )

**Negative segregation:** The solid is usually denser than the liquid and sinks carrying with it less solute (initially solidified one) than the bulk composition (assuming  $k < 1$ ). This can, therefore, lead to a region of negative segregation near the bottom of the ingot. ((b) Gravity effects)

Fig. 4.43 Segregation pattern in a large killed steel ingot. + positive, - negative segregation. (After M.C. Flemings, Scandinavian Journal of Metallurgy 5 (1976) 1.) 26

**Two of the most important application of solidification :  
“Casting” and “Weld solidification”**

**Q: What kinds of ingot structure exist?**

### **Ingot Structure**

- **Chill zone**
- **Columnar zone**
- **Equiaxed zone**

# \* Solidification of **Ingots** and **Castings**

*a lump of metal, usually shaped like a brick.*

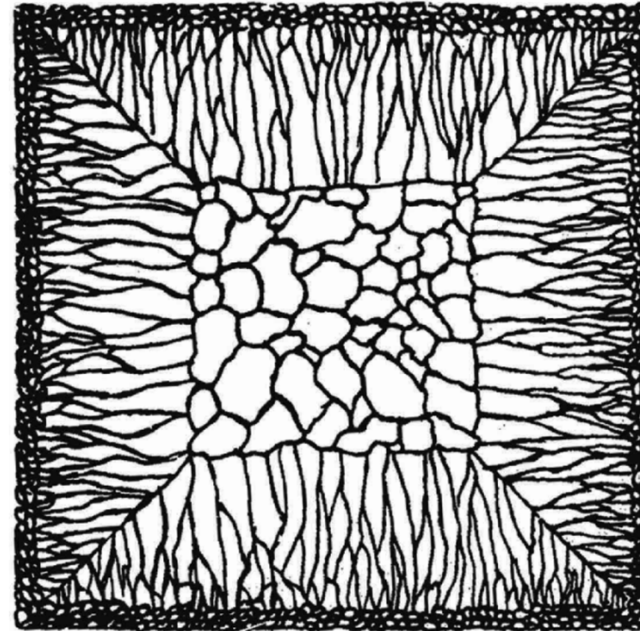
Later to be worked, e.g. by rolling, extrusion or forging >> blank (small)

*an object or piece of machinery which has been made by pouring a liquid such as hot metal into a container*

Permitted to regain their shape afterwards, or reshaped by machining

## Ingot Structure

- **outer Chill zone**  
: equiaxed crystals
- **Columnar zone**  
: elongated or column-like grains
- **central Equiaxed zone**



## Chill zone

- **Solid nuclei form on the mould wall and begin to grow into the liquid.**
  - 1) **If the pouring temp. is low:** liquid~ rapidly cooled below the liquidus temp. → **big-bang nucleation** → **entirely equiaxed ingot structure**, no columnar zone
  - 2) **If the pouring temp. is high:** liquid~remain above the liquidus temp. for a long time → **majority of crystals~remelt under influence of the turbulent melt (“convection current”)** → **form the chill zone**

## Columnar zone

After pouring the **temperature gradient** at the mould walls **decreases** and the crystals in the chill zone grow dendritically in certain crystallographic directions, e.g. **<100>** in the case of cubic metals.

→ **grow fastest and outgrow less favorably oriented neighbors**

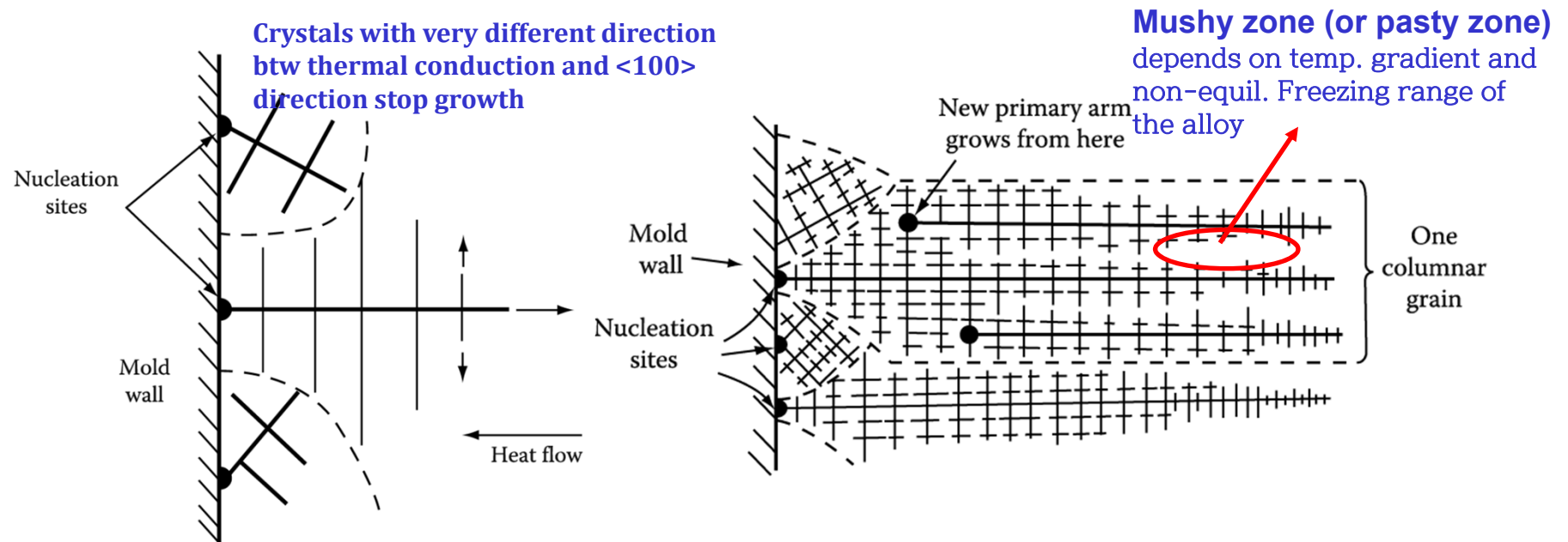


**Fig. 4.41 Competitive growth soon after pouring. Dendrites with primary arms normal to the mould wall, i.e. parallel to the maximum temperature gradient, outgrow less favorably oriented neighbors.**

**Fig. 4.42 Favorably oriented dendrites develop into columnar grains. Each columnar grain originates from the same heterogeneous nucleation site, but can contain many primary dendrite arms.**

- 1) In general, the secondary arms become coarser with distance behind the primary dendrite tips.
- 2) The primary and secondary dendrite arm spacing increase with increasing distance from the mold wall.  
( $\because$  a corresponding decrease in the cooling rate with time after pouring)

 **Mushy zone (or pasty zone)**  
depends on temp. gradient and non-equil. freezing range of the alloy

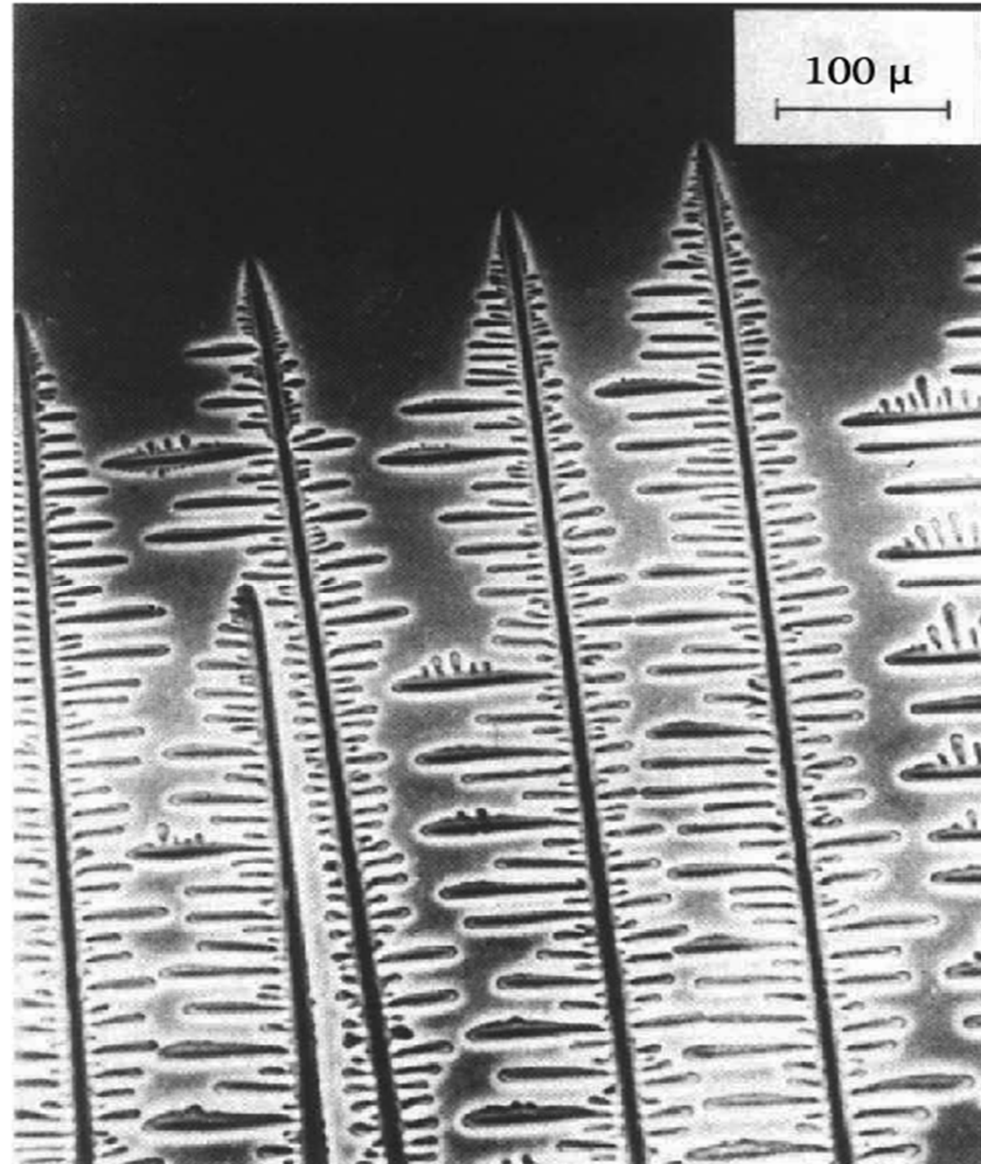


**Fig. 4.28 Columnar dendrites in a transparent organic alloy.**

(After K.A. Jackson in Solidification, American Society for Metals, 1971, p. 121.)

## Equiaxed zone

The equiaxed zone consists of **equiaxed grains randomly** oriented in the centre of the ingot. An important origin of these grains is thought to be **melted-off dendrite side-arms + convection current**

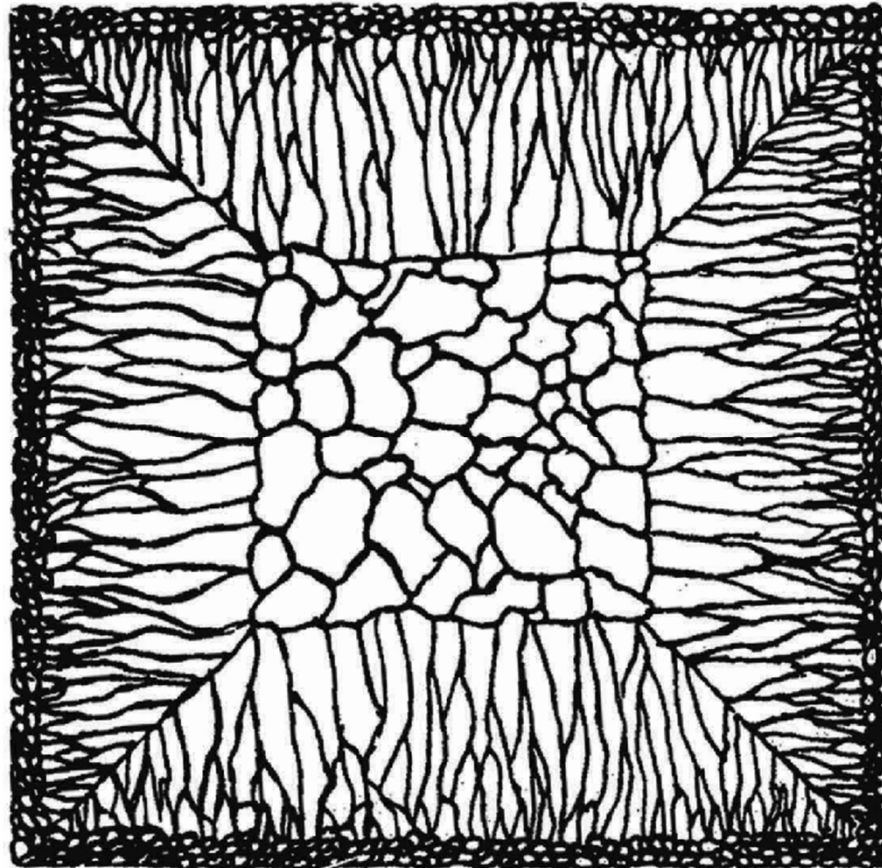
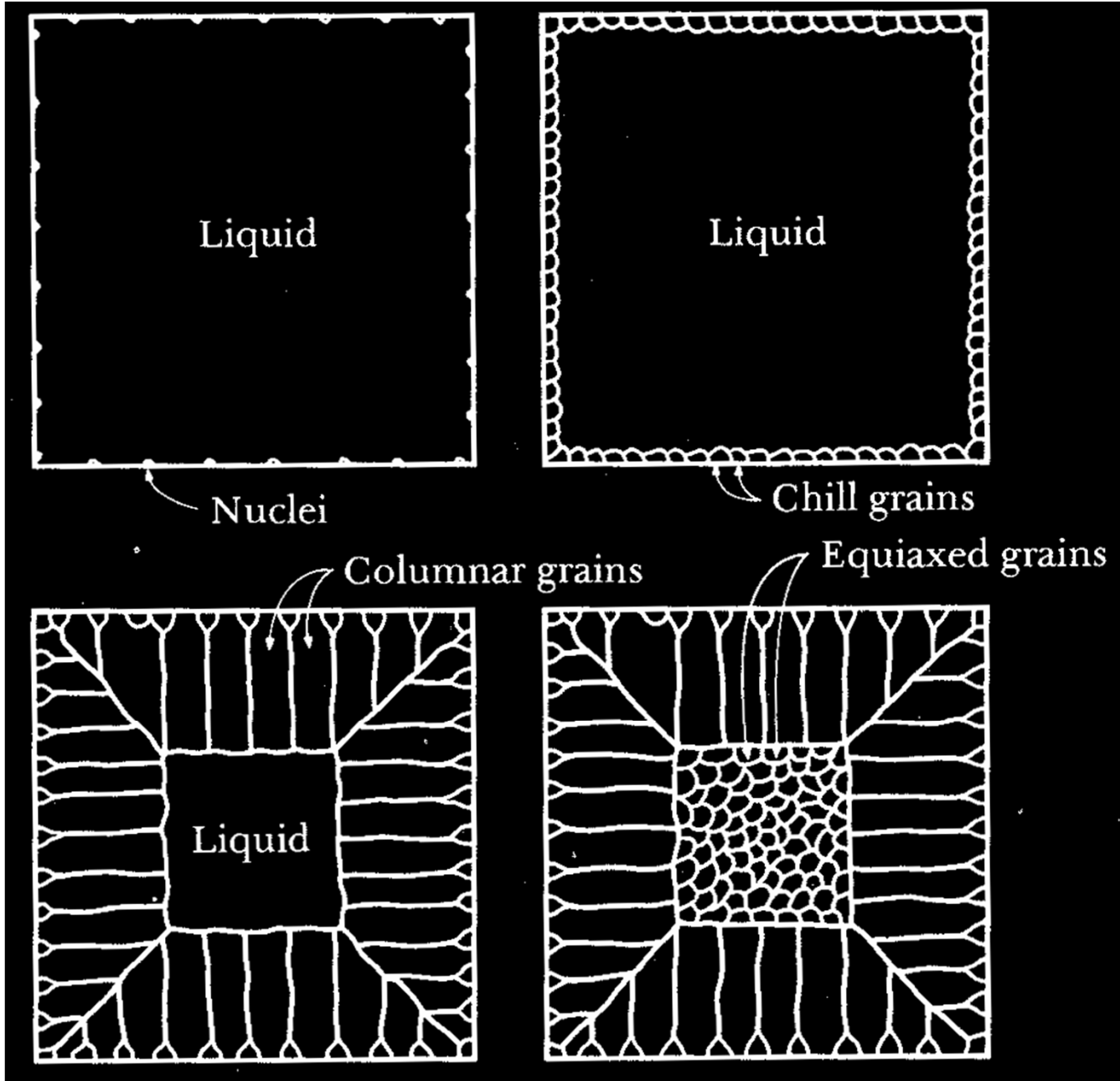


**Fig. 4.40 Schematic cast grain structure.**

(After M.C. Flemings, *Solidification Processing*, McGraw-Hill, New York, 1974.) 31



**Solidification of Pure Metal**

**: Thermal gradient dominant**



**Solidification of single phase alloy: Solute redistribution dominant**

**a) Constitutional Supercooling (C.S.)**

Planar	→ Cellular growth	→ cellular dendritic growth	→ Free dendritic growth
Thin zone formation by C.S. at the sol. Interface	Dome type tip / (surrounding) hexagonal array	T↓ → Increase of C.S. zone Pyramid shape of cell tip / Square array of branches / Growth direction change toward Dendrite growth direction	formed by releasing the latent heat from the growing crystal toward the supercooled liquid Dendrite growth direction/ Branched rod-type dendrite

→ “Nucleation of new crystal in liquid” which is at a higher temp. than the interface at which growth is taking place.

**b) Segregation**

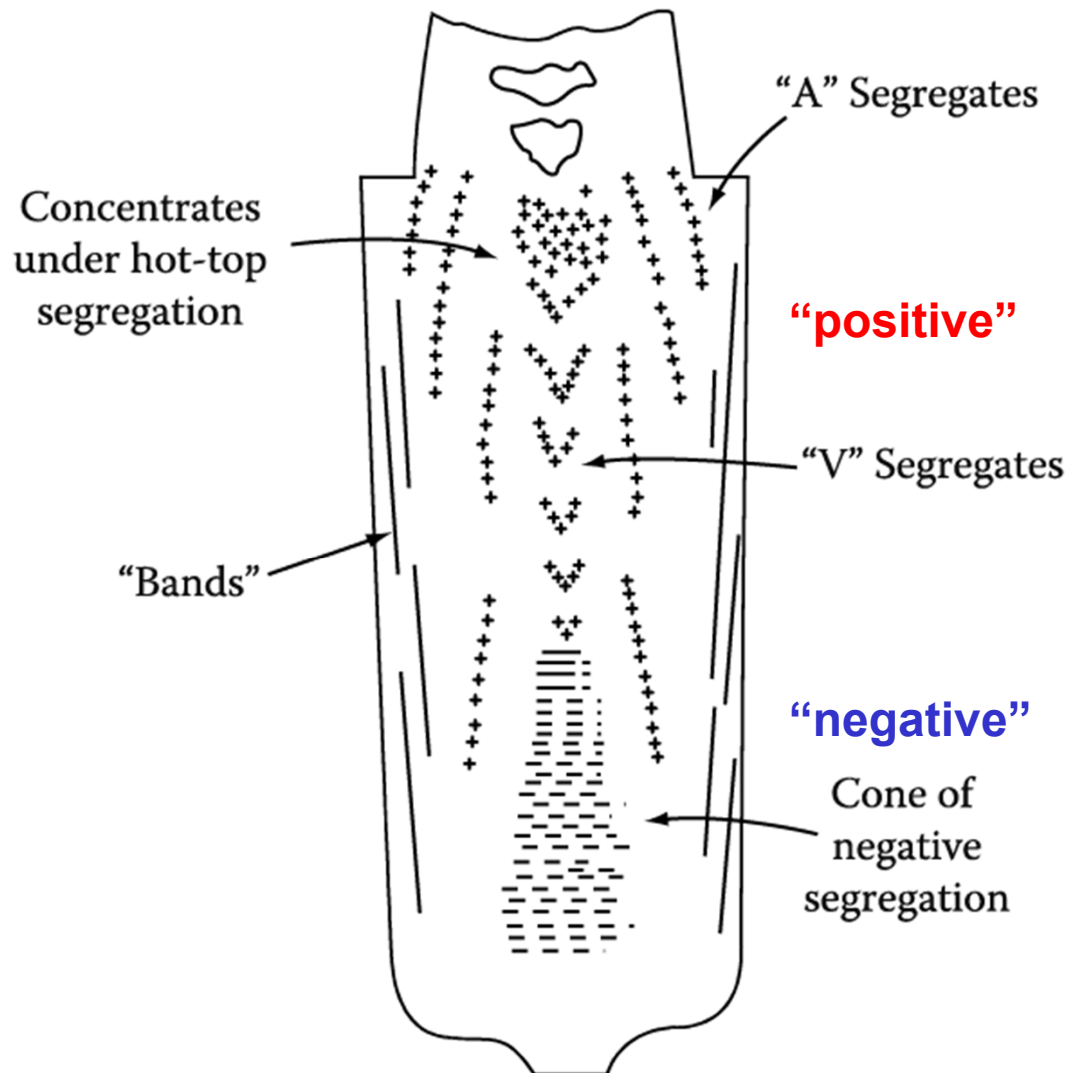
**: normal segregation, grain boundary segregation, cellular segregation, dendritic segregation, inverse segregation, coring and intercrystalline segregation, gravity segregation**

**: undesirable ~ deleterious effects on mechanical properties**

→ subsequent **homogenization heat treatment**, but diffusion in the solid far too slow

→ **good control of the solidification process**

- \* **Segregation:** undesirable ~ deleterious effects on mechanical properties
  - subsequent **homogenization heat treatment**, but diffusion in the solid far too slow
  - **good control of the solidification process**



**Inverse segregation:** As the columnar dendrites thicken solute-rich liquid (assuming  $k < 1$ ) must flow back between the dendrites to **compensate for (a) shrinkage** and this raises the solute content of the outer parts of the ingot relative to the center.

EX) Al-Cu and Cu-Sn alloys with a wide freezing range (relatively low  $k$ )

**Negative segregation:** The solid is usually denser than the liquid and sinks carrying with it less solute (**initially solidified one**) than the bulk composition (assuming  $k < 1$ ). This can, therefore, lead to a region of negative segregation near the bottom of the ingot. ((b) **Gravity effects**)

Fig. 4.43 Segregation pattern in a large killed steel ingot. + positive, - negative segregation. (After M.C. Flemings, Scandinavian Journal of Metallurgy 5 (1976) 1.) 34

## \* Solidification of **Ingots** and **Castings**

*a lump of metal, usually shaped like a brick.*

Later to be worked, e.g. by rolling, extrusion or forging >> blank (small)

*an object or piece of machinery which has been made by pouring a liquid such as hot metal into a container*

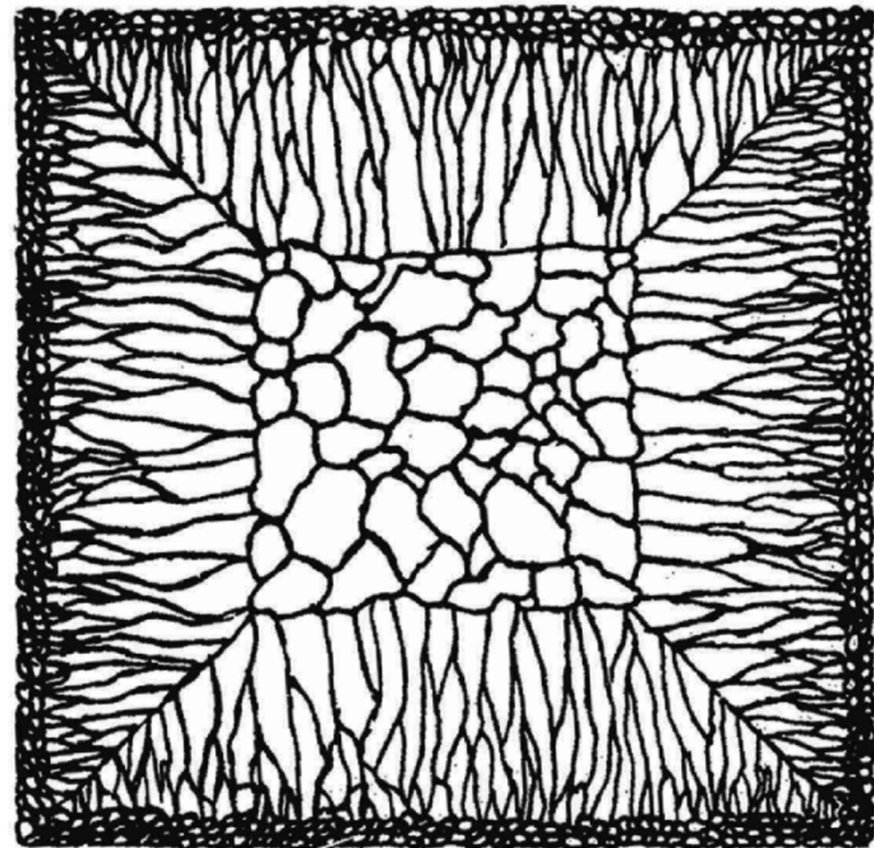
Permitted to regain their shape afterwards, or reshaped by machining

### Ingot Structure

- **outer Chill zone**  
: equiaxed crystals
- **Columnar zone**  
: elongated or column-like grains

**Mushy zone (or pasty zone)**  
depends on temp. gradient and non-equil.  
Freezing range of the alloy

- **central Equiaxed zone**



# Chapter 6 Polyphase solidification

\* Chapter 5 : discussion of the redistribution of solute during solidification was based on the implicit assumption that the whole of the solute could be accommodated in solution to a single solid phase.

However, many important cases more than one solid phase is formed

## Chapter 6 → Binary poly-phase solidification

### 6.1. Evolution of a Gas during solidification

#### (a) Gas-metal equilibria

- metallic system: ignore the pressure (except pressure appear to be relevant is for the consideration of nucleation under transient pressure resulting from cavitation, see Chapter 3) → However, when one of the phases is a gas (other than the vapor of the metal) the pressure has an important influence on the equilibrium relationships:  
Phase diagram with P, T, composition variables

→ However, it is seldom necessary to consider the phase diagram as a whole, because the variation in melting point or in the liquidus and solidus temperatures, due to the presence of the gas is **always small**, unless a new phase, such as a metal-gas compound is formed.

→ ∴ **The important characteristic of gas-metal system from the present point of view is the solubility of the gas in the metal (= the concentration of gas in solution in the solid or the liquid \_ pressure or partial pressure)**

## Chapter 6 Polyphase solidification

\* A diagram relating solubility with temperature for a single pressure (for example, a pressure of one atmosphere) will convey the significant information.

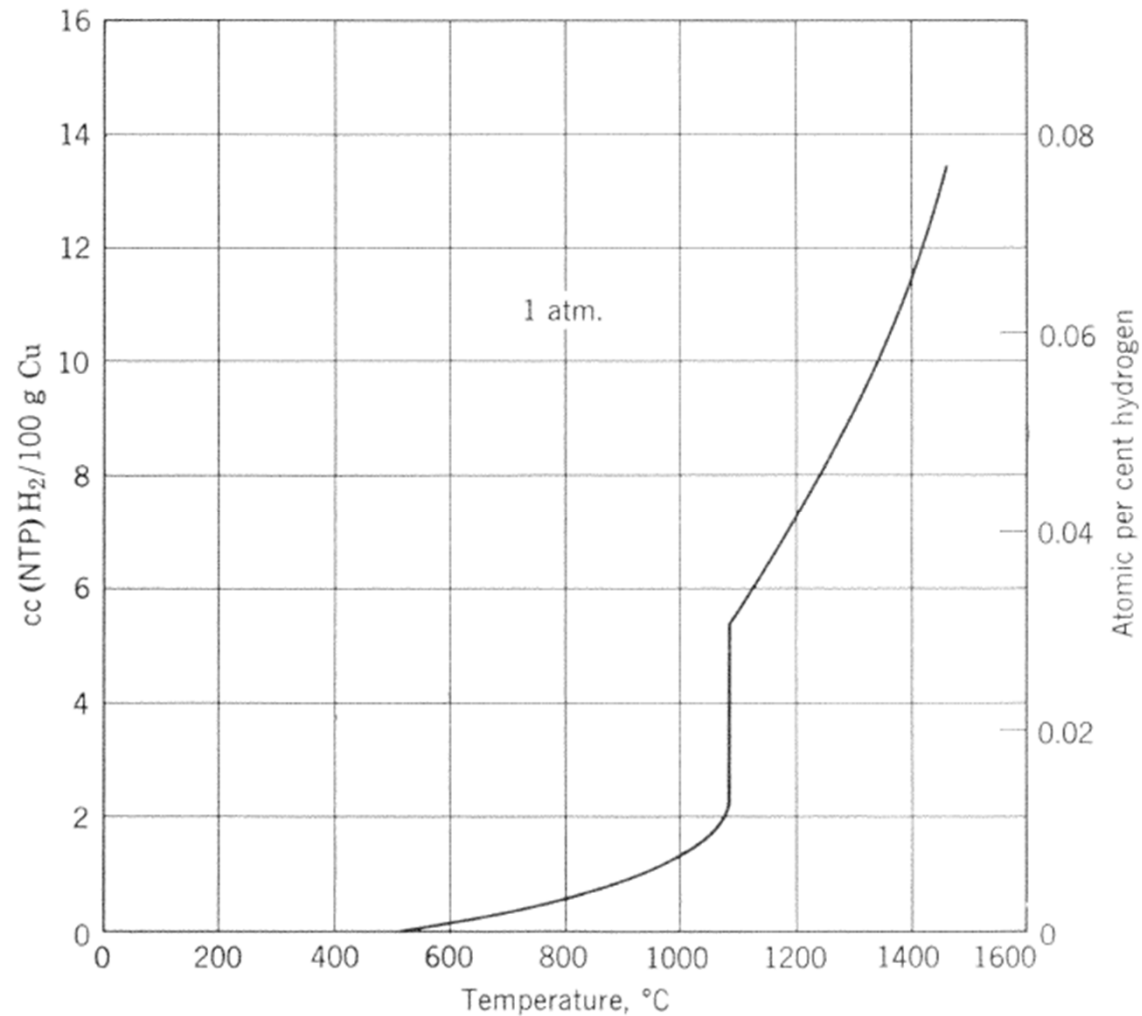


Fig. 6.1. Solubility of hydrogen in copper.

**\* A diagram relating solubility with temperature for a single pressure (for example, a pressure of one atmosphere) will convey the significant information.**

**A typical solubility diagram**

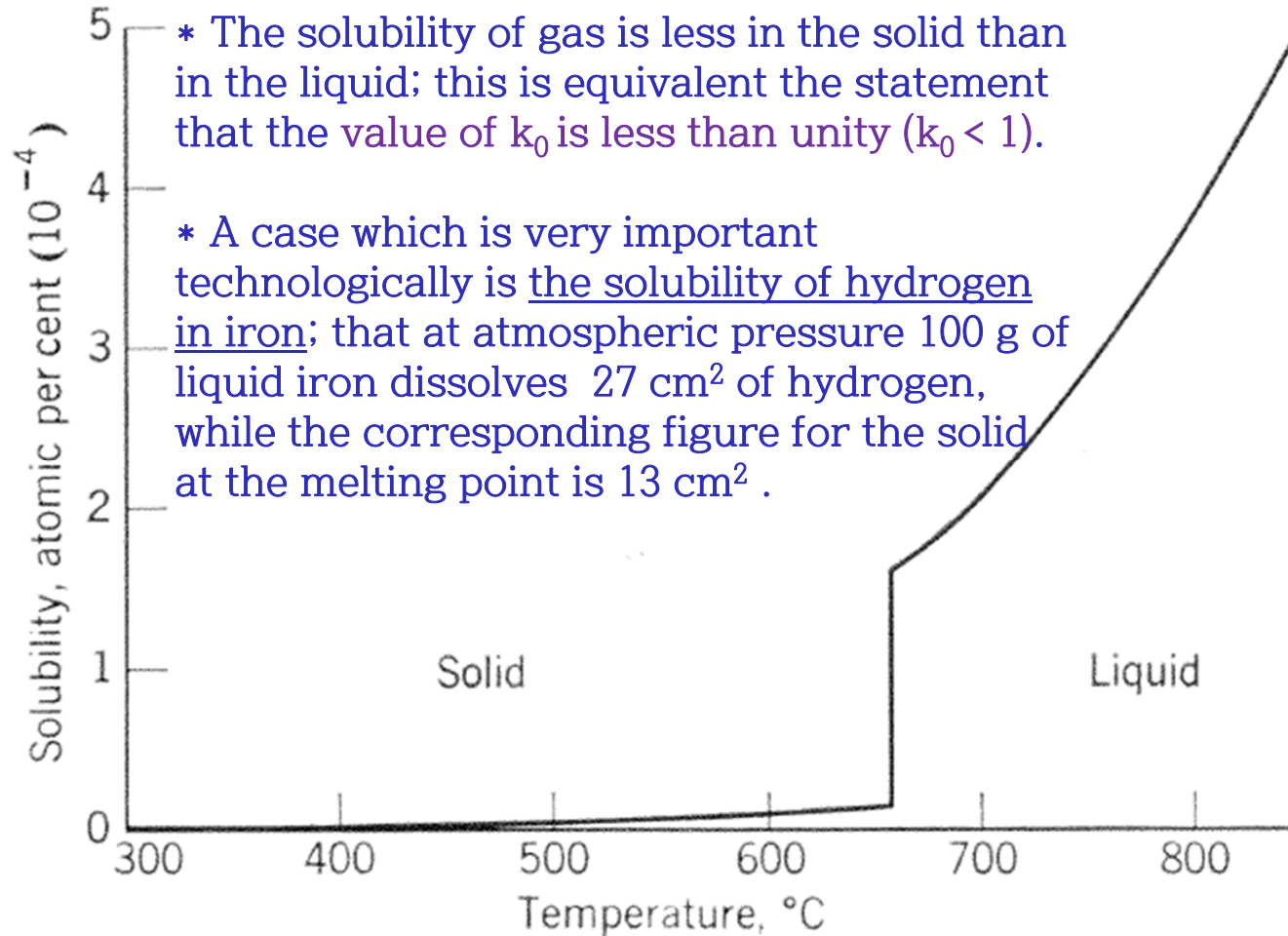


Fig. 6.2. Solubility of hydrogen in aluminum.

\* A diagram relating solubility with temperature for a single pressure (for example, a pressure of one atmosphere) will convey the significant information.

A typical solubility diagram

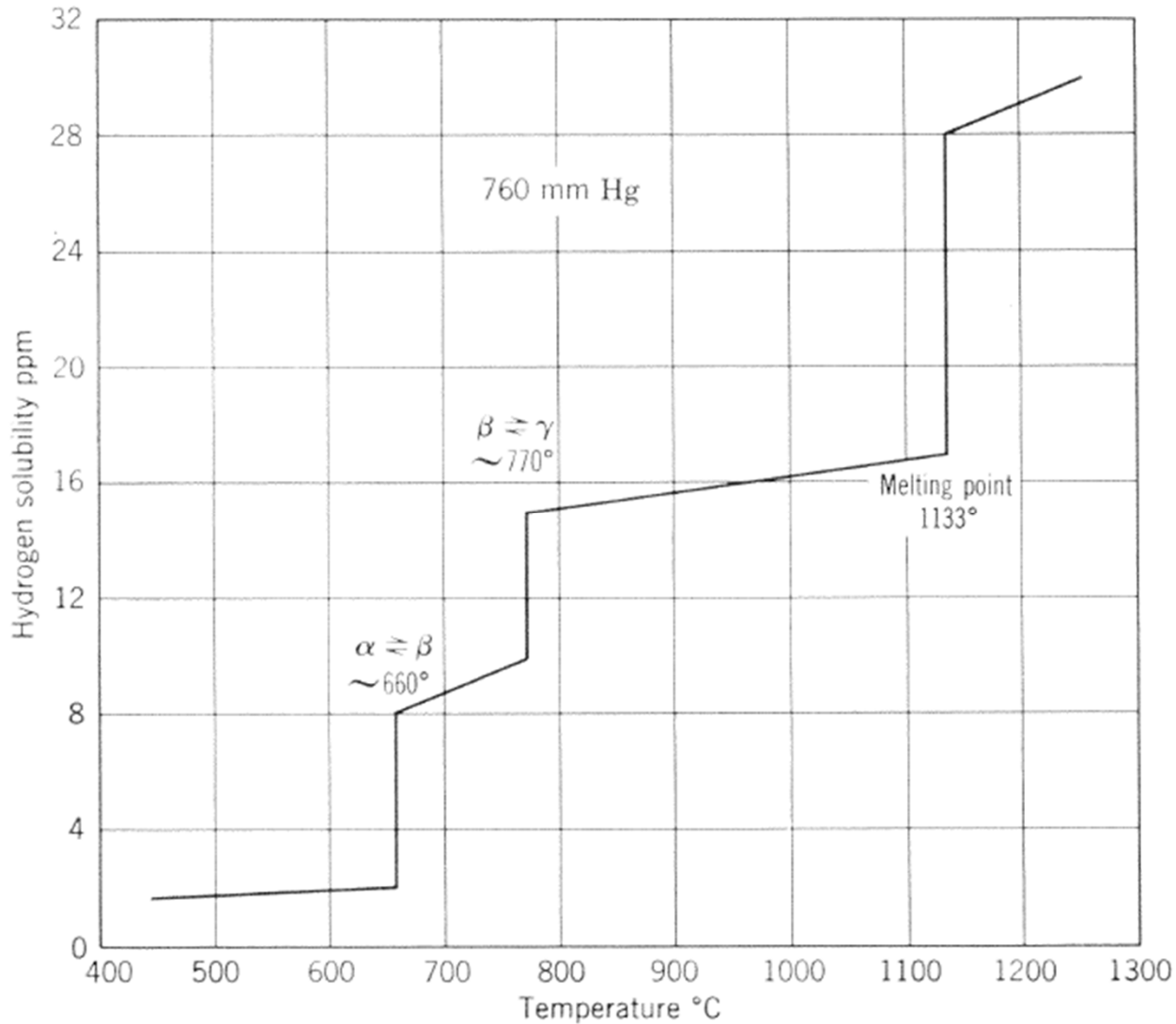


Fig. 6.3. Hydrogen-Uranium phase diagram.

## (b) Bubble formation

- When a metal or alloy containing a gas (such as Oxygen, Nitrogen or hydrogen) in solution solidifies, gas will be rejected at the interface, exactly in the same way as any other solute for which the  $k_0 < 1$ .

→ If the gas in the liquid was already saturated (i.e. if it was at the limit of solubility for the prevailing pressure at  $T_m$ ) then it becomes supersaturated as soon as an enriched layer begins to form at the interface. This means that there is more gas in solution than the equilibrium amount, as therefore there is a thermodynamic driving force tending to reduce the gas content.

→ The amount of gas in solution may decrease either by escape of the gas at a free surface, if one is accessible within the range in which the gas can diffuse in the liquid, or by the formation of a gas bubble in the liquid.

→ Formation of gas bubble requires homogeneous or heterogeneous nucleation :

“The condition for nucleation of a gas bubble is similar to that for nucleation of a solid phase, except that the effect of the pressure of the gas on its free energy must be considered.”

But , a solid-liquid interface should not be an effective nucleant for a bubble;

Equilibrium corresponds to  $\theta < 180^\circ$ ,

$$\sigma_{SL} = \sigma_{SG} + \sigma_{LG} \cos \theta$$

$$\cos \theta = \frac{\sigma_{SL} - \sigma_{SG}}{\sigma_{LG}}$$

$$\sigma_{SG} \gg \sigma_{SL} \text{ \& } \sigma_{SG} > \sigma_{LG}$$

$$\therefore \cos \theta < -1$$

→ Surface E of the bubble is increased by contact with the solid-liquid interface.

**However, gas bubbles are formed at solid-liquid interfaces.**

This location is in part due to the fact that the gas concentration would be highest there during solidification; but it may also be due to the fact that any re-entrant in the interface, such as a cell wall, grain boundary, or inter-dendritic space, would have an even higher gas content because of lateral segregation, as shown in Fig. 6.5.

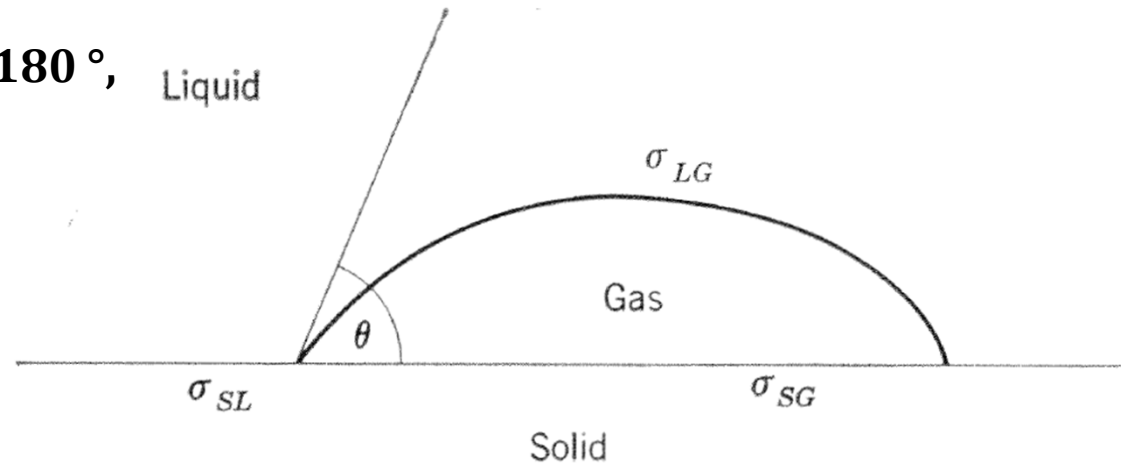
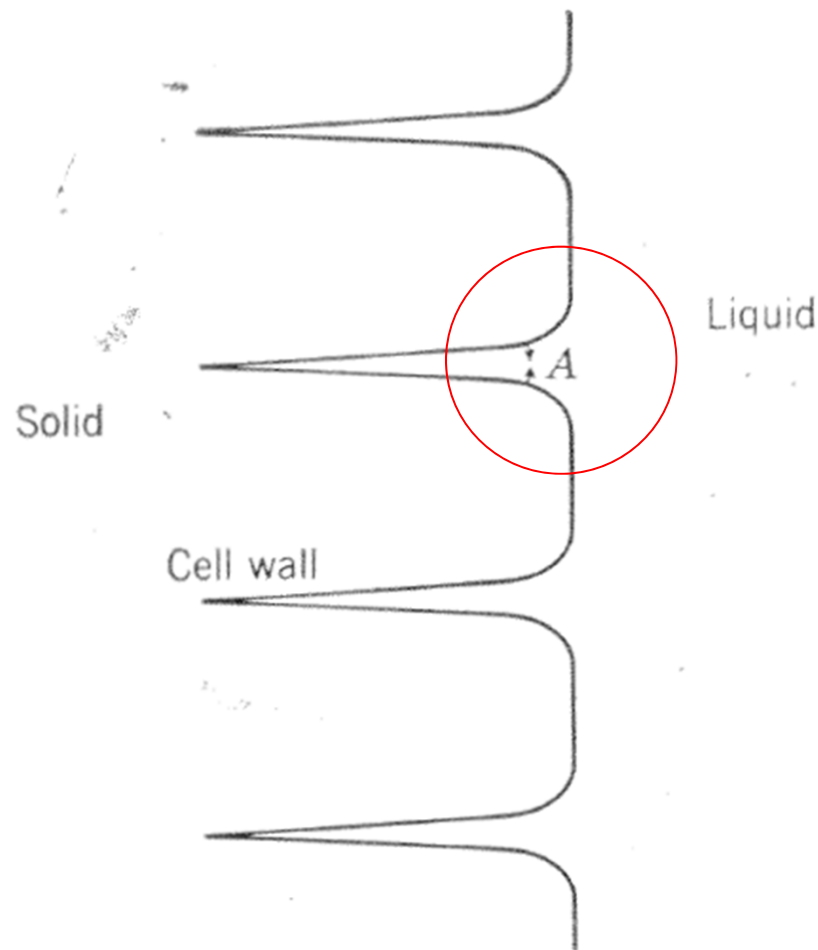


Fig. 6.4. Solid-liquid as nucleant for a gas bubble.

**\* gas bubbles are formed at solid-liquid interfaces.**

In detail, in regions such as A, the terminal transient condition is entered as the 2 walls approach each other; the concentration of solute (in this case, gas rises far above the  $C_0/k$  that would occur at a flat interface, and which might not be sufficient to cause nucleation of gas bubbles.



\* Experimental observations leave no doubt that gas bubbles are in fact nucleated during solidification, when transport of gas away from the interface by diffusion is not sufficiently fast, in terms of the rate of rejection at the interface, to hold the gas content below the nucleation level.

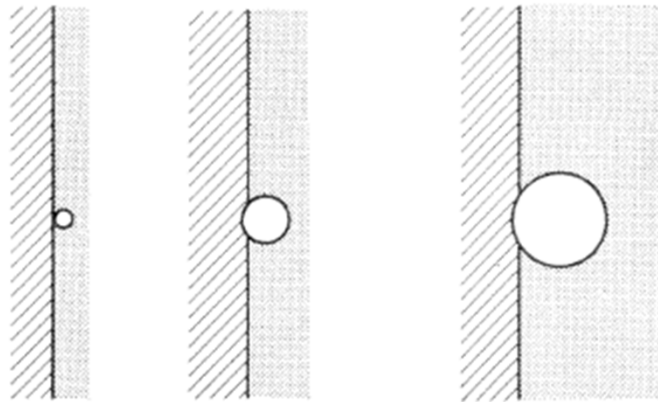
Fig. 6.5. Conditions for the nucleation of gas bubbles in cell wall.

**\* Subsequent behavior of bubble;**

depends upon whether they float away from the surface or remain attached.

- a) If a bubble escapes from the region where it was nucleated, it may float to the surface of the melt, or it may be trapped by other crystals, in which case its subsequent behavior is similar to that of a bubble that remained at its point of origin.
- b) If the bubble is trapped where it forms, it immediately becomes a “sink” into which gas from the neighboring supersaturated liquid can escape. This sets up a concentration gradient which causes gas to diffuse to the bubble from the surrounding liquid. The bubble there fore grows; but while it is doing so, the interface continues to advance.
- **The relative rates of growth of the bubble and of advance of the interface determine whether the bubble will increase in diameter, remain of constant diameter but increase in length, or be overgrown by the solid.**

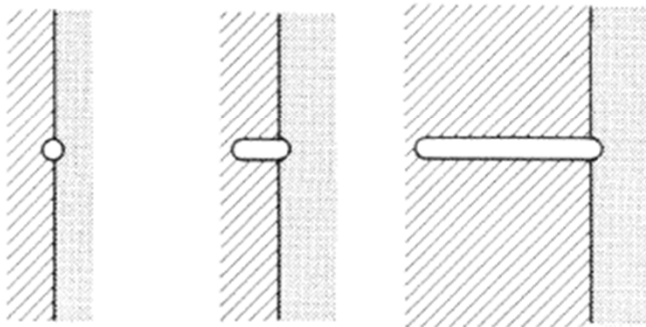
These three possibilities :



(a)

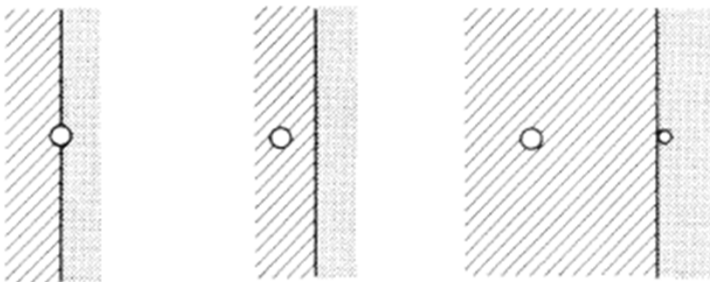
\* Growth rate of bubble > Advanced speed of interface  
 → increase of bubble diameter

The diameter of the bubble is maintained  
 in the longitudinal direction



(b)

\* Growth rate of bubble ~ Advanced speed of interface  
 → Bubble growth progresses in the longitudinal  
 direction while maintaining bubble diameter



(c)

\* Growth rate of bubble < Advanced speed of interface  
 → bubble are trapped in the solid.

Fig. 6.6. Effect of speed of growth of a bubble on its shape and size.  
 (a) Slow growth, (b) intermediate speed, (c) fast growth.

\* A bubble that starts by growing (Fig. 6.6a) may reach a size at which the conditions of Fig. 6.6b are satisfied, and a cylindrical bubble becomes stable. The stability of the cylindrical bubble at intermediate speeds, and its breakdown at high and at low speeds, has been demonstrated for water containing dissolved air.

\* Cylindrical type of bubble (=wormhole) can easily be seen in ice cubes produced by freezing water containing dissolved air; an example is shown in Fig. 6.7.

→ The bubbles do not nucleate until the ice has grown inward for a few millimeters; this is presumably distance required for the critical supersaturation to be produced.

\* Clear ice (=wormhole free ice) can be obtained by causing the water to flow continuously over the freezing interface. This prevents the concentration of dissolved air from reaching the critical level.

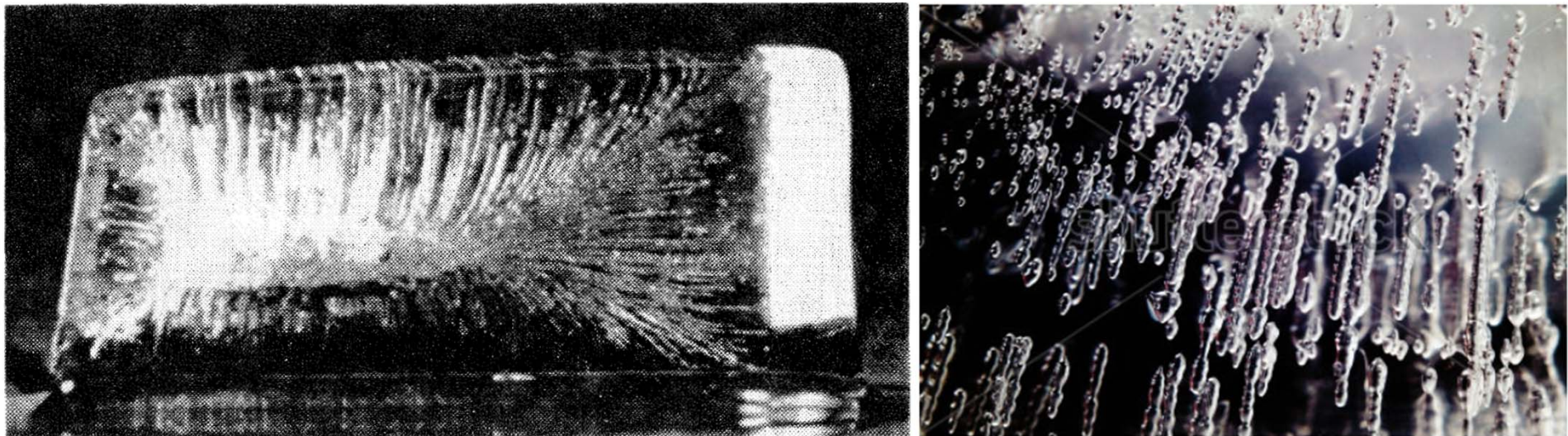


Fig. 6.7. Bubbles in ice cube

- **Growth of gas bubbles in a solidifying metal**

The process is essentially the same as in water. → The pressure at a point in a solidifying liquid may be lower than would be expected from purely hydrostatic conditions. In the extreme case, a region of liquid may be completely surrounded by solid. Further solidification, accompanied by decrease in volume, would rapidly decrease the pressure, leading to the nucleation of bubbles.

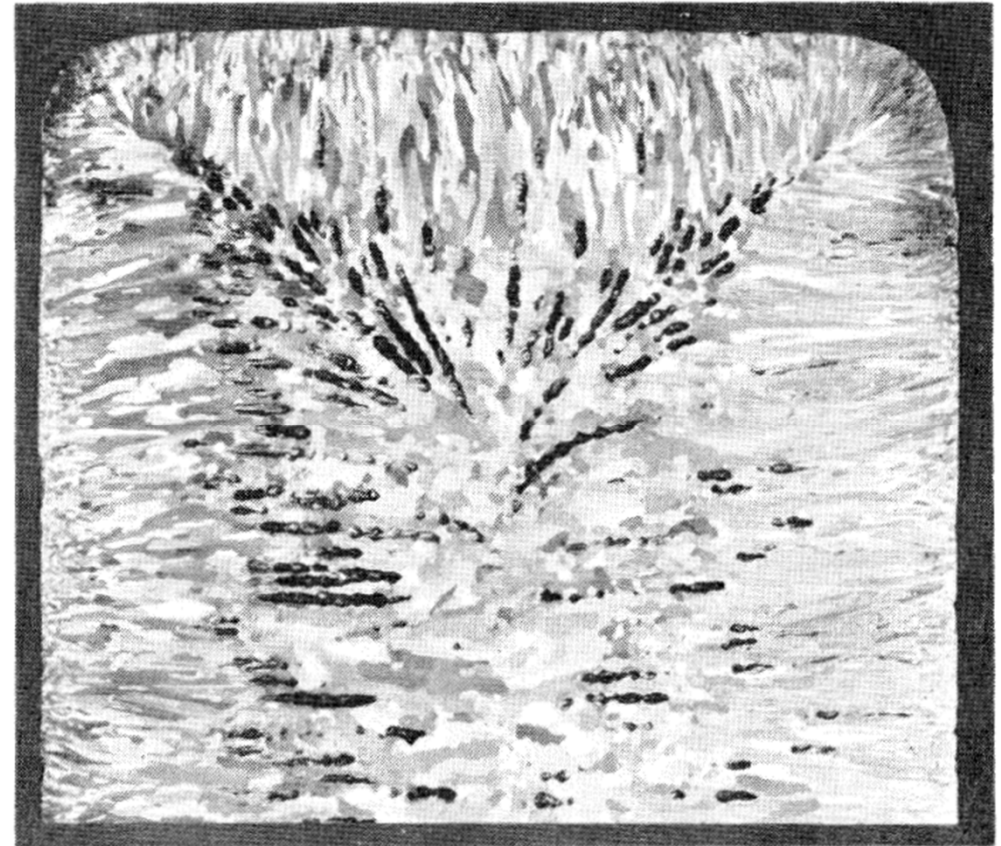


Fig. 6.8. Gas bubbles in a metal.

**(c) Formation of compounds by dissolved gases**

\* **A second possible effect of dissolved gases on solidification is that compounds, such as oxides, may be formed when the gas concentration reaches a high level, especially during the terminal transient stage of solidification.**

→ **Oxide and other inclusions that are often found at grain boundaries in cast metals may have been formed in this way, rather than being present in the liquid prior to solidification.**

## 6.2 Eutectics: limited solubility, most fusible (가장 잘 녹는, Greek)

\* Most of the discussion of eutectic solidification will be based on binary eutectic.

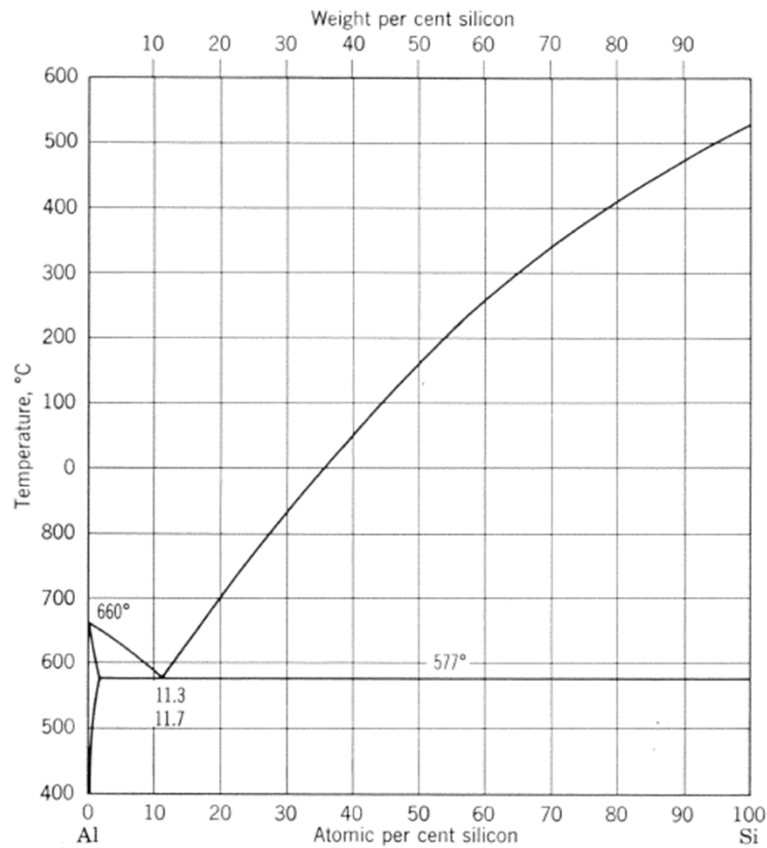


Fig. 6.9. Phase diagram for the Al-Si system

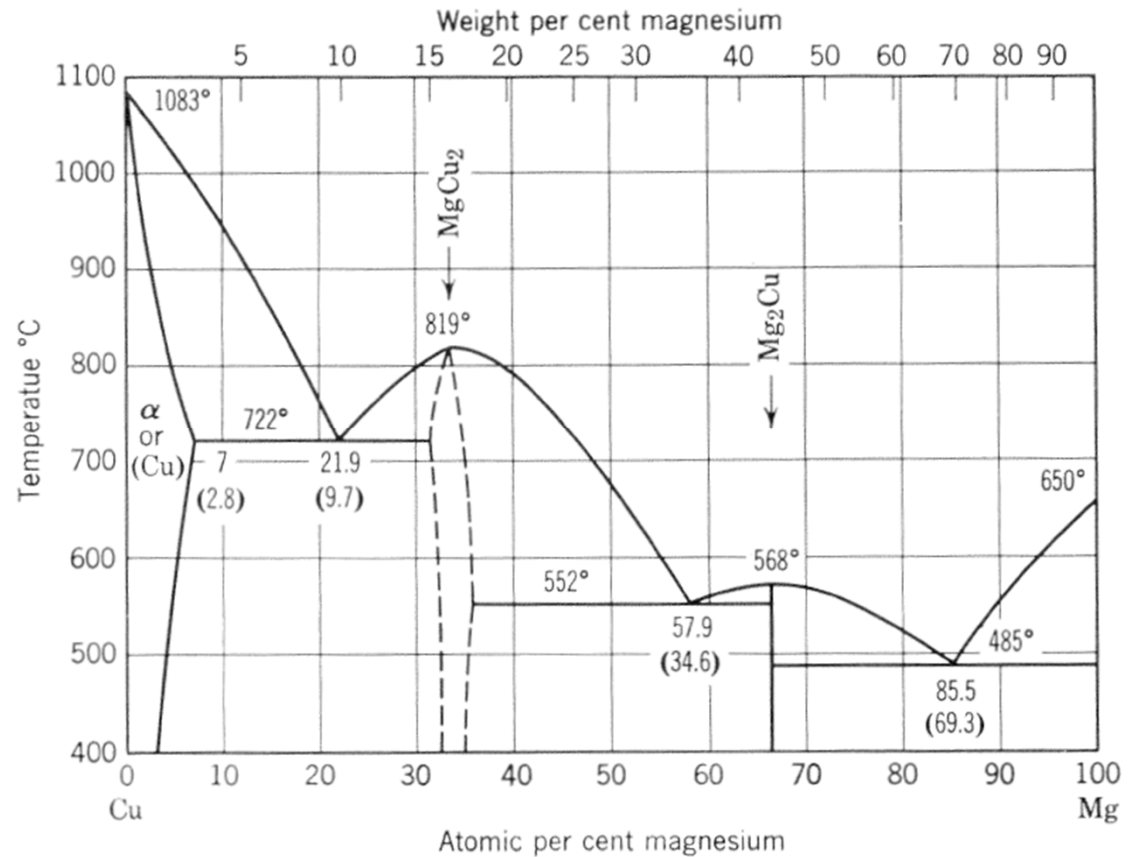


Fig. 6.10. Phase diagram for the Cu-Mg system

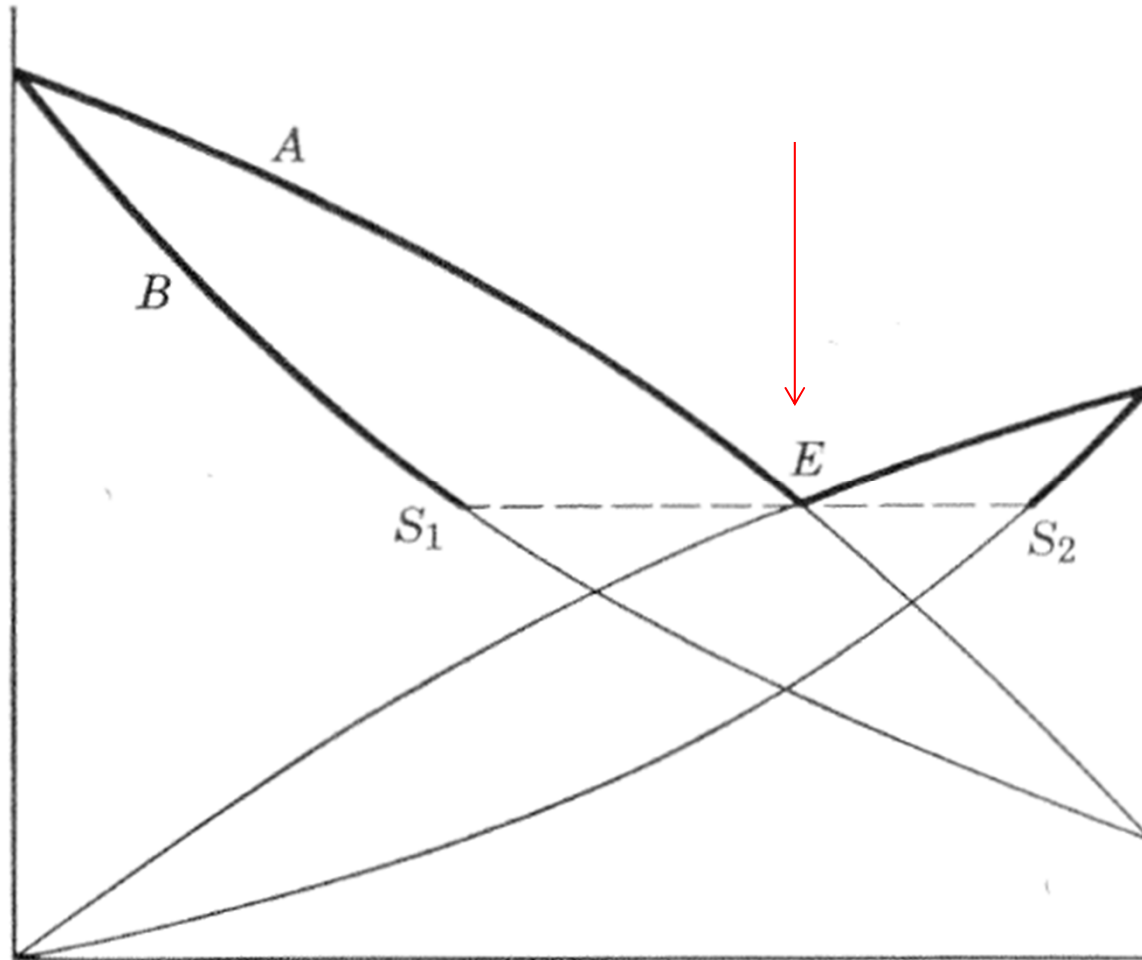


Fig. 6.11. Eutectic phase diagram

# \* Ternary eutectic system

: Minimum point of the liquidus surface

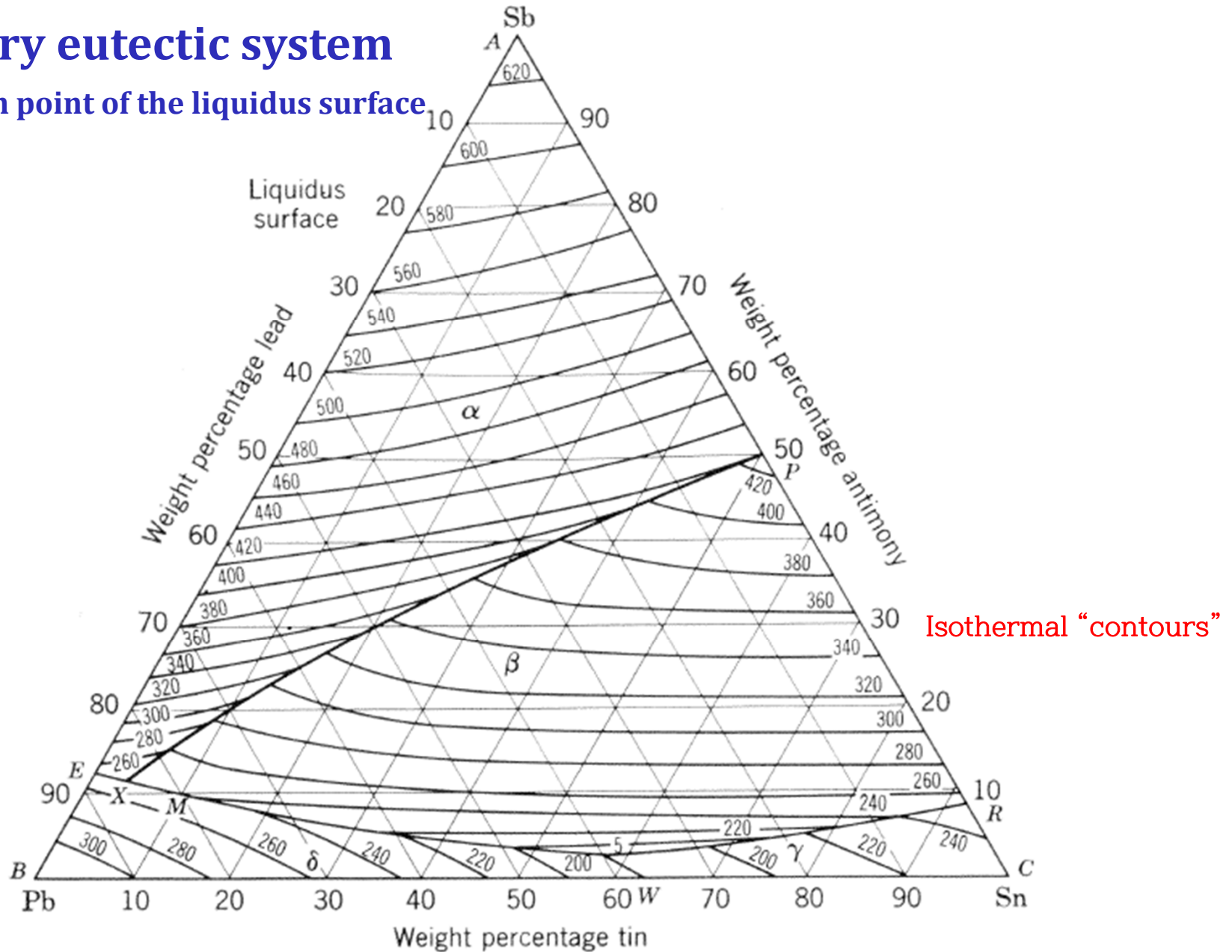
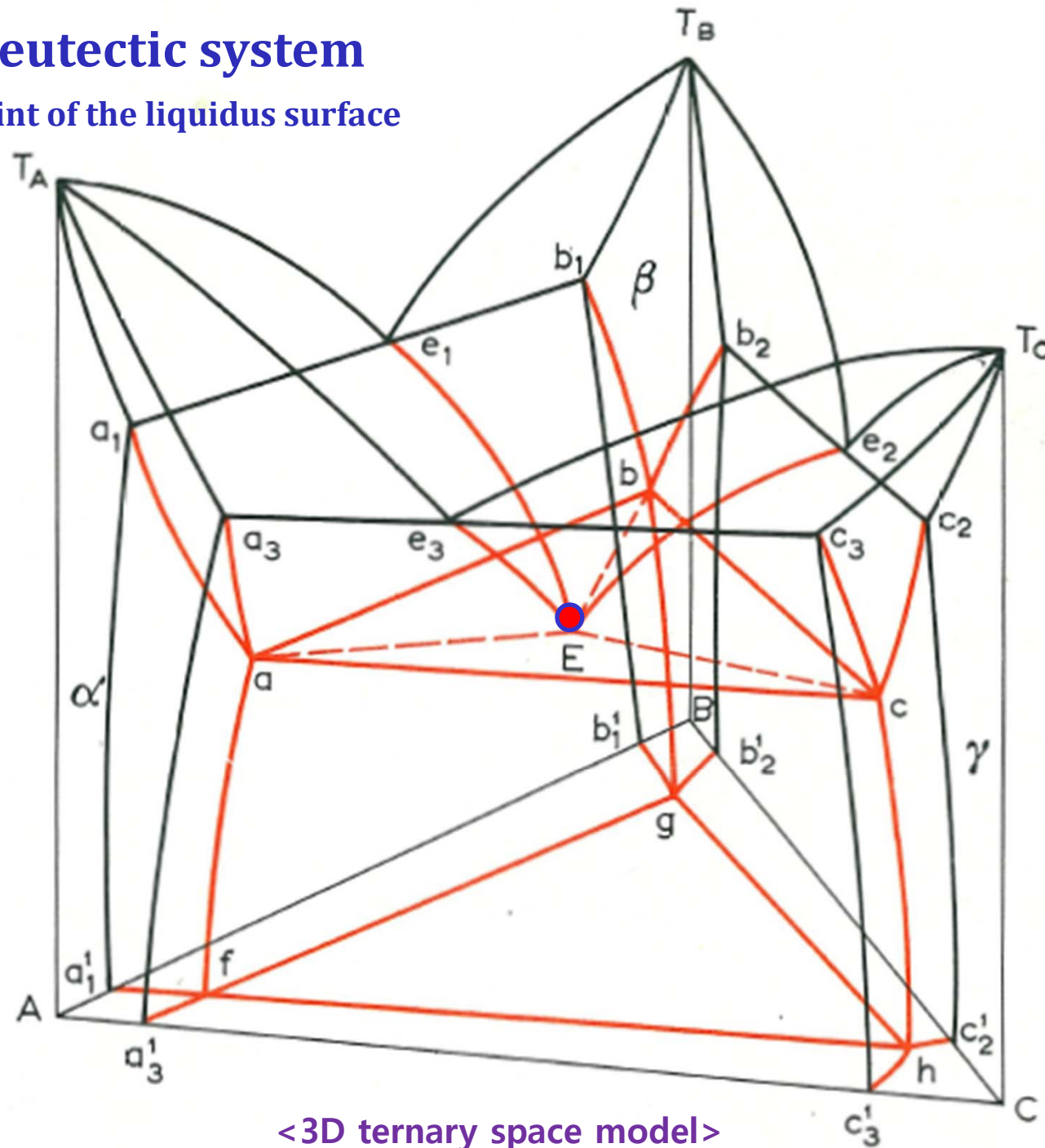


Fig. 6.12. The liquidus surface of the Pb-Sb-Sn system (X is the ternary eutectic point; liquidus temperature, 239 °C)

# \* Ternary eutectic system

: Minimum point of the liquidus surface

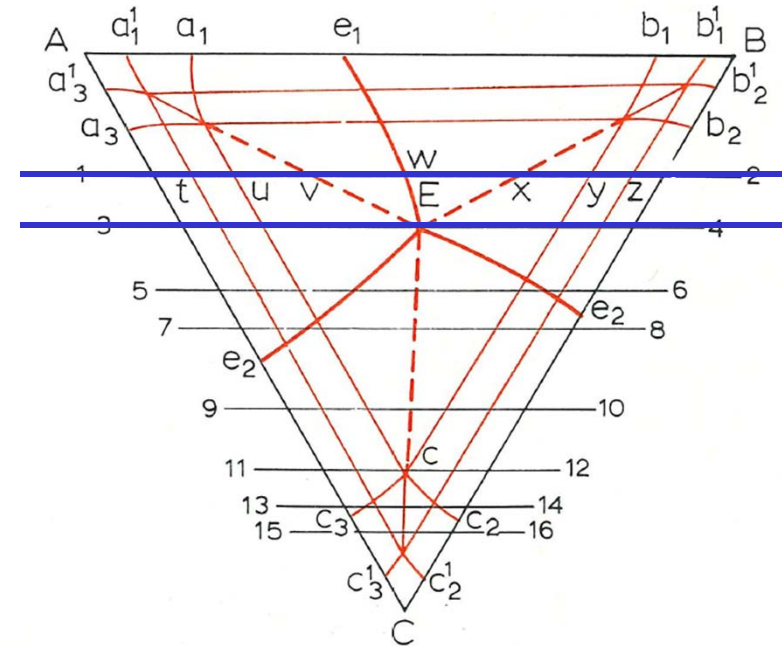


<3D ternary space model>

# \* Ternary eutectic system

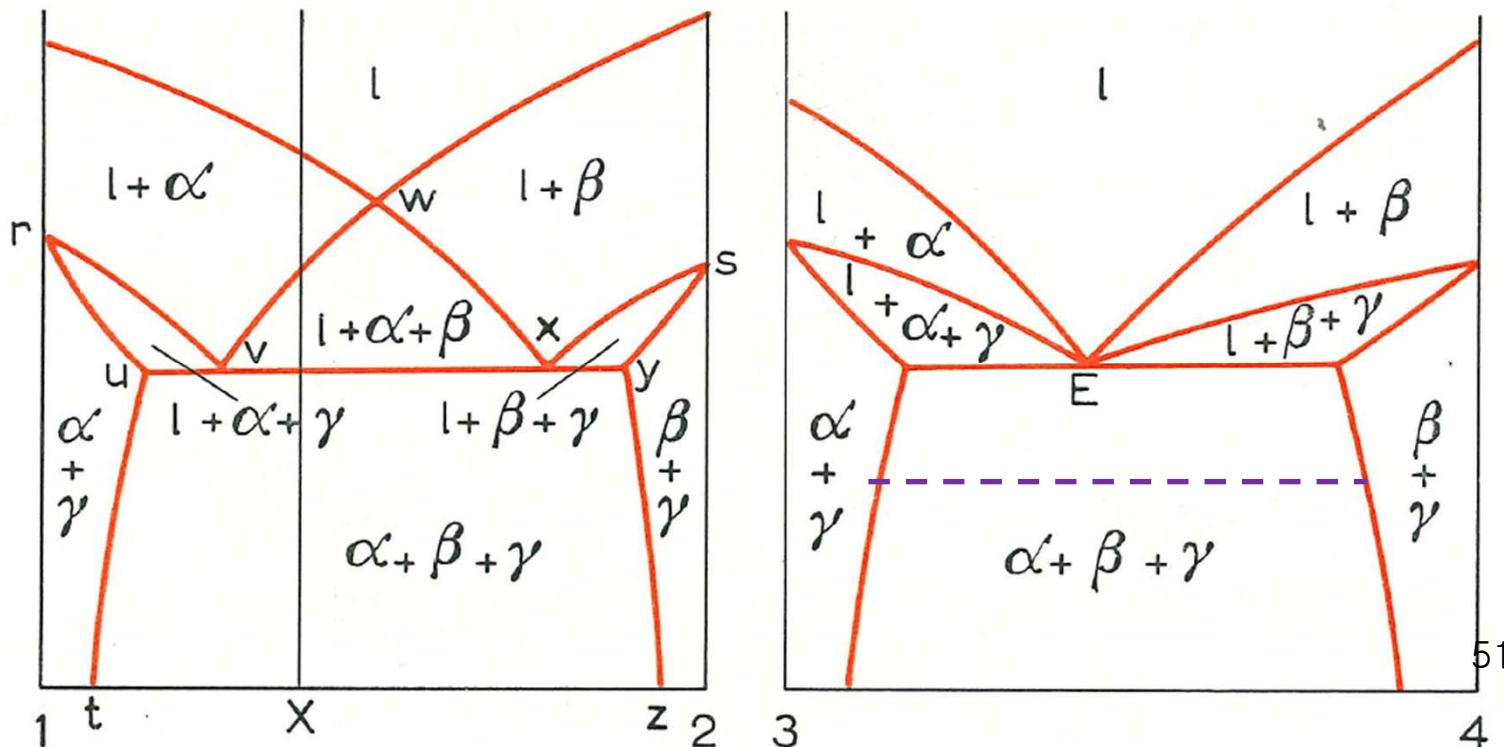
: Minimum point of the liquidus surface

Location of vertical section



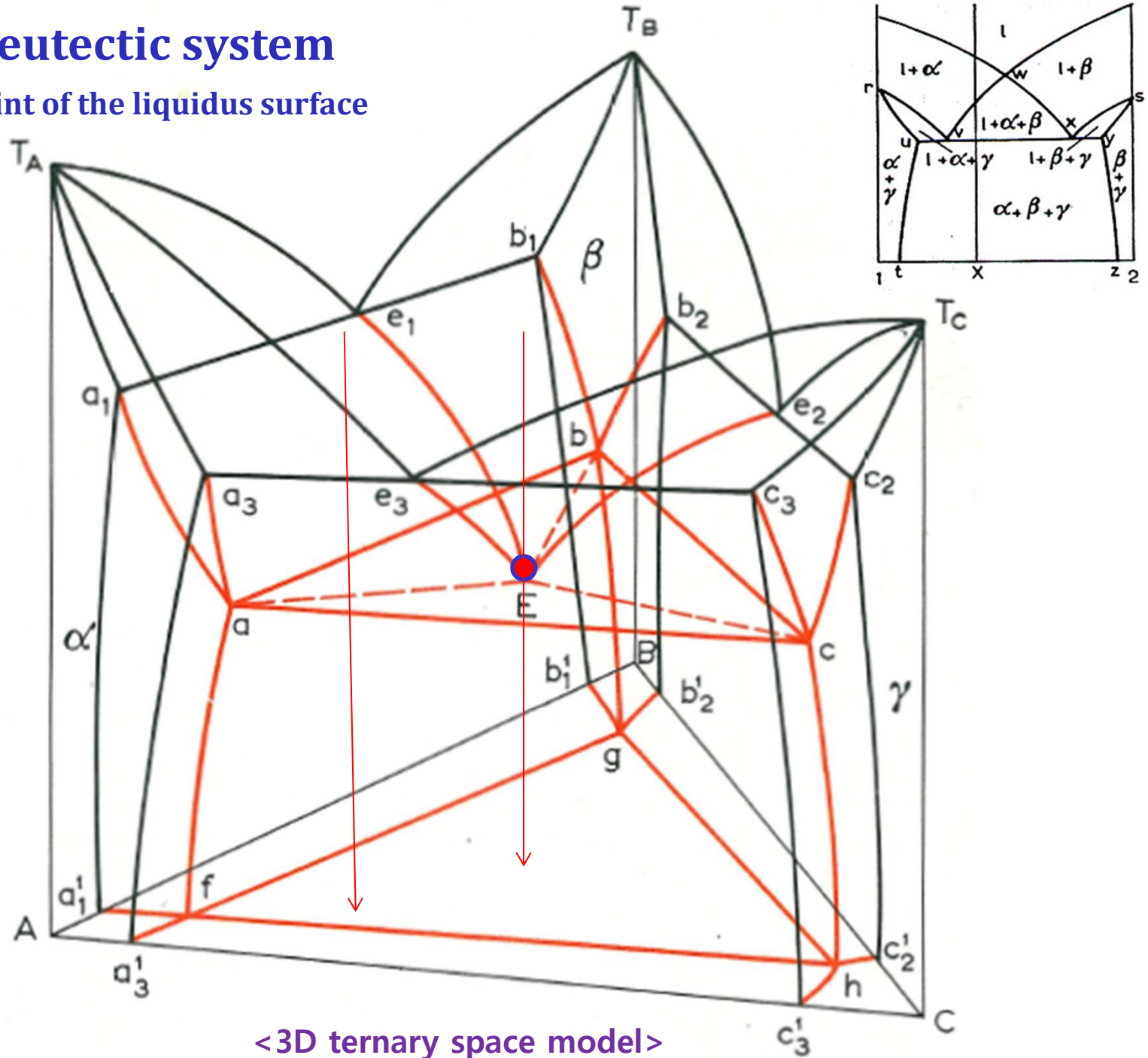
## \* Vertical section : Solidification Sequence

- \* The horizontal lines are not tie lines. (no compositional information)
- \* Information for equilibrium phases at different temperatures



# \* Ternary eutectic system

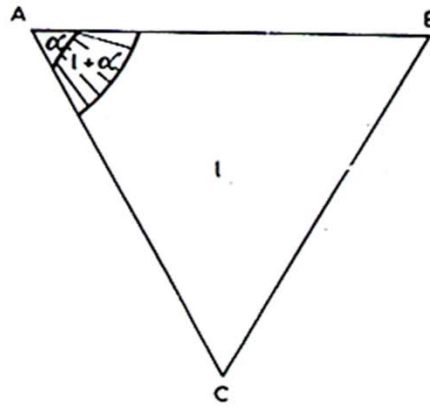
: Minimum point of the liquidus surface



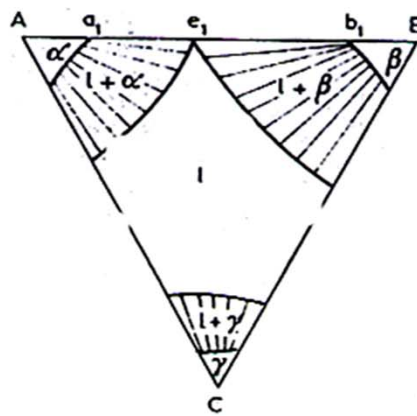
<3D ternary space model>

\* **THE EUTECTIC EQUILIBRIUM ( $l = \alpha + \beta + \gamma$ )**

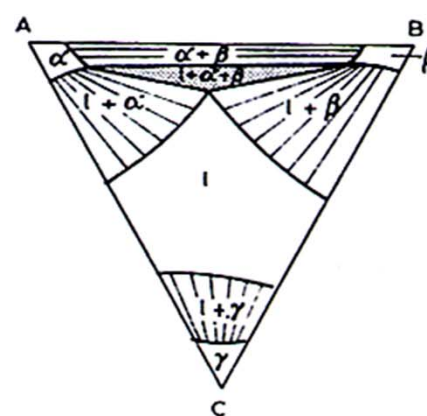
- **Isothermal section ( $T_A > T > T_B$ )**



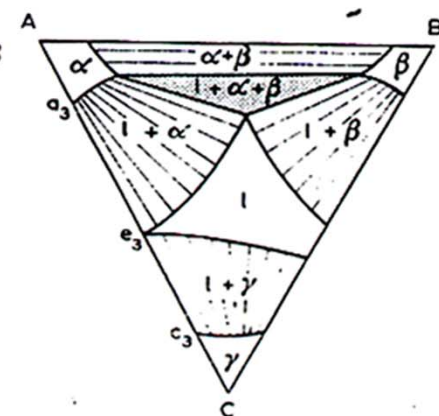
**(a)  $T_A > T > T_B$**



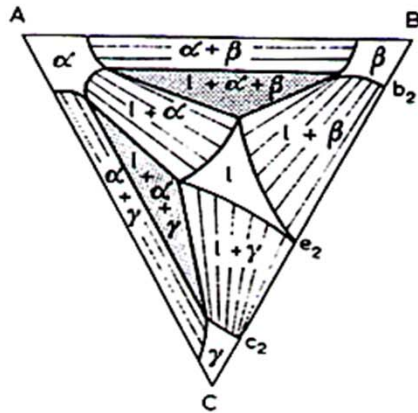
**(b)  $T = e_1$**



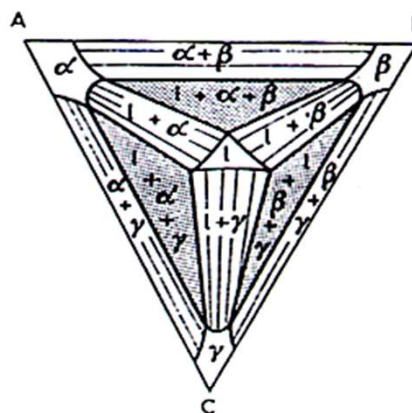
**(c)  $e_1 > T > e_3$**



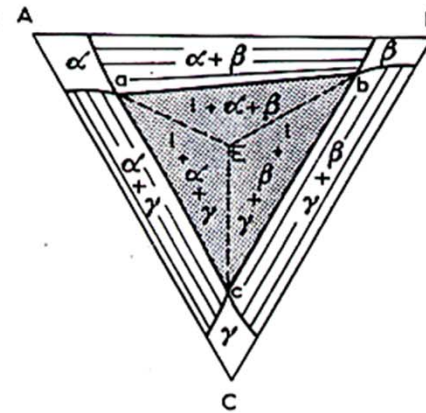
**(d)  $T = e_3$**



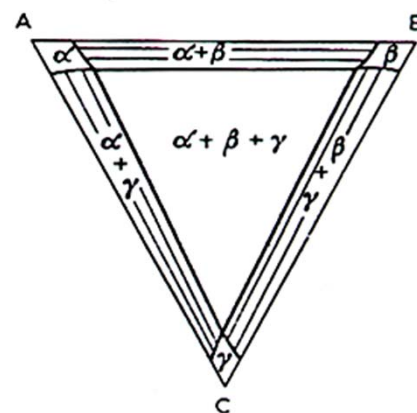
**(e)  $T = e_2$**



**(f)  $e_2 > T > E$**



**(g)  $T_A = E$**



**(h)  $E = T$**

\* Quaternary eutectic  $l \rightleftharpoons \alpha + \beta + \gamma + \delta$

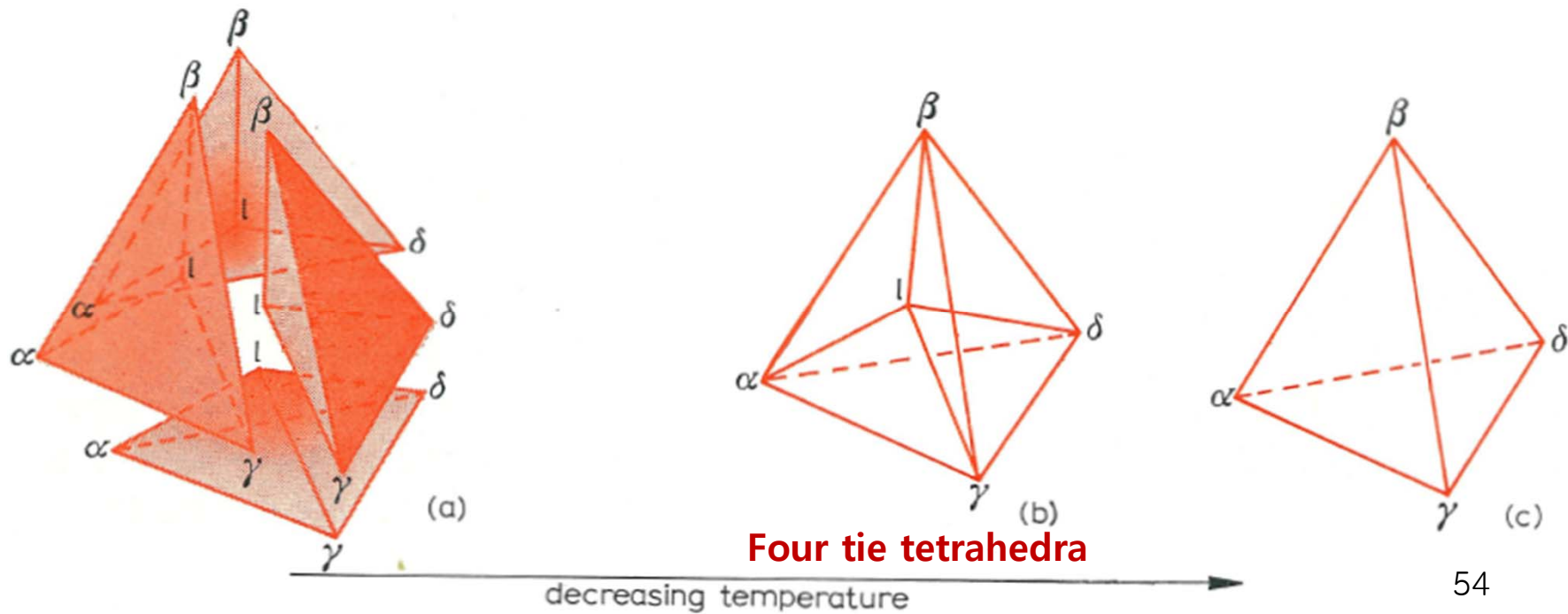
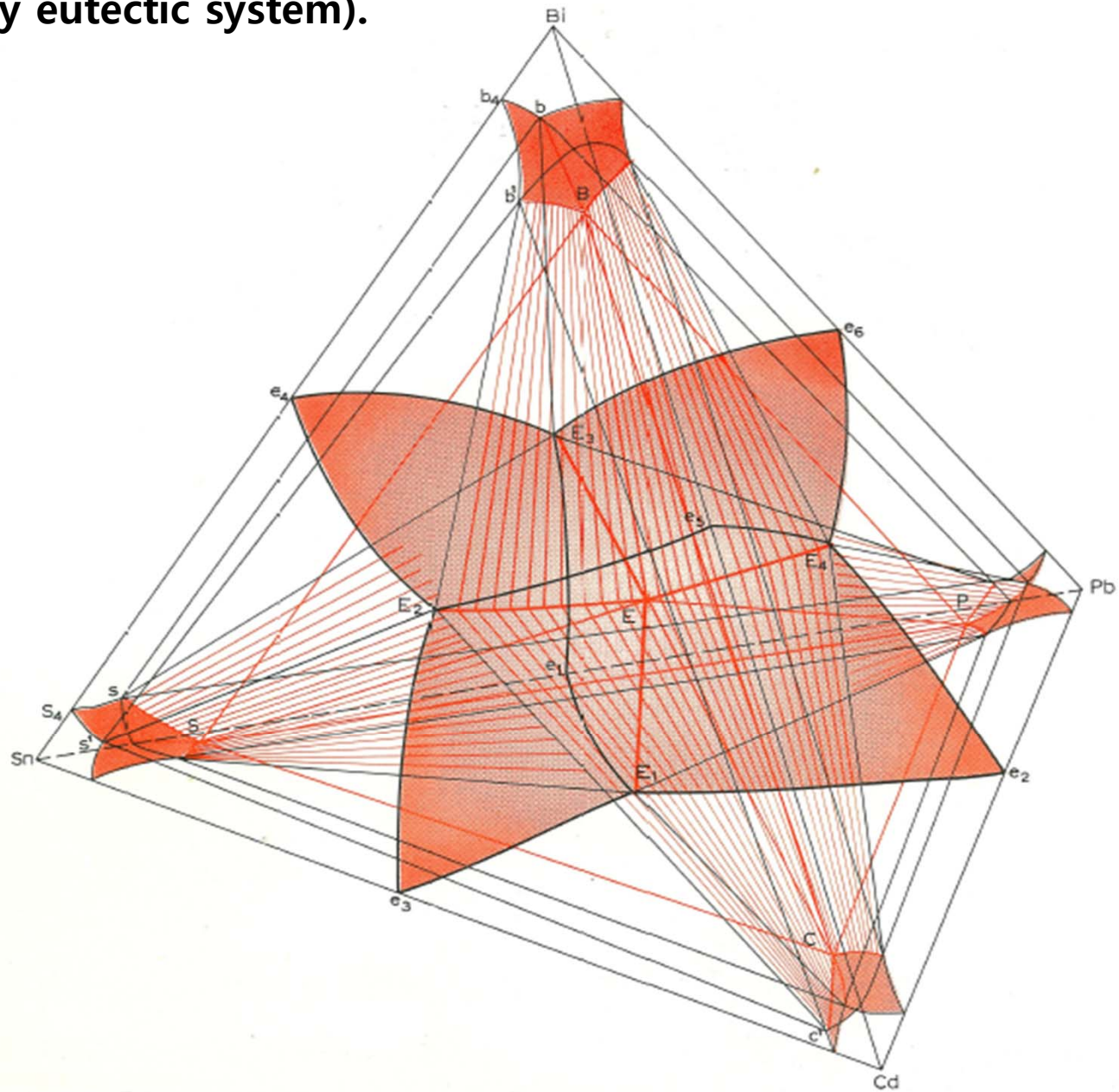


Fig. Sequence of tie-tetrahedron on cooling through the quaternary eutectic temperature

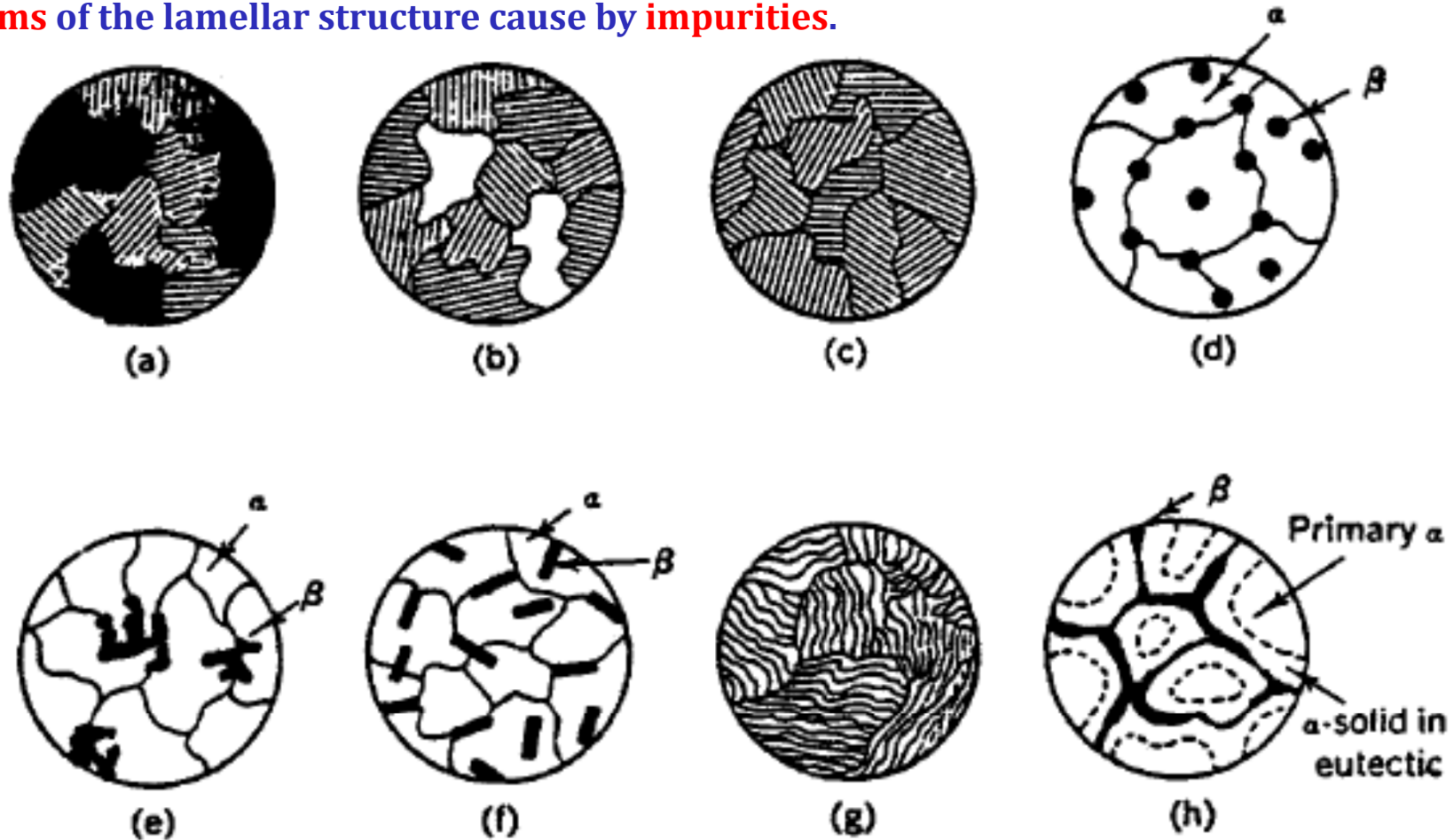
Polythermal projectin of a quaternary system involving five-phase equilibrium of the type  $l \rightleftharpoons \alpha + \beta + \gamma + \delta$  (schematic representation of the Bi-Cd-Pb-Sn quaternary eutectic system).



**Q: Various different types of eutectic solidification ( $L \rightarrow \alpha + \beta$ ) ?**

# 1) Microstructure of Eutectics

\* Many eutectics are lamellar with a very regular structure if the metals used are sufficiently "pure" and that may of the other structures that are observed are degenerate forms of the lamellar structure cause by impurities.



~~various~~

Fig. 14 Schematic representation possible in eutectic structures. (a), (b) and (c) are alloys shown in fig. 13; (d) nodular; (e) Chinese script; (f) acicular; (g) lamellar; and (h) divorced.

## 4.3.2 Eutectic Solidification

Various different types of eutectic solidification → Both phases grow simultaneously.

### Normal eutectic

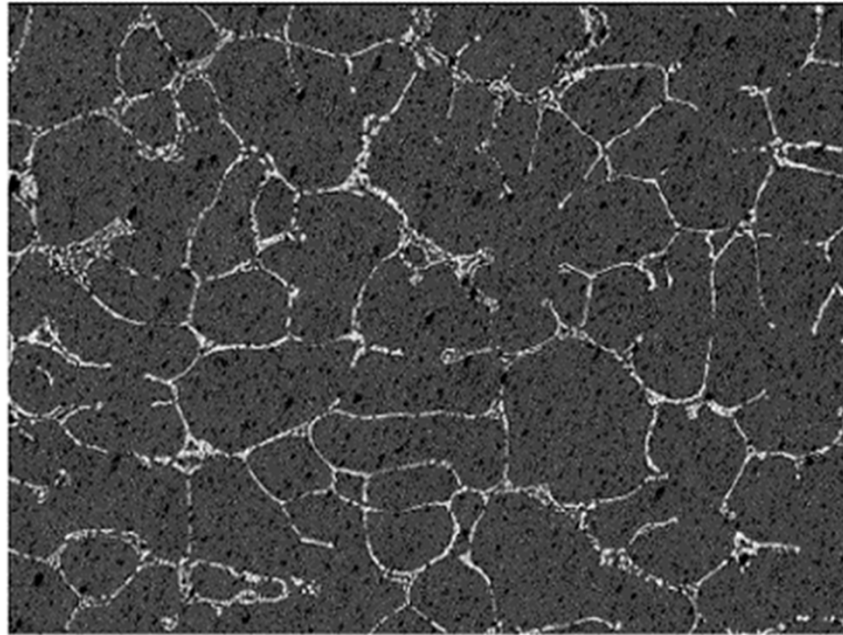
both phases have low entropies of fusion.



Fig. 4.30 Rod-like eutectic.  $\text{Al}_6\text{Fe}$  rods in Al matrix. Transverse section. Transmission electron micrograph ( x 70000).

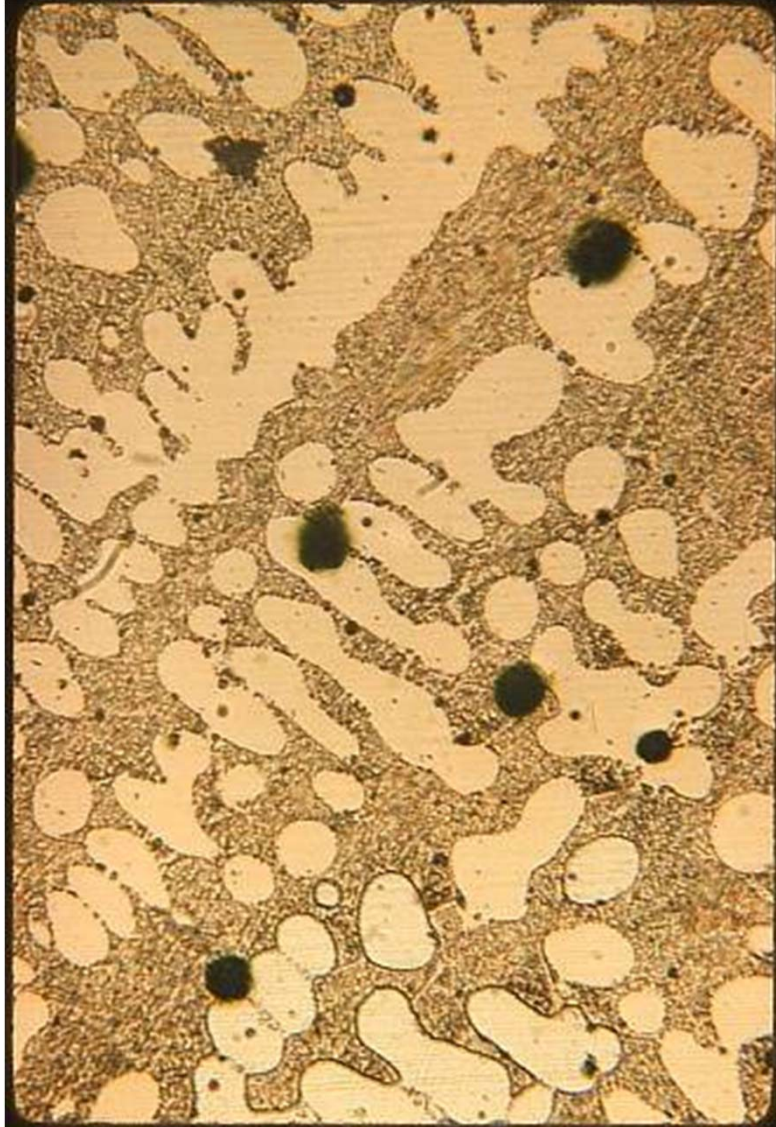
### Anomalous eutectic

One of the solid phases is capable of faceting, i.e., has a high entropy of melting.

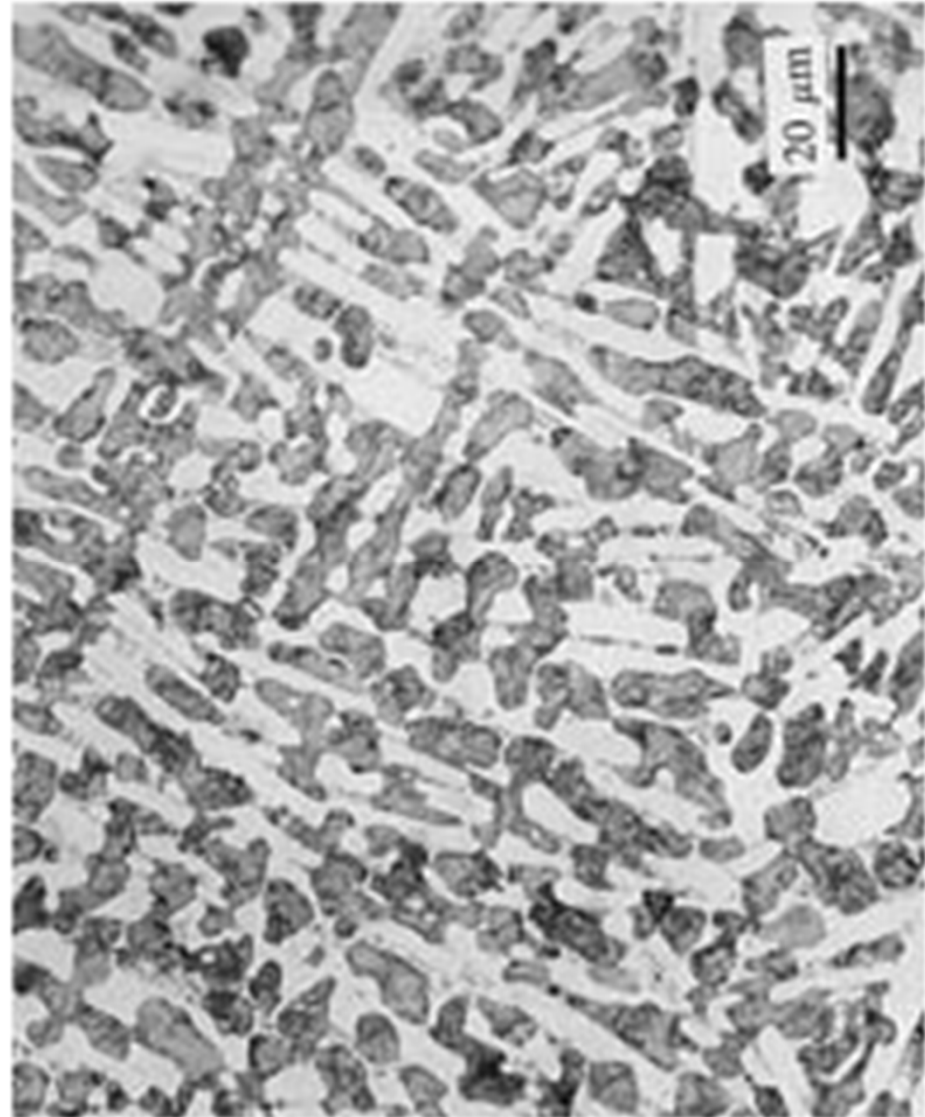


The microstructure of the **Pb-61.9%Sn (eutectic) alloy** presented a coupled growth of the (Pb)/ $\beta$ Sn eutectic. There is a remarkable change in morphology **increasing the degree of undercooling** with transition from regular lamellar to **anomalous eutectic**.

## Eutectic



## Divorced Eutectic



## 2) Pure binary eutectic

(zone-refined) high purity tin-lead  
→ extremely regular lamellar structure

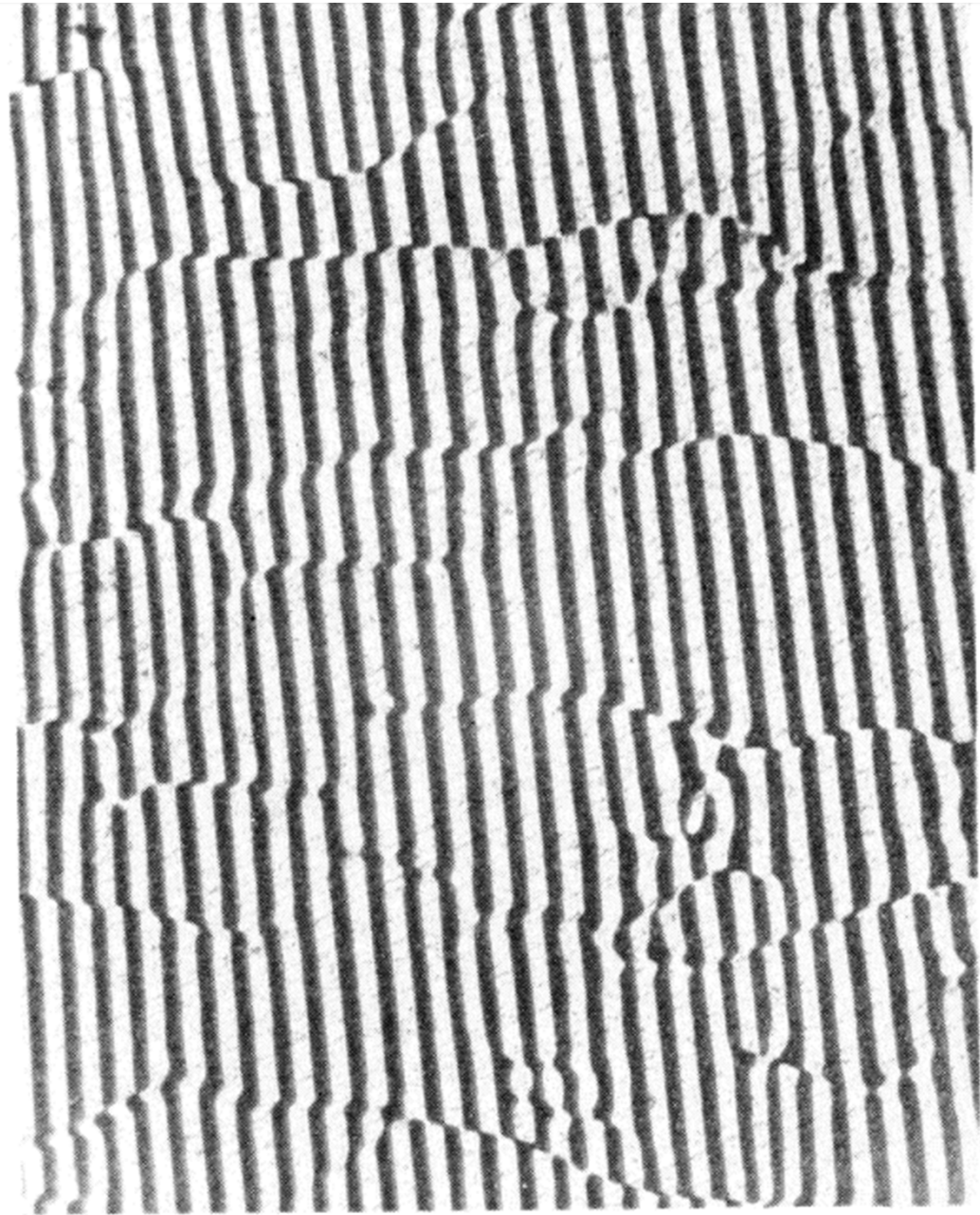


Fig. 6.13. Morphology of a pure eutectic (tin-lead).

**Lamellae:** straight and uniform thickness (ex, Al-Cu eutectic: several centimeters)

except where an “offset” or “termination” occurs

a) Constant orientation → **simple crystallographic relationship**

**Sn-Zn**       $(100) \text{ Sn} \parallel (0001) \text{ Zn}; [001] \text{ Sn} \parallel [01\bar{1}0] \text{ Zn}$

**Sn-Pb**       $(101) \text{ Sn} \parallel (111) \text{ Pb}; [010] \text{ Sn} \parallel [112] \text{ Pb}$

Ag Cu: all planes and directions parallel

b) Cu-CuAl<sub>2</sub> eutectic → **preferred relationship develops during the growth of a eutectic “single crystal”**

: a relationship not only btw the orientation of the two phases, but also btw the interlamellar surface and the crystal orientations

$(111) \text{ Al} \parallel (211) \text{ CuAl}_2$

$[101] \text{ Al} \parallel (120) \text{ CuAl}_2$

Lamellar interface parallel to  $(111) \text{ Al}$

### 3) Solidification of lamellar eutectic

Two representative opinions:

- 1) **Tammann** : alternation of layers of the two phases
- 2) **Vogel**: two phase grew simultaneously → interlamellar interfaces were approximately normal to the mean solid–liquid interface

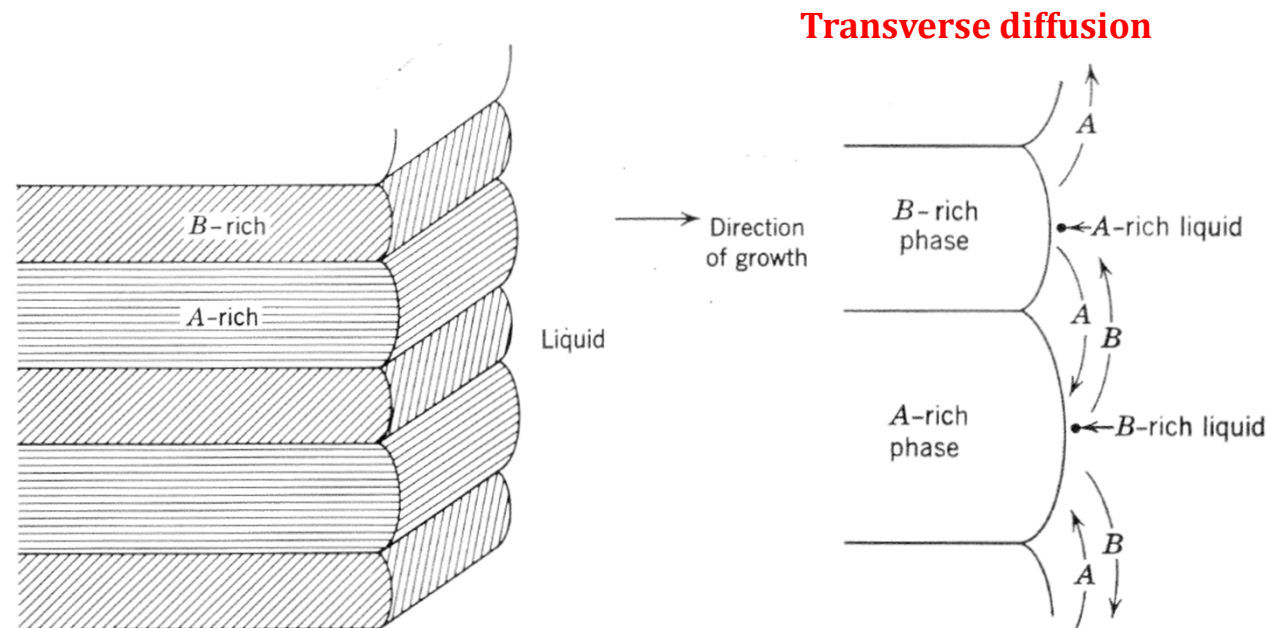
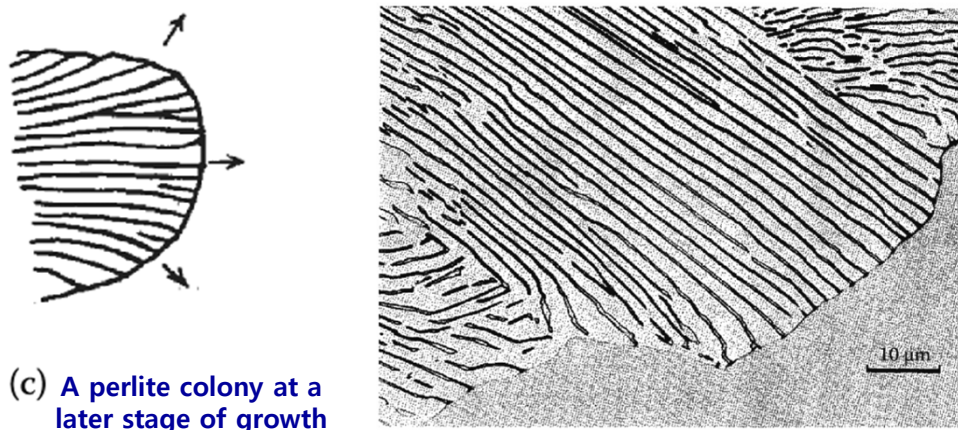
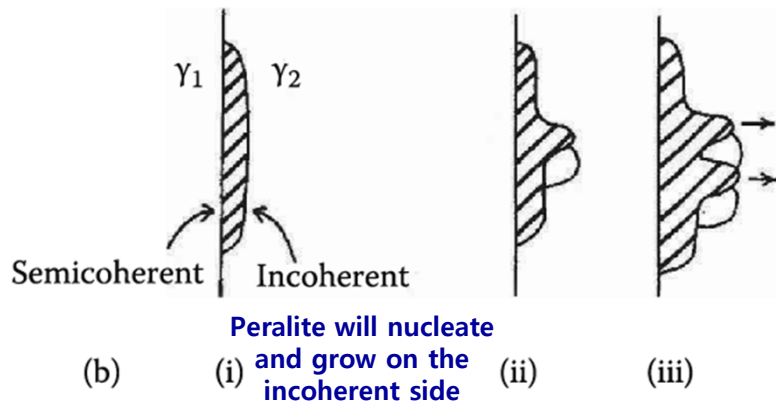
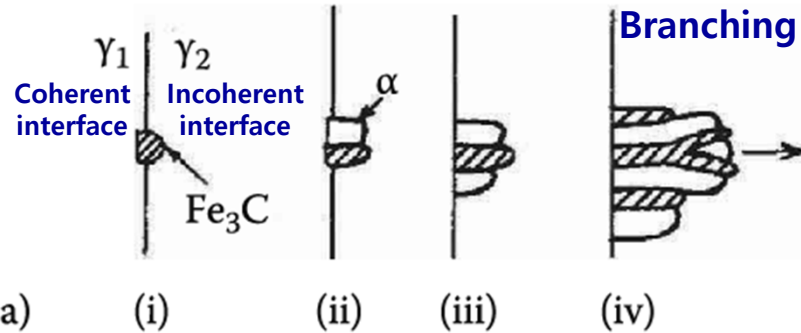


Fig. 6.14. Growth, mechanism, and diffusion paths for lamellar eutectic.

**\* Formation of Lamellae: a single nucleus of each phases → a nucleus of one phase forms first → second phase nucleates on the surface of the first**

**Reference: Pearlite Reaction in Fe-C Alloys: nucleation and growth**

**Branching Nucleation:** depend on GB structures and composition



(a) On a “clean” GB.

(i) **Cementite nucleates on GB** with coherent interface and orientation relationship with  $\gamma_1$  and incoherent interface with  $\gamma_2$ .

(ii)  **$\alpha$  nucleates adjacent to cementite** also with a coherent interface and orientation relationship with  $\gamma_1$ . (This also produces an orientation relationship between the cementite and the ferrite).

(iii) The **nucleation process repeats side ways**, while incoherent interfaces grow into  $\gamma_2$ .

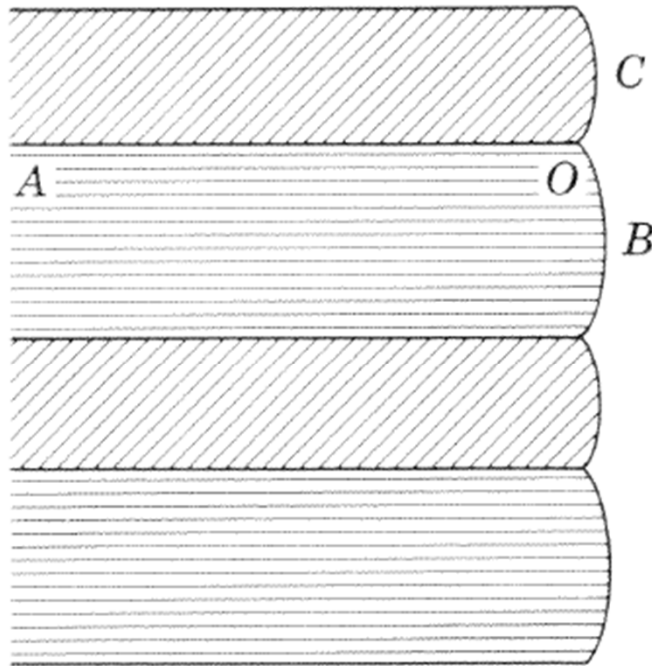
(iv) New plates can also form by a **branching mechanism**.

(b) When a proeutectoid phase (cementite or ferrite) already exists on that boundary, pearlite will **nucleate and grow on the incoherent side**. A different orientation relationship between the cementite and the ferrite results in this case.

(c) **Pearlite colony** at a latest stage of growth. Pearlite grows into the austenite grain with which it does not have an orientation relationship.

## 4) Shape of the interface

Fig. 6.15. Possible interface shapes.

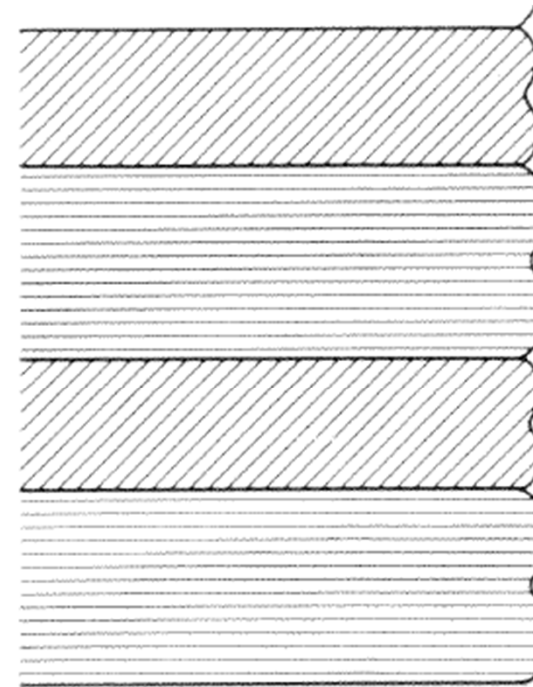


(a)

**Normally convex**

- Equilibrium of vector OA, OB, OC  
(O point → line in the real 3D case)

: the composition of the liquid in contact with the interface is constant over each lamella



(b)

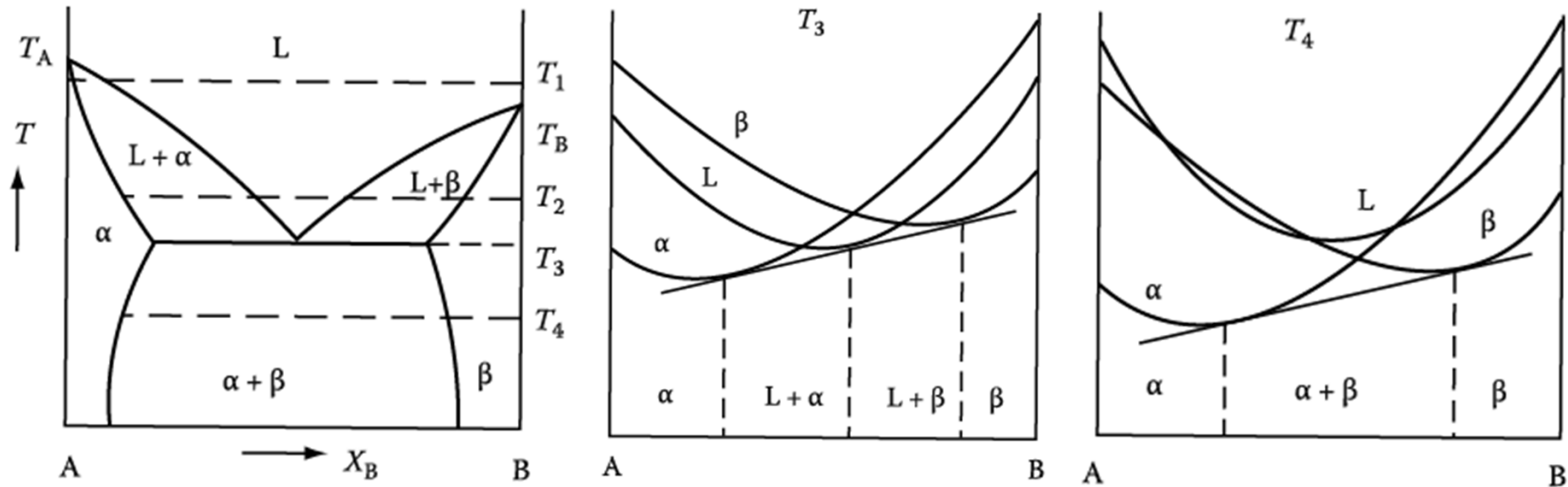
**Extreme case Concave**

- : Max. concentration of solute at Lamellae center & Min. concentration of solute at Lamellae edge

**Q: Thermodynamics and Kinetics of eutectic solidification ( $L \rightarrow \alpha + \beta$ ) ?**

This section will only be concerned with normal structures, and deal mainly with lamellar morphologies.

## 2. Eutectic Solidification (Thermodynamics)



Plot the diagram of Gibbs free energy vs. composition at  $T_3$  and  $T_4$ .

What is the driving force for the eutectic reaction ( $L \rightarrow \alpha + \beta$ ) at  $T_4$  at  $C_{\text{eut}}$ ?

What is the driving force for nucleation of  $\alpha$  and  $\beta$ ? “ $\Delta T$ ”

# Eutectic Solidification (Kinetics)

:  $\Delta T \rightarrow$  formation of interface + solute redistribution

If  $\alpha$  is nucleated from liquid and starts to grow, what would be the composition at the interface of  $\alpha/L$  determined?

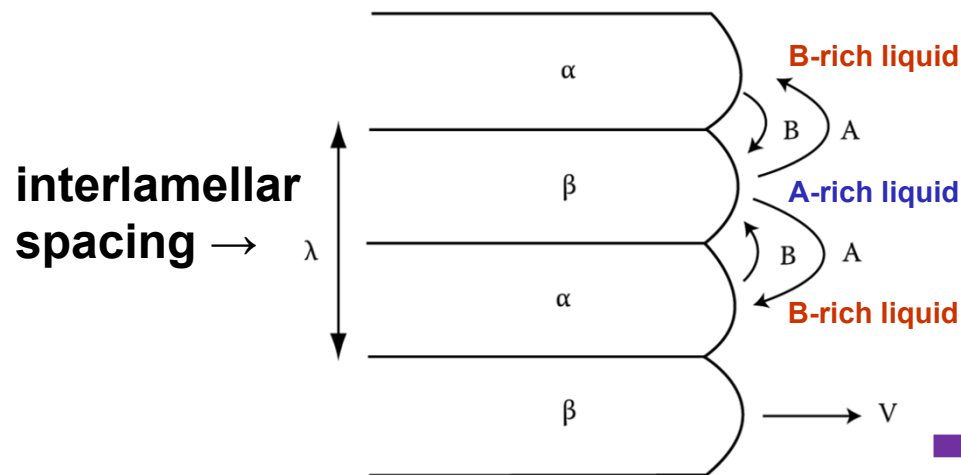
$\rightarrow$  rough interface (diffusion interface) & local equilibrium

How about at  $\beta/L$ ? Nature's choice? Lamellar structure

$$\rightarrow G = G_{\text{bulk}} + G_{\text{interface}} = G_0 + \gamma A$$

$$\sum A_i \gamma_i + \Delta G_S = \text{minimum}$$

Interface energy + Misfit strain energy



**Eutectic solidification**  
: diffusion controlled process

1)  $\lambda \downarrow \rightarrow$  eutectic growth rate  $\uparrow$

but 2)  $\lambda \downarrow \rightarrow \alpha/\beta$  interfacial  $E, \gamma_{\alpha\beta} \uparrow$   
 $\rightarrow$  lower limit of  $\lambda$

fastest growth rate at a certain  $\lambda$

What would be a role of the curvature at the tip?

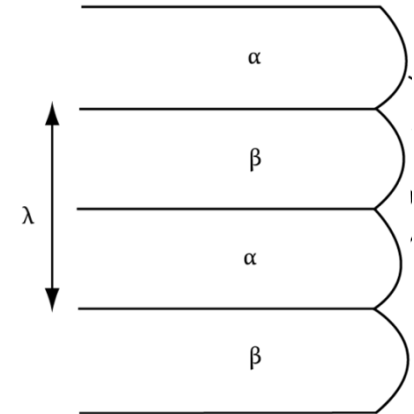
$\rightarrow$  Gibbs-Thomson Effect

# Eutectic Solidification (Kinetics)

:  $\Delta T \rightarrow$  a) formation of interface + b) solute redistribution

How many  $\alpha/\beta$  interfaces per unit length?

$\rightarrow 1/\lambda \times 2$



a) Formation of interface:  $\Delta G$

For an interlamellar spacing,  $\lambda$ , there is a total of  $(2/\lambda) \text{ m}^2$  of  $\alpha/\beta$  interface per  $\text{m}^3$  of eutectic.

$$\Delta G = \Delta\mu \cong \frac{L\Delta T}{T_m}$$

$$\rightarrow \Delta G = \Delta\mu = \frac{2\gamma}{\lambda} \times V_m$$

Driving force for nucleation = Total interfacial E of eutectic phase

For very large values of  $\lambda$ , interfacial E  $\sim 0$

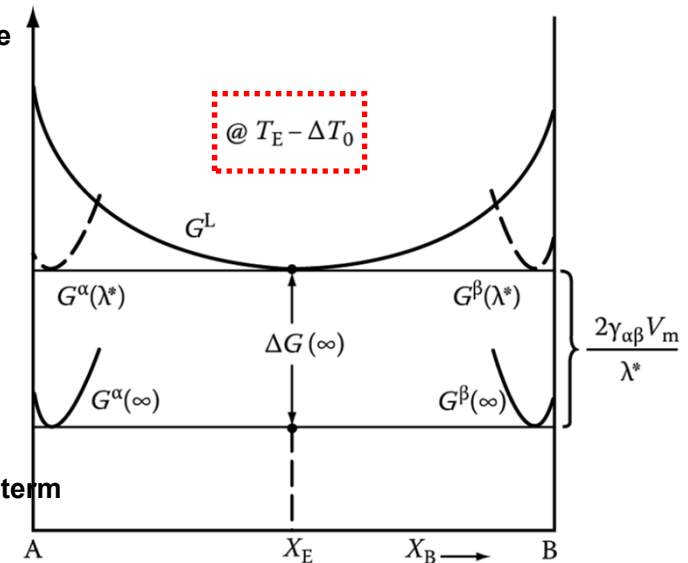
No interface (ideal case)

$$\lambda \rightarrow \infty, \quad \Delta G(\infty) = \Delta\mu = \frac{\Delta H \Delta T_0}{T_E}$$

With interface (real case)

$$\Delta G(\lambda) = ? = -\Delta G(\infty) + \frac{2\gamma V_m}{\lambda}$$

Solidification will take place if  $\Delta G$  is negative (-).



a) All  $\Delta T \rightarrow$  use for interface formation = min.  $\lambda$

What would be the minimum  $\lambda$ ?

Critical spacing,  $\lambda^* : \Delta G(\lambda^*) = 0$

최소 층상 간격

$$\Delta G(\infty) = \frac{2\gamma V_m}{\lambda^*}$$

$$\lambda^* = + \frac{2T_E \gamma V_m}{\Delta H \Delta T_0}$$

Gibbs-Thomson effect

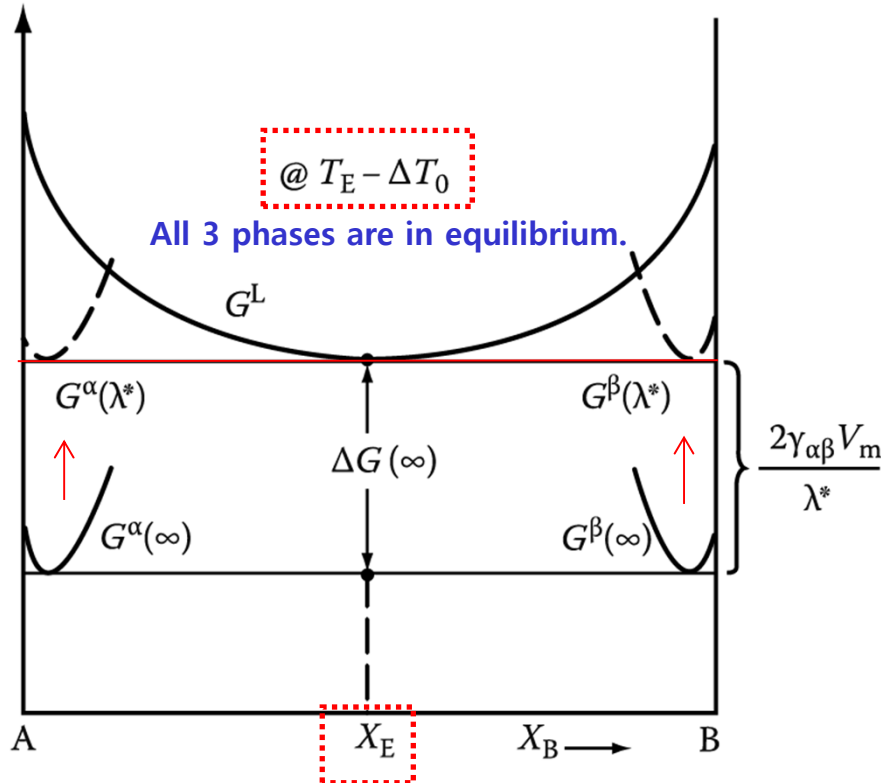
$$\lambda^* = -\frac{2T_E \gamma V_m}{\Delta H \Delta T_0} \rightarrow \text{identical to critical radius of dendrite tip in pure metal}$$

$$\text{cf) } r^* = \frac{2\gamma_{SL}}{\Delta G_V} = \left( \frac{2\gamma_{SL} T_m}{L_V} \right) \frac{1}{\Delta T}$$

$L_V$ : latent heat per unit volume  
 $L = \Delta H = H^L - H^S$

\* Growth Mechanism: Gibbs-Thomson effect in a  $\Delta G$ -composition diagram?

1) At  $\lambda = \lambda^* (< \infty)$ ,



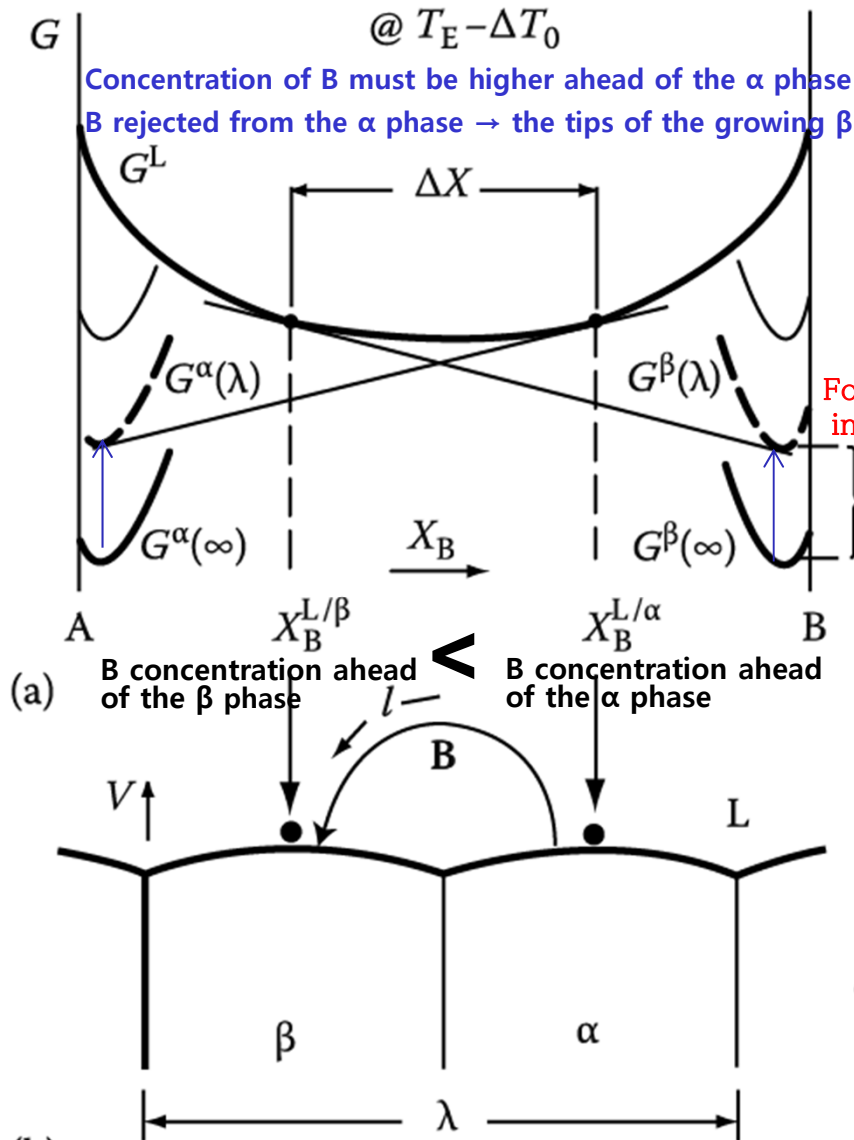
The cause of **G increase** is the curvature of the  $\alpha/L$  and  $\beta/L$  interfaces arising from the need to **balance the interfacial tensions at the  $\alpha/\beta/L$  triple point**, therefore the increase will be different for the two phases, but for simple cases it can be shown to be

$$\frac{2\gamma_{\alpha\beta} V_m}{\lambda} \text{ for both.}$$

1) If  $\lambda = \lambda^*$ , growth rate will be ***infinitely slow*** because the liquid in contact with both phases has the same composition,  $X_E$  in Figure 4.32.

2) At  $\lambda = (\infty >) \lambda (> \lambda^*)$ ,

If  $\infty > \lambda > \lambda^*$ ,  $G_\alpha$  and  $G_\beta$  are correspondingly reduced because less free energy is locked in the interfaces.  $\rightarrow X_B^{L/\alpha} > X_B^{L/\beta}$



\* Eutectic growth rate,  $v$

$\rightarrow$  if  $\alpha/L$  and  $\beta/L$  interfaces are highly mobile

$\rightarrow$  proportional to flux of solute through liquid

$\rightarrow$  diffusion controlled process

$$v \propto D \frac{dC}{dl} \propto (X_B^{L/\alpha} - X_B^{L/\beta})$$

$$\propto 1/\text{effective diffusion distance.. } 1/\lambda$$

$$v = k_1 D \frac{\Delta X}{\lambda} \quad (1)$$

$$\lambda = \lambda^*, \Delta X = 0$$

$$\lambda = \infty, \Delta X = \Delta X_0$$

(next page)

$$\Delta X = \Delta X_0 \left(1 - \frac{\lambda^*}{\lambda}\right) \quad (2)$$

$$\Delta X_0 \propto \Delta T_0 \quad (3)$$

$$(2)+(3) \rightarrow (1) \quad v = k_2 D \frac{\Delta T_0}{\lambda} \left(1 - \frac{\lambda^*}{\lambda}\right)$$

Maximum growth rate at a fixed  $\Delta T_0 \rightarrow \lambda = 2\lambda^*$

Fig. 4.33 (a) Molar free energy diagram at  $(T_E - \Delta T_0)$  for the case  $\lambda^* < \lambda < \infty$ , showing the composition difference available to drive diffusion through the liquid ( $\Delta X$ ). (b) Model used to calculate the growth rate.

$\Delta X$  will it self depend on  $\lambda$ .  $\sim$  maximum value,  $\Delta X_0$

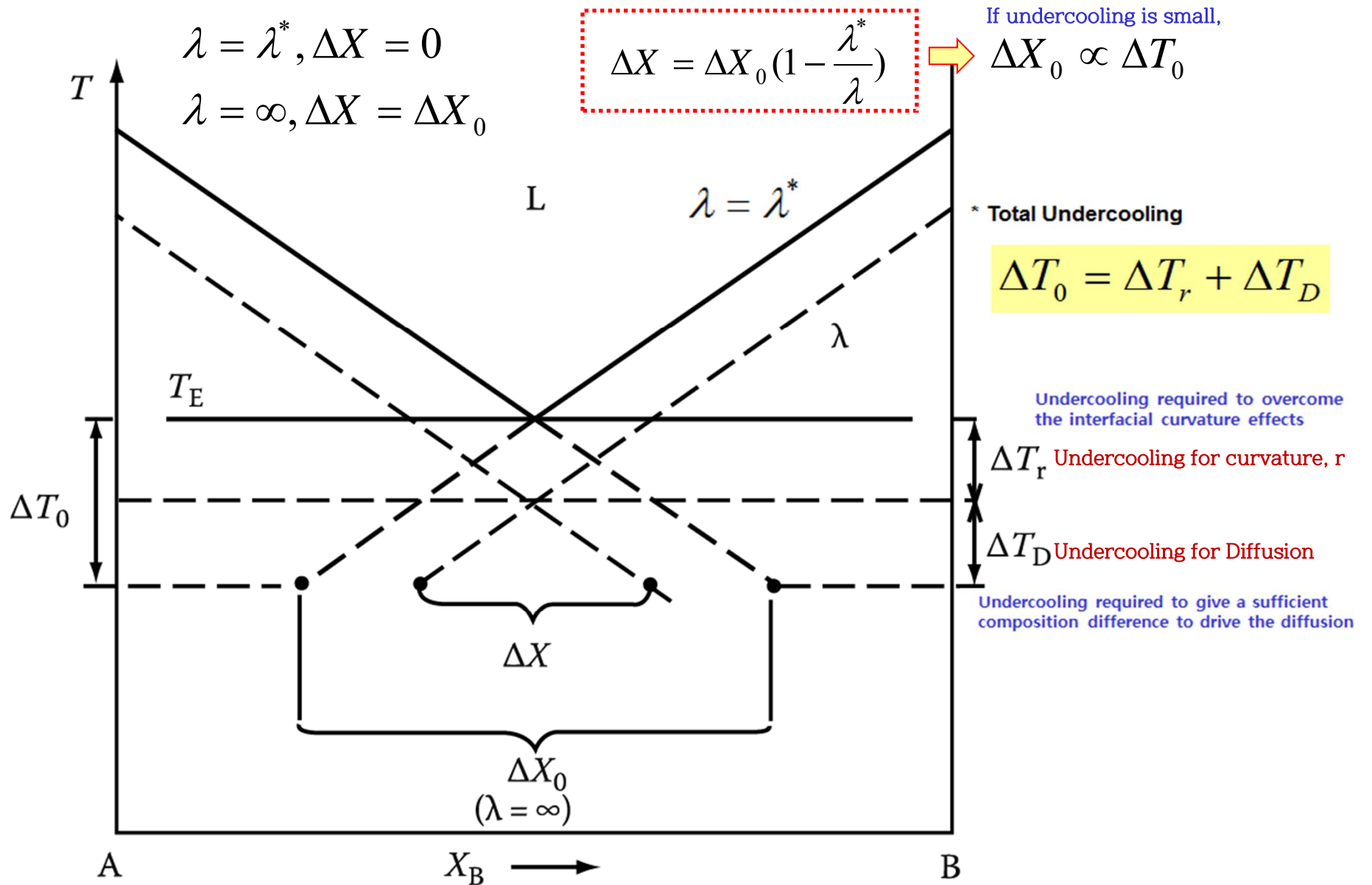
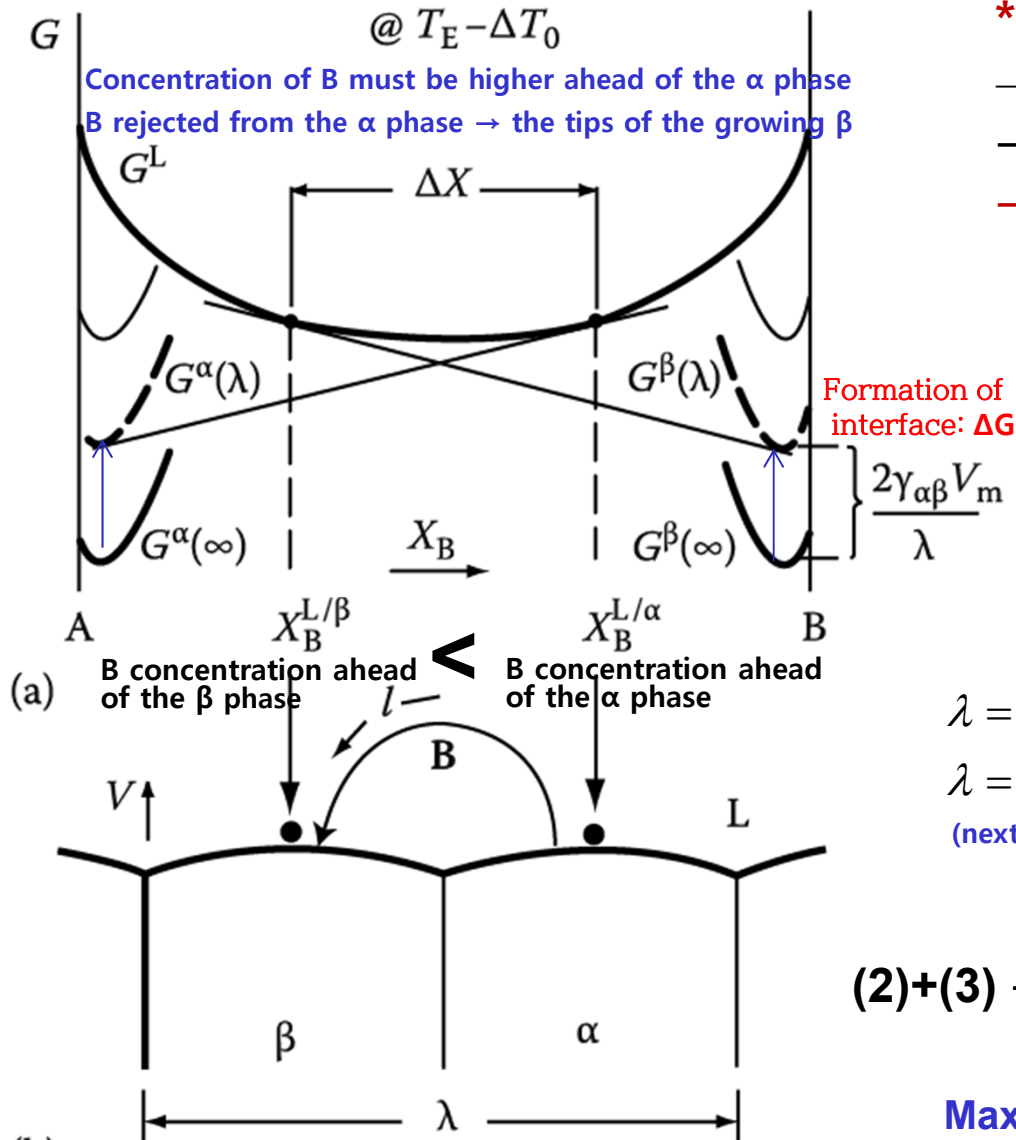


Fig. 4.34 Eutectic phase diagram showing the relationship between  $\Delta X$  and  $\Delta X_0$  (exaggerated for clarity)

2) At  $\lambda = (\infty >) \lambda (> \lambda^*)$ ,

If  $\infty > \lambda > \lambda^*$ ,  $G_\alpha$  and  $G_\beta$  are correspondingly reduced because less free energy is locked in the interfaces.  $\rightarrow X_B^{L/\alpha} > X_B^{L/\beta}$



\* Eutectic growth rate,  $v$

$\rightarrow$  if  $\alpha/L$  and  $\beta/L$  interfaces are highly mobile

$\rightarrow$  proportional to flux of solute through liquid

$\rightarrow$  diffusion controlled process

$$v \propto D \frac{dC}{dl} \propto (X_B^{L/\alpha} - X_B^{L/\beta})$$

$$\propto 1/\text{effective diffusion distance.. } 1/\lambda$$

$$v = k_1 D \frac{\Delta X}{\lambda} \quad (1)$$

$$\lambda = \lambda^*, \Delta X = 0$$

$$\lambda = \infty, \Delta X = \Delta X_0$$

(next page)

$$\Delta X = \Delta X_0 \left(1 - \frac{\lambda^*}{\lambda}\right) \quad (2)$$

$$\Delta X_0 \propto \Delta T_0 \quad (3)$$

$$(2)+(3) \rightarrow (1) \quad v = k_2 D \frac{\Delta T_0}{\lambda} \left(1 - \frac{\lambda^*}{\lambda}\right)$$

Maximum growth rate at a fixed  $\Delta T_0 \rightarrow \lambda = 2\lambda^*$

Fig. 4.33 (a) Molar free energy diagram at  $(T_E - \Delta T_0)$  for the case  $\lambda^* < \lambda < \infty$ , showing the composition difference available to drive diffusion through the liquid ( $\Delta X$ ). (b) Model used to calculate the growth rate. 72

# Closer look at the tip of a growing dendrite

different from a planar interface because heat can be conducted away from the tip in three dimensions.

Assume the solid is isothermal ( $T'_S = 0$ )

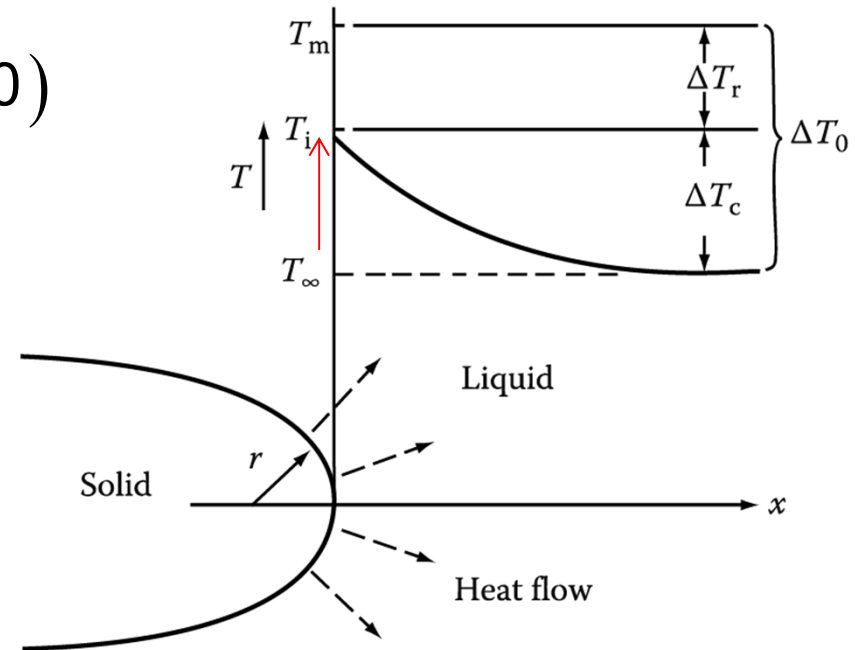
From  $K_S T'_S = K_L T'_L + v L_V$

If  $T'_S = 0$ ,  $v = \frac{-K_L T'_L}{L_V}$

A solution to the heat-flow equation for a hemispherical tip:

$$T'_L (\text{negative}) \cong \frac{\Delta T_C}{r} \quad \Delta T_C = T_i - T_\infty$$

$$v = \frac{-K_L T'_L}{L_V} \cong \frac{K_L}{L_V} \cdot \frac{\Delta T_C}{r} \quad v \propto \frac{1}{r}$$



However,  $\Delta T$  also depends on  $r$ .  
How?

## Thermodynamics at the tip?

Gibbs-Thomson effect:  
melting point depression

$$\Delta G = \frac{L_V}{T_m} \Delta T_r = \frac{2\gamma}{r} \quad \Delta T_r = \frac{2\gamma T_m}{L_V r}$$

## Minimum possible radius ( r )?

$$r_{min} : \Delta T_r \rightarrow \Delta T_0 = T_m - T_\infty \rightarrow r^*$$

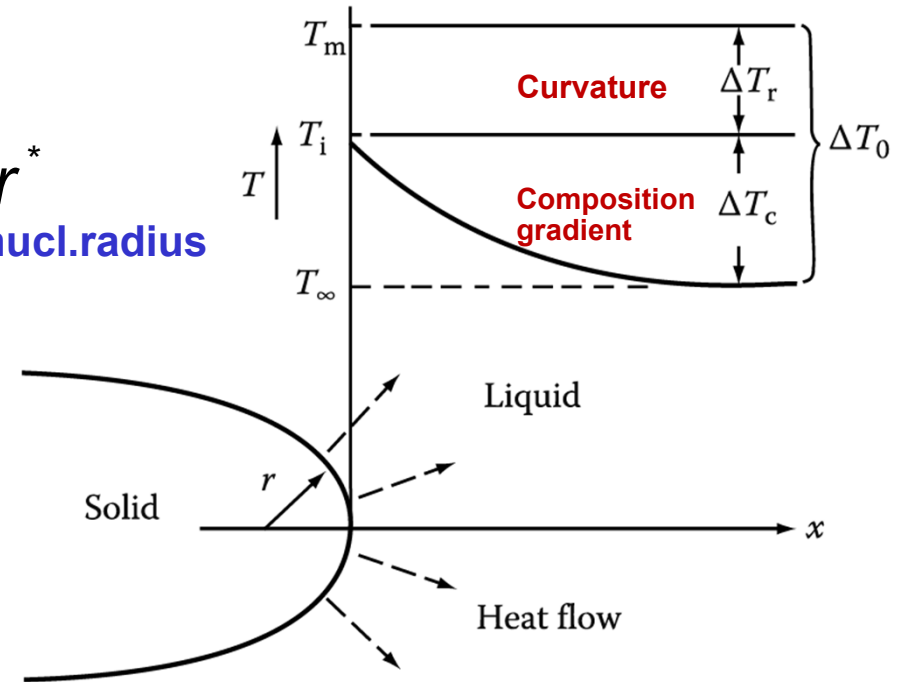
The crit.nucl.radius

$$r^* = \frac{2\gamma T_m}{L_v \Delta T_0}$$

$$\Delta T_r = \frac{2\gamma T_m}{L_v r}$$

Express  $\Delta T_r$  by  $r$ ,  $r^*$  and  $\Delta T_0$ .

$$\Delta T_r = \frac{r^*}{r} \Delta T_0$$



$$v \cong \frac{K_L}{L_v} \cdot \frac{\Delta T_c}{r} = \frac{K_L}{L_v} \cdot \frac{(\Delta T_0 - \Delta T_r)}{r} = \frac{K_L}{L_v} \cdot \frac{\Delta T_0}{r} \left( 1 - \frac{r^*}{r} \right)$$

$v \rightarrow 0$  as  $r \rightarrow r^*$  due to Gibbs-Thomson effect  
as  $r \rightarrow \infty$  due to slower heat conduction

Maximum velocity?

$$\rightarrow r = 2r^*$$

# Undercooling $\Delta T_0$

$$\Delta T_0 = \underbrace{\Delta T_r}_{\text{Curvature}} + \underbrace{\Delta T_D}_{\text{Composition gradient}} \quad \rightarrow \quad \Delta G_{total} = \underbrace{\Delta G_r}_{\text{Curvature}} + \underbrace{\Delta G_D}_{\text{Composition gradient}} \quad \rightarrow \quad v = k_2 D \frac{\Delta T_0}{\lambda} \left(1 - \frac{\lambda^*}{\lambda}\right)$$

$$\Delta G_r = \frac{2\gamma_{\alpha\beta} V_m}{\lambda}$$

$\rightarrow$  free energy dissipated in forming  $\alpha/\beta$  interfaces

$\Delta G_D \rightarrow$  free energy dissipated in diffusion

By varying the interface undercooling ( $\Delta T_0$ ) it is possible to vary the growth rate ( $v$ ) and spacing ( $\lambda$ ) independently.

Therefore, it is impossible to predict the spacing that will be observed for a given growth rate. **However, controlled growth experiments show that a specific value of  $\lambda$  is always associated with a given growth rate.**

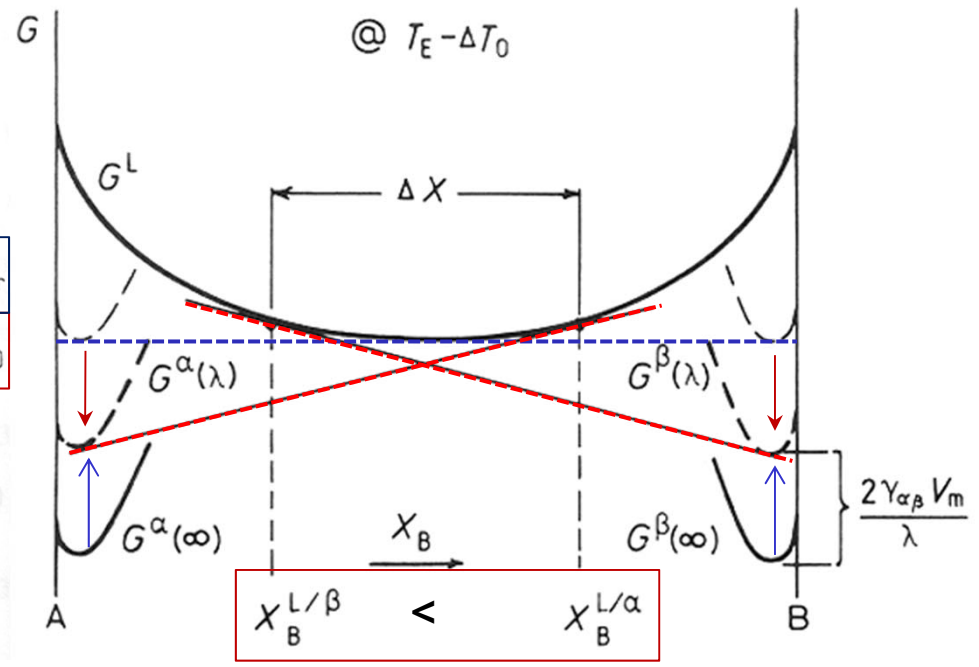
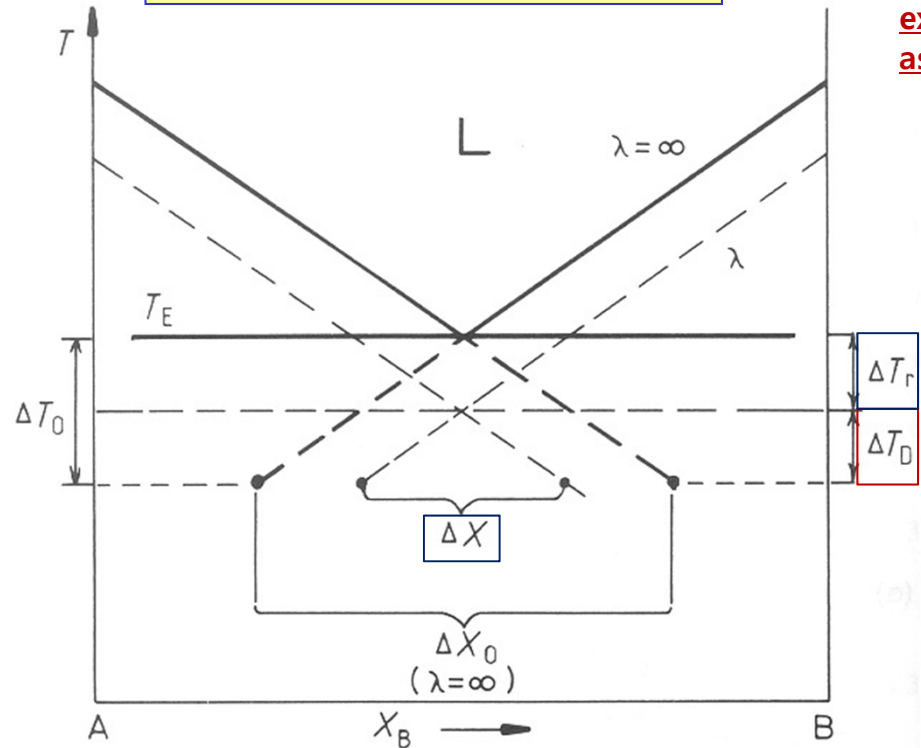
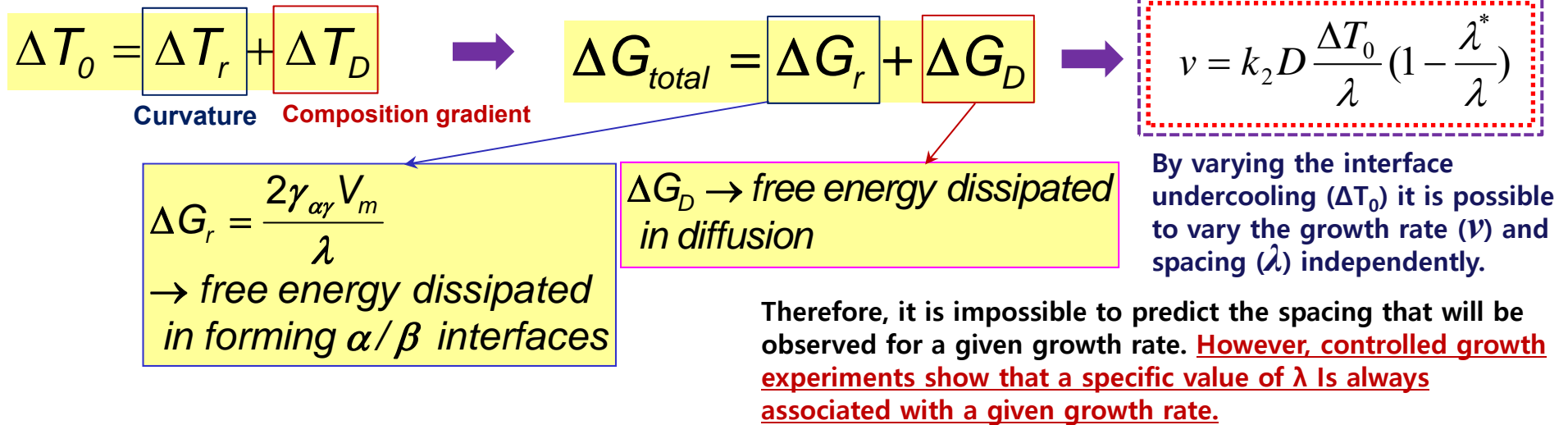


Fig. 4.34 Eutectic phase diagram showing the relationship between  $\Delta X$  and  $\Delta X_0$  (exaggerated for clarity)

# Undercooling $\Delta T_0$



\* For example,

Maximum growth rate at a fixed  $\Delta T_0 \rightarrow \lambda_0 = 2\lambda^*$

(4)  $v = k_2 D \frac{\Delta T_0}{\lambda} \left(1 - \frac{\lambda^*}{\lambda}\right)$  →  $v_0 = k_2 D \Delta T_0 / 4\lambda^*$  (5)

From Eq. 4.39

$\lambda^* = + \frac{2T_E \gamma V_m}{\Delta H \Delta T_0}$  →  $\Delta T_0 \propto 1/\lambda^*$  (6)

So that the following relationships are predicted:

(5) + (6) →

$v_0 \lambda_0^2 = k_3$  (constant)  
 $\frac{v_0}{(\Delta T_0)^2} = k_4$

Ex) Lamellar eutectic in the Pb-Sn system

$k_3 \sim 33 \mu\text{m}^3/\text{s}$  and  $k_4 \sim 1 \mu\text{m}/\text{s}\cdot\text{K}^2$

→  $v = 1 \mu\text{m}/\text{s}$ ,  $\lambda_0 = 5 \mu\text{m}$  and  $\Delta T_0 = 1 \text{ K}$

## \* Total Undercooling

$$\Delta T_0 = \Delta T_r + \Delta T_D$$

Undercooling required to overcome the interfacial curvature effects

Undercooling required to give a sufficient composition difference to drive the diffusion

Strictly speaking,

$\Delta T_i$  term should be added **but, negligible for high mobility interfaces**

Driving force for atom migration across the interfaces

$\Delta T_D \rightarrow$  Vary continuously from the middle of the  $\alpha$  to the middle of the  $\beta$  lamellae

$\Delta T_0 = \text{const}$   $\leftarrow$  Interface is essentially isothermal.

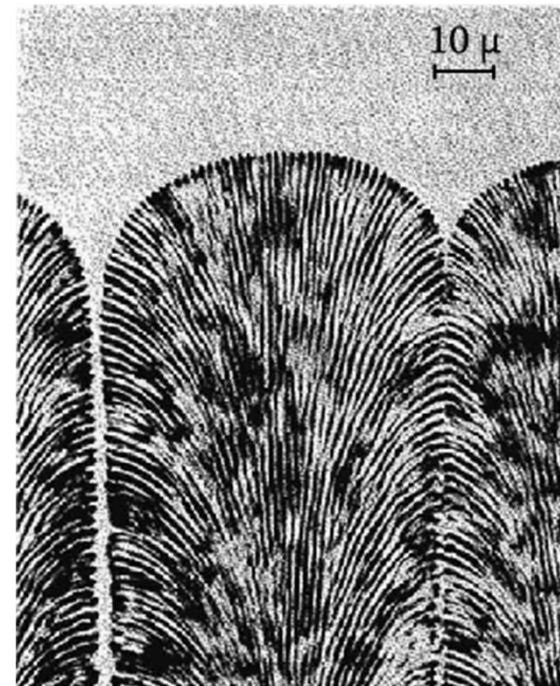
$\Delta T_D \rightarrow$   $\Delta T_r$  **The interface curvature will change across the interface.**  
Should be compensated

## \* A planar eutectic front is not always stable.

Binary eutectic alloys contains **impurities** or **other alloying elements**  $\rightarrow$  "Form a cellular morphology"  
analogous to single phase solidification restrict in a sufficiently high temp. gradient.

$\rightarrow$  The solidification direction changes as the cell walls are approached and the lamellar or rod structure fans out and may even change to an irregular structure.

$\rightarrow$  **Impurity elements (here, mainly copper) concentrate at the cell walls.**



## A planar eutectic front is not always stable.

Binary eutectic alloys contains **impurities** or **other alloying elements**

“Form a cellular morphology”

→ analogous to single phase solidification restrict in a sufficiently high temp. gradient.

- The solidification direction changes as the cell walls are approached and the lamellar or rod structure fans out and may even change to an irregular structure.
- Impurity elements (here, mainly copper) concentrate at the cell walls.

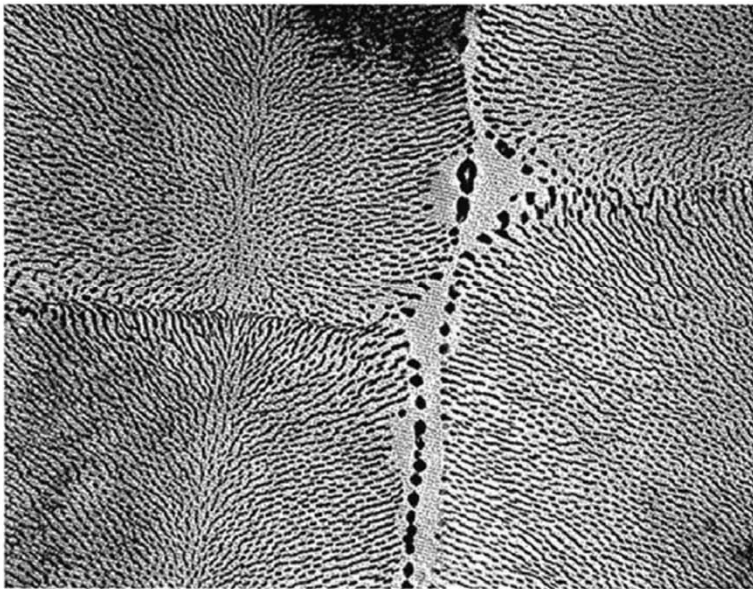
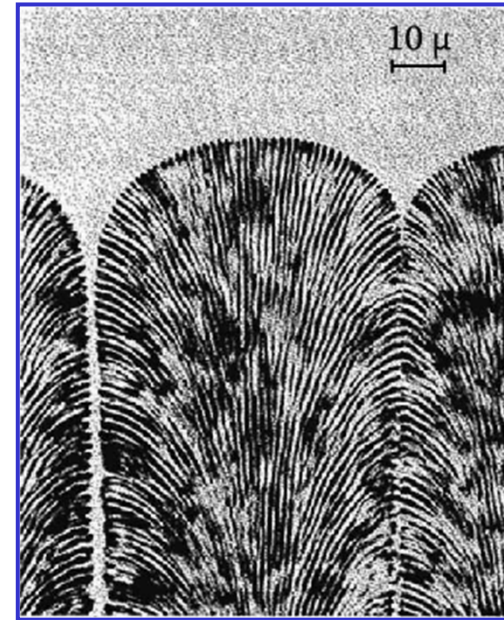


Fig. 4.35 Transverse section through the cellular structure of an Al-Al<sub>6</sub>Fe rod eutectic (x3500).

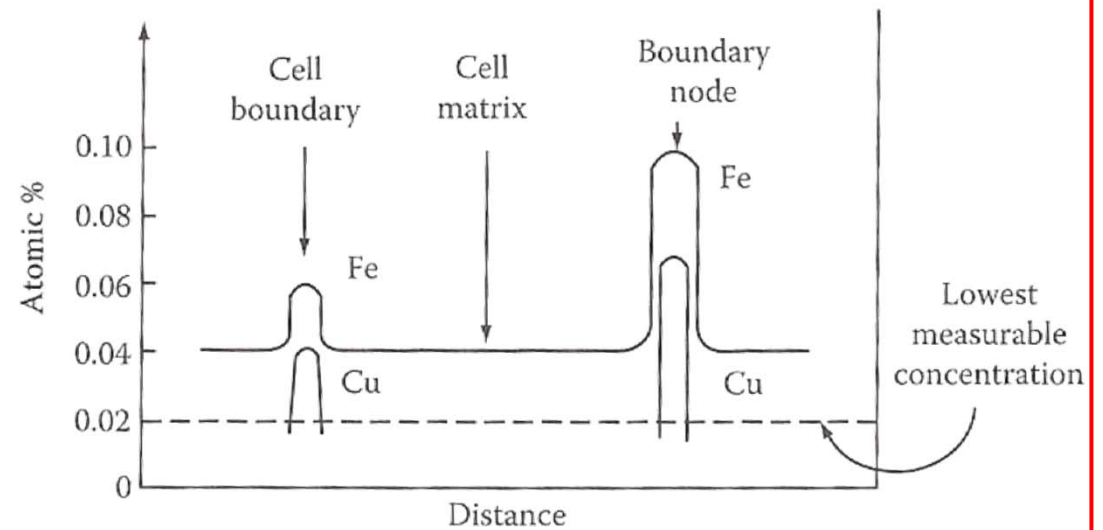


Fig. 4.36 Composition profiles across the cells in Fig. 4.35b.